Application to Food Standards Australia New Zealand for the Inclusion of Soybean MON 94637 in *Standard 1.5.2 - Food Produced Using Gene Technology*

Submitted by:

Bayer CropScience Pty Ltd

Level 4, 109 Burwood Rd

Hawthorn, Victoria 3122

July 22, 2024

© 2024 Bayer Group. All Rights Reserved.

This document is protected under national and international copyright law and intellectual property right treaties. This document and any accompanying materials are for use only by the regulatory authority to which it has been submitted by the Bayer Group, including all subsidiaries and affiliated companies, and only in support of actions requested by the Bayer Group. Any other use, copying, or transmission, including internet posting, of this document and the materials described in or accompanying this document, without prior consent of Bayer Group, is strictly prohibited; except that Bayer Group hereby grants such consent to the regulatory authority where required under applicable law or regulation. The intellectual property, information and materials described in or accompanying this document are owned by Bayer Group, who has filed for or been granted patents on those materials. By submitting this document and any accompanying materials, Bayer Group does not grant any party or entity any right or license to the information, materials or intellectual property described or contained in this submission.

TABLE OF CONTENTS

LIST OF FIGURES

LIST OF TABLES

CHECKLIST

General Requirements (3.1.1)	Page No.
A Form of application	
☑ *Application in English*	
☑ *Executive Summary (separated from main application electronically)*	
☑ *Relevant sections of Part 3 clearly identified*	
☑ *Pages sequentially numbered*	
☑ *Electronic copy (searchable)*	
☑ *All references provided*	
☑ **B Applicant details**	*Page 1*
☑ **C Purpose of the application**	*Page 1*
D Justification for the application	
☑ *Regulatory impact information*	*Page 2*
☑ *Impact on international trade*	*Page 3*
E Information to support the application	
☑ *Data requirements*	*Page 3*
F Assessment procedure	
☑ *General*	*Page 3*
☐ *Major*	
☐ *Minor*	
☐ *High level health claim variation*	
G Confidential Commercial Information	
☑ *CCI material separated from other application material*	
☐ *Formal request including reasons*	*Page 3*
☐ *Non-confidential summary provided*	
H Other confidential information	
☑ *Confidential material separated from other application material*	*Page 3*
☐ *Formal request including reasons*	
I Exclusive Capturable Commercial Benefit	
☑ *Justification provided*	*Page 4*

J International and Other National Standards	
☑ *International standards*	*Page 4*
☑ *Other national standards*	*Page 4*
K Statutory Declaration	*Page 4*
L Checklist/s provided with Application	
☑ *3.1.1 Checklist*	*Page x*
☑ *All page number references from application included*	
☑ Any other relevant checklists for Sections 3.2 – 3.7	*Checklist 3.5.1*
Foods Produced using Gene Technology (3.5.1)	
☑ A.1 Nature and identity	*Page 5*
☑ A.2 History of use of host and donor organisms	*Page 6*
☑ A.3 Nature of genetic modification	*Page 9*
☑ B.1 Characterisation and safety assessment of new substances	*Page 49*
☑ B.2 New proteins	*Page 93*
☑ B.3 Other (non-protein) new sustances	*Page 121*
☑ B.4 Novel herbicide metabolites in GM herbicide-tolerant plants	*Page 122*
☑ B.5 Compositional assessment	*Page 122*
☑ C Information related to the nutritional impact of the food produced using gene technology	*Page 140*
☑ D Other information	*Page 140*

ABBREVIATIONS AND DEFINITIONS

AA	Amino Acid
ADF	Acid Detergent Fiber
AFSI	Agriculture and Food Systems Institute
BLAW	black armyworm
BSA	Bovine Serum Albumin
Bt	*Bacillus thuriengensis*
CAB	chlorophyll a/b-binding
CCDB	Crop Composition Database
COMPARE	COMprehensive Protein Allergen REsource
Cry	Crystalline protein
DNA	Deoxyribonucleic Acid
dw	Dry Weight
DWCF	Dry Weight Conversion Factor
E. coli	*Escherichia coli*
ECL	Enhanced Chemiluminescence
EFSA	European Food Safety Authority
ELISA	Enzyme-linked Immunosorbent Assay
EPA	Environmental Protection Agency (U.S.)
EU	European Union
E-score	Expectation score
FA	Fatty Acid
FCID	Food Commodity Intake Database
FDA	Food and Drug Adminstration (U.S.)
fw	Fresh Weight
g	Gram
GLP	Good Laboratory Practice
GRAS	Generally Recognized as Safe
HRP	Horseradish Peroxidase
IAC	Immunoaffinity Chromatography
ICP-OES	Inductively Coupled Plasma Optical Emission Spectroscopy
ILSI	International Life Science Institute
IUPAC-IUB	Union of Pure and Applied Chemistry - International Union of Biochemistry
kb	Kilobase
kDa	Kilodalton
LOD	Limit of Detection
LOQ	Limit of Quantitation
M	Methionine
MOE	Margin of Exposure
mRNA	Messenger Ribonucleic Acid
MW	Molecular Weight

NDF	Neutral Detergent Fiber
NGS	Next Generation Sequencing
NHANES/WWEIA	National Health and Nutrition Examination Survey/"What We Eat in America"
NOAEL	No Observed Adverse Effect Level
OECD	Organization for Economic Co-operation and Development
ORF	Open Reading Frame
OSL	Over-Season Leaf
PCR	Polymerase Chain Reaction
PIP	Plant-incorporated Protectant
PUFA	Polyunsaturated fatty acid
PVDF	Polyvinylidene difluoride membrane
RO	Reverse Osmosis
ROP	Repressor of Primer
RSR	Regulatory Status Review
SBL	Soybean looper
SE	Standard Error
TCA	Trichloroacetic Acid
U.S.	United States
USDA	United States Department of Agriculture
USP	United States Pharmacopoeia
UTR	Untranslated Region
µg	Microgram
VBC	Velvetbean caterpillar

PART 1 GENERAL INFORMATION

B Applicant Details

(a) Applicant's name/s	Bayer CropScience Pty Ltd
(b) Name of contact person	[redacted]
(c) Address (street and postal)	Level 4, 109 Burwood Road, Hawthorn, Victoria 3122
(d) Telephone number	[redacted]
(e) Email address	[redacted]
(f) Nature of applicant's business	Technology Provider to the Agricultural and Food Industries
(g) Details of other individuals, companies or organisations associated with the application	

C Purpose of the Application

This application is submitted to Food Standards Australia New Zealand by Bayer CropScience Proprietary Limited on behalf of Bayer Group.

The purpose of this submission is to make an application to vary **Standard 1.5.2** – *Food Produced Using Gene Technology* of the *Australia New Zealand Food Standards Code* to seek the addition of Insect-protected soybean MON 94637 and products derived from Insect-protected soybean MON 94637 (hereafter referred to as MON 94637) to Schedule 26-3 Food produced using gene technology of plant origin (see below).

Commodity	Food derived from:
Soybean	Insect-protected soybean MON 94637

D Justification for the Application

(a) The need for the proposed change

Bayer CropScience has developed insect-protected soybean MON 94637 to produce two insecticidal proteins, Cry1A.2 and Cry1B.2, which protect against feeding damage caused by targeted lepidopteran insect pests. Cry1A.2 is a chimeric protein comprised of domains I from Cry1Ah, domain II and the C-terminal domain from Cry1Ac, and domain III from Cry1Ca. Cry1B.2 is a chimeric protein comprised of domains I and II from Cry1Be, domain III from Cry1Ka2, and the C-terminal domain from Cry1Ab.

(b) The advantages of the proposed change over the status quo, taking into account any disadvantages

MON 94637 was developed to provide growers in South America an additional tool for controlling target lepidopteran soybean pests, including soybean looper and velvetbean caterpillar. MON 94637 will be combined through traditional breeding with other deregulated traits to provide protection against feeding damage caused by lepidopteran pests, as well as tolerance to multiple herbicides. The production of the Cry1A.2 and Cry1B.2 proteins in MON 94637 provides two additional *Bt* Cry insecticidal proteins for managing potential insect resistance and prolonging product durability (Chen *et al.*, 2021).

There are no plans currently to commercialize MON 94637 in the U.S., but it is intended to be cultivated in small-scale breeding, testing, and seed increase nurseries to develop seed for future products in South America.

D.1 Regulatory Impact Information

D.1.1 Costs and benefits of the application

If the proposed variation to permit the sale and use of food produced from MON 94637 is approved, possible affected parties may include consumers, industry sectors and government. The consumers who may be affected are those that consume food containing ingredients derived from soybean. Industry sectors affected may be food importers and exporters, distributors and retailers, processors and manufacturers. Lastly, government enforcement agencies may be affected.

A cost/benefit analysis quantified in monetary terms is difficult to determine. In fact, most of the impacts that need to be considered cannot be assigned a dollar value. Criteria would need to be deliberately limited to those involving broad areas such as trade, consumer information and compliance. If the proposed variation is approved:

(a) The cost and benefits to the consumers e.g. health benefits:

- There would be benefits in the broader availability of soybean products.
- There is unlikely to be any significant increase in the prices of foods if manufacturers are able to use comingled soybean products.
- Consumers wishing to do so will be able to avoid GM soybean products as a result of labeling requirements and marketing activities.

(b) The costs and benefits to industry and business in general, noting any specific effects on small businesses e.g. savings in production costs:

- Sellers of processed foods containing soybean derivatives would benefit as foods derived from soybean MON 94637 would be compliant with the Code, allowing broader market access and increased choice in raw materials. Retailers may be able to offer a broader range of soybean products or imported foods manufactured using soybean derivatives.
- Possible cost to food industry as some food ingredients derived from soybean MON 94637 would be required to be labelled.

(c) the costs and benefits to government e.g. increased regulatory costs:

- Benefit that if soybean MON 94637 was detected in food products, approval would ensure compliance of those products with the Code. This approval would ensure no potential for trade disruption on regulatory grounds.
- Approval of soybean MON 94637 would ensure no potential conflict with WTO responsibilities.
- In the case of approved GM foods, monitoring is required to ensure compliance with the labeling requirements, and in the case of GM foods that have not been approved, monitoring is required to ensure they are not illegally entering the food supply. The costs of monitoring are thus expected to be comparable, whether a GM food is approved or not.

D.1.2 Impact of International Trade

If the proposed variation to permit the sale and use of food produced from soybean MON 94637 was rejected it would result in the requirement for segregation of any soybean derived products containing soybean MON 94637 from those containing approved soybean or conventional soybean, which would be likely to increase the costs of imported soybean-derived foods.

It is important to note that if the proposed variation is approved, soybean MON 94637 will not have a mandatory introduction. The consumer will always have the right to choose not to use/consume this product.

E Information to support the application

See Part 2.

F Assessment procedure

Bayer CropScience is submitting this application in anticipation that it will fall within the General Procedure category.

G Confidential commercial information (CCI)

Any CCI information has been identified as CCI and has been treated according to the FSANZ Application Handbook 2019.

H Other confidential information

Any non CCI information that Bayer CropScience wants to be treated as confidential has been treated according to the FSANZ Application Handbook 2019.

I Exclusive capturable commercial benefit

This application is likely to result in an amendment to the Code that provides exclusive benefits and therefore Bayer CropScience intends to pay the full cost of processing the application.

J International and other national standards

J.1 International standards

Bayer CropScience makes all efforts to ensure that safety assessments are aligned, as closely as possible, with relevant international standards such as the Codex Alimentarius Commission's *Principles for the Risk Analysis of Foods Derived from Modern Biotechnology* and supporting *Guideline for the Conduct of Food Safety Assessment of Foods Derived from Recombinant-DNA Plants* (Codex Alimentarius, 2009).

In addition, the composition analysis is conducted in accordance with OECD guidelines and includes the measurement of OECD-defined soybean nutrients and anti-nutrients based on conventional commercial soybean varieties (OECD, 2012).

J.2 Other national standards or regulations

Bayer CropScience has submitted a food and feed safety and nutritional assessment summary for MON 94637 to the United States Food and Drug Administration (FDA) and has also requested a Regulatory Status Review (RSR) for a determination of plant pest risk potential of MON 94637, including all progenies derived from crosses between MON 94637 and conventional soybean, or deregulated biotechnology-derived soybean by the Animal and Plant Health Inspection Service (APHIS) of the U.S. Department of Agriculture (USDA).

Consistent with our commitments to the Excellence Through Stewardship® (ETS) Program[1], regulatory submissions have been or will be made to countries that import significant soybean or food and feed products derived from South America soybean and have functional regulatory review processes in place.

K Statutory declaration

See Part 3.

L Checklist

The checklists can be found on page x.

[1] Excellence Through Stewardship is a registered trademark of Excellence Through Stewardship, Washington, DC. (http://www.excellencethroughstewardship.org)

PART 2 SPECIFIC DATA REQUIREMENTS FOR FOODS PRODUCED USING GENE TECHNOLOGY

A. TECHNICAL INFORMATION ON THE FOOD PRODUCED USING GENE TECHNOLOGY

A.1 Nature and Identity of the Genetically Modified Food

A.1(a) A description of the GM organism from which the new GM food is derived. The description must include the nature and purpose of the genetic modification

Bayer CropScience has developed insect-protected soybean MON 94637 that produces two insecticidal proteins, Cry1A.2 and Cry1B.2 derived from *Bacillus thuringiensis* (*Bt*), to protect soybean plants against feeding damage caused by lepidopteran pests. Control of lepidopteran pests remains a high priority for South American soybean production because these pests are responsible for significant annual crop losses (Oerke, 2006; Heinrichs and Muniappan, 2018). MON 94637 will be offered in South America for control of commercial target pests *Chrysodeixis includens* (soybean looper) and *Anticarsia gemmatalis* (velvetbean caterpillar). Soybean looper is the main lepidopteran pest species that attacks soybean in Brazil, followed by velvetbean caterpillar. Both soybean looper and velvetbean caterpillar have high potential to cause injury through the defoliation of plants, consequently reducing yield (Bueno *et al.*, 2013; Horikoshi *et al.*, 2021).

A.1(b) Name, line number and OECD Unique Identifier of each of the new lines or strains of GM organism from which the food is derived

In accordance with OECD's "Guidance for the Designation of a Unique Identifier for Transgenic Plants" MON 94637 has been assigned the unique identifier MON-94637-8.

A.1(c) The name the food will be marketed under (if known)

Soybean containing the transformation event MON 94637 will be produced in South America. There are currently no plans to produce this product in Australia or New Zealand. A commercial trade name for the product has not been determined at the time of this submission and will be available prior to commercial launch of the product in South America.

A.2 History of Use of the Host and Donor Organisms

A.2(a) For the donor organism(s) from which the genetic elements are derived:

A.2(a)(i) Any known pathogenicity, toxicity or allergenicity relevance to the food

A.2(a)(i)(i) Source of the *cry1A.2* and *cry1B.2* genes introduced into MON 94637

The Cry1A.2 and Cry1B.2 proteins are derived from genetic elements that code for crystalline proteins (Cry) that are expressed as parasporal inclusions (or δ-endotoxins) in the ubiquitous gram-positive bacterium *Bacillus thuriengensis* (*Bt)* (Gill *et al.*, 1992; Schnepf *et al.*, 1998; Vachon *et al.*, 2012). *Bt* isolates have a long, documented history of safe use in agriculture and safe human consumption. Since the first *Bt* isolate was registered as a pesticide in 1961, over 180 microbial *Bt* products have been registered in the United States (U.S.), with more than 120 microbial products registered in the European Union (EU) (Hammond, 2004). *Bt* microbial biopesticides have been safely and directly applied to consumed agricultural commodities including berry crops, cabbage, grapes, tomatoes, celery, lettuce, and spinach (U.S. EPA, 1998). For certain crops, a significant percentage of the total US grown crop has been treated with *Bt* crystal/spore preparations (*e.g.*, blackberries (50%), celery (46%), and cabbage (39%)) (U.S. EPA, 1998). In Europe, residual levels of *Bt* microbes of up to 100,000 CFUs (colony forming units) were observed on fresh vegetables following application of *Bt* microbial pesticides (Frederiksen *et al.*, 2006). Thus, the use of *Bt* microbials for pest control in agriculture, including in organic farming, provides a 50-year history of safe consumption of food crops sprayed with *Bt* microbial pesticides.

Genes from Bt microbes including *Bt* subsp. *kurstaki* and *Bt* subsp. *Aizawai* have been used in several GM plants including MON 89034 (A595), MON 87751 (A1110), MON 88702 (A1154), MON 95379 (A1226) and MON 95275 (A1262). Those plants were assessed for the safety by FSANZ and approved in 2008, 2016, 2018, 2022 and 2023, respectively.

Several different *Bt* subspecies, including *Bt* subsp. *kurstaki* and *Bt* subsp. *aizawai*, have been subjected to toxicity testing and showed no evidence for adverse effects on human health (Baum *et al.*, 1999; Betz *et al.*, 2000; McClintock *et al.*, 1995; Siegel, 2001; U.S. EPA, 1986; Federici and Siegel, 2008; Hammond, 2004; Mendelsohn *et al.*, 2003; U.S. EPA, 2001). These subspecies are extensively used in formulations for commercial biopesticides and express a diverse array of Cry1 proteins (e.g., Cry1Aa, Cry1Ab, Cry1Ac, Cry1C, Cry1D and Cry1B proteins) (Betz *et al.*, 2000; EFSA, 2012). Additionally, direct toxicity assessments of *Bt* microbial biopesticide formulations containing these subspecies, such as Dipel®[2], Cutlass® OF[3], Xentari®[4] WG, Turex® 50 WG[5] and Thuricide®[6] have shown no evidence for adverse effects on human and mammalian health (VKM, 2016; Hadley *et al.*, 1987; Fisher and Rosner, 1959; U.S. EPA, 1986; U.S. EPA, 1996; McClintock *et al.*, 1995; Betz *et al.*, 2000). Taken together, the long history of safe use in agriculture and the comprehensive toxicity testing of *Bt* subspecies and *Bt*-derived biopesticides provides strong support for the conclusions that the

[2] Dipel is a registered trademark of Abbott Inc.
[3] Cutlass is a registered trademark of Certis USA
[4] Xentari is a registered trademark of Valent USA
[5] Turex is a registered trademark of Certis USA
[6] Thuricide is a registered trademark of Certis USA

Cry1A.2 and Cry1B.2 donor organism (*Bt*) presents no health hazard to humans when present in food.

A.2(a)(i)(ii) Source of other genetic materials introduced into MON 94637

The codon optimized *cry1A.2* coding sequence in MON 94637 is under the regulation of the promoter, 5' untranslated region (UTR) and intron from *Arabidopsis thaliana* of the polyubiquitin gene *UBQ10* (Norris *et al.*, 1993).

The codon optimized *cry1B.2* coding sequence in MON 94637 is under the regulation of the promoter and 5' UTR of a chlorophyll a/b-binding (CAB) protein from *Cucumis melo* (melon), which directs transcription in plant cells (Hernandez-Garcia and Finer, 2014). The *cry1B.2* coding sequence also utilizes a 3' UTR sequence from *Medicago truncatula* (barrel medic) of a lipoxygenase gene, which directs polyadenylation of the mRNA (Hunt, 1994).

Cucumis melo, *Medicago truncatula*, and *Arabidopsis thaliana* have a long history of safe use. *Cucumis melo* (melon) has been in human diet for centuries. *Medicago truncatula*, and *Arabidopsis thaliana* are popular model organism in legume biology, plant biology and genetics, whose genomes have been extensively studied.

Additionally, genes from *A. thaliana* and *M. truncatula* have been used in several GM plants including MON 87701 (A1080) and MON 94100 (A1216) Those plants were assessed for the safety by FSANZ and approved in 2014 and 2021.

A.2(a)(ii) History of use of the organism in food supply or history of human exposure to the organism through other than intended food use (e.g. as a normal contaminant)

As described in Section A.2(a)(i), *Bt* isolates have a long, documented history of safe use in agriculture and safe human consumption.

A.2(b) For the host organism into which the genes were transferred:

A.2(b)(i) Its history of safe use for food

Soybean is the most widely grown oilseed in the world, with approximately 368 million metric tons (MMT) of harvested seed produced in 2020/2021, which represented 61% of world oilseed production that year (ASA, 2022). Soybean is grown as a commercial crop in over 35 countries. The major producers of soybean are Brazil, U.S, Argentina, China, Paraguay, India and Canada, which accounted for approximately 94% of the global soybean production in 2020/2021 (ASA, 2022). Approximately 31% of the 2020/2021 world soybean production was produced in the U.S. (ASA, 2022). With 61.5 MMT exported, the U.S. was second to Brazil (81.7 MMT) in world soybean exports. Approximately 58.3 MMT of soybeans were crushed in the U.S. in 2020/2021 and used to supply the feed industry for livestock use or the food industry for edible vegetable oil and soybean protein isolates (ASA, 2022).

Soybean is the second most planted field crop in the U.S. after corn. According to data from American Soybean Association, soybean was planted on approximately 87.2 million acres in the U.S. in 2021, producing 120.7 MMT of soybean (ASA, 2022).

A.2(b)(ii) The part of the organism typically used as food

The part of the organism from soybean to be used as food is whole grain.

A.2(b)(iii) The types of products likely to include the food or food ingredient

Soybean is used in various food products, including tofu, soy sauce, soymilk, energy bars, and meat products. A major food use for soybean is purified oil, for use in margarines, shortenings, cooking, and salad oils. Soybean oil generally has a smaller contribution to soybean's overall value compared to soybean meal because the oil constitutes just 18 to 19% of the soybean's weight. Nonetheless, soybean oil accounted for approximately 29% of all the vegetable oils consumed globally in 2021, and was the second largest source of vegetable oil worldwide, slightly behind palm oil at approximately 36% share (ASA, 2022).

Soybean meal is a high-value component obtained from processing of soybean, and is used as a supplement in feed rations for livestock. Industrial edible and industrial uses of soybean range from a carbon/nitrogen source in the production of yeasts via fermentation to the manufacture of soaps, inks, paints, disinfectants, and biodiesel. Industrial uses of soybean have been summarized by the American Soybean Association (ASA, 2022).

A.2(b)(iv) Whether special processing is required to render food drived from the organism safe to eat

In general, soyfoods can be roughly classified into four major categories (Liu, 2004).

Traditional soyfoods, primarily made from whole soybean: The non-fermented traditional soyfoods include soymilk, tofu, and soybean sprouts, whereas the fermented soyfoods include soybean paste (miso), soybean sauce, natto, and tempeh.

Soybean oil: soybean oil constitutes approximately 29% of global consumption of vegetable oil, and is the second largest source of vegetable oil worldwide slightly behind palm oil at approximately 36% share (ASA, 2022).

Refined, bleached, and deodorized (RDB) soybean oil can be further processed and utilized in the manufacture of cooking oils, shortening, margarine, mayonnaise, salad dressings, and a wide variety of products that are either based entirely on fats and oils or contain fat or oil as a principal ingredient. Soybean oil is comprised primarily of five major fatty acids: saturated fatty acids; 16:0 palmitic and 18:0 stearic acids, monounsaturated; 18:1 oleic acid, and the Polyunsaturated fatty acids (PUFAs); 18:2 linoleic and 18:3 linolenic acids. These five major fatty acids have very different oxidative stabilities and chemical functionalities. Conventional soybean oil typically contains 60-65% PUFAs, mostly in the form of 18:2 linoleic acid. This composition makes soybean oil unsuitable for certain food applications since the high concentrations of PUFAs in the oil are susceptible to oxidation and degradation at high temperature resulting in off-flavors and odors. Therefore, hydrogenation of soybean oil is necessary to reduce levels of polyunsaturated fatty acids by converting them to saturated fatty acids resulting in higher stability oil suitable for a range of food uses.

Soybean protein products: soybean protein products are made from defatted soybean flakes, and include soybean flour, soybean protein concentrate, and soybean protein isolate. Soybean flour has a protein content of approximately 50% and is used mainly as an ingredient in the bakery industry. Soybean protein concentrate has a protein content of approximately 70% and is used widely in the meat industry as a key ingredient of meat alternative products such as soybean burgers and meatless "meatballs." Soybean protein isolate has a protein content of 90%, and possesses many functional properties such as gelation and emulsification. As a result,

it can be used in a wide range of food applications, including soups, sauce bases, energy bars, nutritional beverages, infant formula, and dairy replacements.

Dietary supplements: soybean is a rich source of certain phytochemicals used as dietary supplements, which include isoflavones and tocopherols. Isoflavones have been shown to inhibit the growth of cancer cells, lower cholesterol levels, and inhibit bone resorption (Messina, 1999). Tocopherols have long been recognized as a free radical scavenging antioxidant whose deficiency impairs mammalian fertility. In addition, biological activities have been reported for the desmethyl tocopherols, such as γ-tocopherol, which possess antiinflammatory, antineoplastic, and natriuretic functions (Schafer *et al.*, 2003; Hensley *et al.*, 2004). Detailed reviews of soybean fractions and soybean-derived phytochemicals have been published (Liu, 2004).

A.3 The Nature of the Genetic Modification

Characterisation of the genetic modification in MON 94637 was conducted using a combination of sequencing, PCR, and bioinformatics. The results of this characterisation demonstrate that MON 94637 contains a single copy of the intended T-DNA I containing the *cry1A.2* and *cry1B.2* expression cassettes, which is stably integrated at a single locus and is inherited according to Mendelian principles over multiple generations. These conclusions are based on the following:

- Molecular characterisation of MON 94637 by next generation sequencing (NGS) demonstrated that MON 94637 contained a single copy of T-DNA I insert. These whole-genome sequence analyses (Kovalic *et al.*, 2012) provided a comprehensive assessment of MON 94637 to determine the presence of sequences derived from PV-GMIR527237 and demonstrated that MON 94637 contained a single copy of T-DNA I insert with no detectable plasmid backbone or T-DNA II sequences.

- Directed sequencing (locus-specific PCR, DNA sequencing and analyses) performed on MON 94637 was used to determine the complete sequence of the single DNA insert from PV-GMIR527237, the adjacent flanking DNA, and the 5' and 3' insert-to-flank junctions. This analysis confirmed that the sequence and organization of the DNA insert is identical to the corresponding region in the PV-GMIR527237 T-DNA I. Furthermore, the genomic organization at the insertion site was assessed by comparing the T-DNA I insert and sequences flanking the T-DNA I insert in MON 94637 to the sequence of the insertion site in conventional soybean. This analysis identified a 14 bp deletion that likely occurred during integration of the T-DNA I sequence and determined that no major DNA rearrangement occurred at the insertion site in MON 94637 upon DNA integration.

- Generational stability analysis by NGS demonstrated that the single PV-GMIR527237 T-DNA I insert in MON 94637 has been maintained through five breeding generations, thereby confirming the stability of the T-DNA I in MON 94637.

- Segregation data confirm that the inserted T-DNA I segregated following Mendelian inheritance patterns, which corroborates the insert stability demonstrated by NGS and independently establishes the nature of the T-DNA I at a single chromosomal locus.

Taken together, the characterisation of the genetic modification in MON 94637 demonstrates that a single copy of the intended T-DNA I was stably integrated at a single locus of the soybean genome and that no T-DNA II or plasmid backbone sequences are present in MON 94637.

A.3(a) A description of the method used to transform the host organism

MON 94637 was created through an *Agrobacterium*-mediated transformation in A3555 soybean meristem explants with the PV-GMIR527237 binary plasmid vector DNA based on the methods described by Ye et al. (2008). After co-culturing with *Agrobacterium* AB30 strain carrying the plasmid vector, meristem explants were placed on selection medium containing spectinomycin to select transgenic events and carbenicillin, cefotaxime and timentin to inhibit the overgrowth of *Agrobacterium*. The putative transgenic plants (R0) with normal phenotypic characteristics were selected and screened using copy number assay and linkage analysis. Events which passed the advancement criteria (such as a single copy of the T-DNA I insert unlinked to the scorable/selectable markers (T-DNA II), absence of vector backbone, insertion not occurring in repetitive regions or gene sequences) were selected and transferred to soil for growth and further assessment.

The R0 plants generated through the transformation process described above were self-pollinated to produce R1 seed, the unlinked insertions of T-DNA I (containing the *cry1A.2* and *cry1B.2* expression cassettes) and T-DNA II (containing the selectable and scorable marker genes) were segregated. The *splA* scorable phenotype (wrinkled seed) and polymerase chain reaction (PCR) analyses were used to evaluate presence/absence of the aadA coding sequence and were used to eliminate any seeds or plants from further development that contained T-DNA II. R1 plants homozygous for T-DNA I were selected using TaqMan-based Real-time PCR assay. Homozygous R1 progenies were subjected to further development, that included additional molecular analysis, measurement of protein expression, insect protection/efficacy test, and phenotypic assessments. As is typical of a commercial event production and selection process, hundreds of different transformation events (regenerants) were generated in the laboratory using the PV-GMIR527237 vector. After careful selection and evaluation of these events in the laboratory, greenhouse and field, MON 94637 was selected as the lead event based on superior efficacy, agronomic, phenotypic, and molecular characteristics. Studies on MON 94637 were initiated to further characterise the genetic insertion and the expressed products, and to establish the food safety and unaltered environmental risk compared to commercial soybean. The major development steps of MON 94637 are depicted in Figure 1.

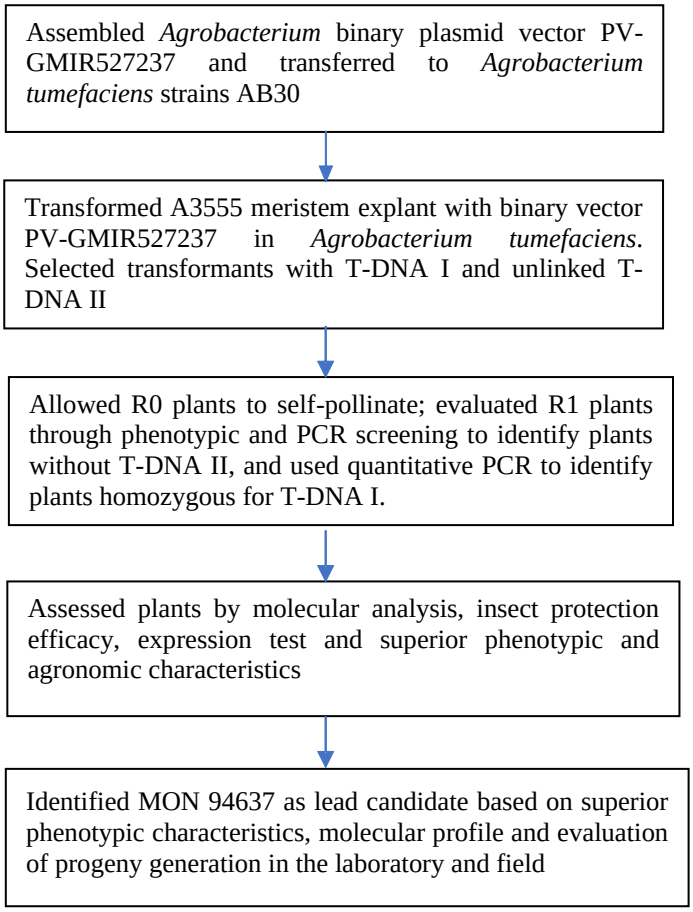

Figure 1. Schematic of the Development of MON 94637

A.3(b) A description of the construct and the transformation vectors used, including:

A.3(b)(i) The size, source and function of all the genetic components including marker genes, regulatory and other elements

Plasmid vector PV-GMIR527237 was used for the transformation of conventional soybean to produce MON 94637 and its plasmid map is shown in A.3(b)(ii). A description of the genetic elements and their prefixes (e.g. B, P, TS, CS, T, I, OR, and E) in PV-GMIR527237 is provided in Table 1. PV-GMIR527237 is approximately 26.6 kb and contains two separate T-DNAs, each delineated by Left and Right Border regions, and the vector backbone sequences. The first T-DNA, designated as T-DNA I, contains the *cry1A.2* and *cry1B.2* expression cassettes. The second T-DNA, designated as T-DNA II, contains the *splA* and *aadA* expression cassettes. When *splA* is expressed during embryo development, it interferes with sucrose metabolism, leading to a recognizable wrinkled seed phenotype to provide a visual demonstration that T-DNA II is present (Piper *et al.*, 1999). The expression of *aadA* provides antibiotic resistance and a second method for selecting transformants carrying T-DNA II. During transformation, both T-DNAs were inserted into the soybean genome (Section A.3(a)). Subsequently, segregation, selection and screening were used to isolate those plants that contained the *cry1A.2* and *cry1B.2* expression cassettes (T-DNA I) and did not contain T-DNA II containing the selectable marker genes *splA* and *aadA* or the backbone sequences from the transformation vector.

The *cry1A.2* coding sequence in MON 94637 is under the regulation of the *ubq10-At1* promoter, leader and intron from *Arabidopsis thaliana* of the polyubiquitin gene *ubq10* (Norris *et al.*, 1993), which directs transcription in plant cells. Additionally, the *cry1A.2* coding sequence utilizes the *Zfp-Mt1* 3' UTR sequence from *Medicago truncatula* (barrel medic) of a gene encoding a putative zinc finger protein, which directs polyadenylation of the mRNA (Hunt, 1994).

The *cry1B.2* coding sequence in MON 94637 is under the regulation of the *Cab-Cm1* Promoter and leader of a chlorophyll a/b-binding (CAB) protein from *Cucumis melo* (melon), which directs transcription in plant cells (Hernandez-Garcia and Finer, 2014). Additionally, the *cry1B.2* coding sequence utilizes the *Lox-Mt1* 3' UTR sequence from *Medicago truncatula* (barrel medic) of a lipoxygenase gene, which directs polyadenylation of the mRNA (Hunt, 1994).

The *splA* expression cassette is regulated by *Usp* promoter from *Vicia faba* (broad bean) encoding an unknown seed protein gene that is involved in regulating gene expression (Bäumlein *et al.*, 1991), and *nos* 3' UTR sequence of the *nopaline synthase* (*nos*) gene from *Agrobacterium tumefaciens* pTi encoding NOS that directs polyadenylation (Bevan *et al.*, 1983; Fraley *et al.*, 1983). The *aadA* expression cassette is regulated by *FMV* enhancer from the 35S RNA of figwort mosaic virus (FMV) (Richins *et al.*, 1987) that enhances transcription in most plant cells (Rogers, 2000), promoter, leader, and intron sequences of the *EF–1α* gene from *Arabidopsis thaliana* encoding elongation factor EF–1α (Axelos *et al.*, 1989) that directs transcription in plant cells, the *CTP2* Targeting sequence of the *ShkG* gene from *Arabidopsis thaliana* encoding the EPSPS transit peptide region that directs transport of the protein to the chloroplast (Herrmann, 1995; Klee *et al.*, 1987), and the *E9* 3' UTR sequence from *Pisum sativum* (pea) *rbcS* gene family encoding the small subunit of ribulose bisphosphate carboxylase protein (Coruzzi *et al.*, 1984) that directs polyadenylation of the mRNA.

Additionally, the backbone region of PV-GMIR527237 contains two origins of replication for maintenance of the plasmid vector in bacteria (*ori-pRi*, *ori-pBR322*), a bacterial selectable marker gene (*nptII*) controlled by a promoter of the ribosomal RNA operon from *Agrobacterium tumefaciens* that drives transcription in plant cells, a non-functional portion of the bacterial selectable marker gene *ble1*, and a coding sequence for repressor of primer (ROP) protein for the maintenance of the plasmid vector copy number in *Escherichia coli* (*E. coli*).

Table 1. Summary of Genetic Elements in PV-GMIR527237

Genetic Element	Location in Plasmid Vector	Function (Reference)
T-DNA I		
B[1]-Right Border Region	1-285	DNA region from *Agrobacterium tumefaciens* containing the right border sequence used for transfer of the T–DNA (Depicker *et al.*, 1982; Zambryski *et al.*, 1982)
Intervening Sequence	286-398	Sequence used in DNA cloning
P[2]-*ubq10-At1*	399-1600	Promoter, leader and intron from *Arabidopsis thaliana* of the polyubiquitin gene *UBQ10* (Norris *et al.*, 1993), which directs transcription in plant cells
Intervening Sequence	1601-1609	Sequence used in DNA cloning
CS[3]-*Cry1A.2*	1610-5179	Codon optimized gene fusion comprised of sequences encoding Cry1Ah, Cry1Ac and Cry1Ca domains from *Bacillus thuringiensis* (*Bt*), which confers protection against lepidopteran insects (Chen *et al.*, 2021)
Intervening Sequence	5180-5187	Sequence used in DNA cloning
T[4]-*Zfp-Mt1*	5188-5787	3' UTR sequence from *Medicago truncatula* (barrel medic) of a gene encoding a putative zinc finger protein, which directs polyadenylation of the mRNA (Hunt, 1994)
Intervening Sequence	5788-5889	Sequence used in DNA cloning
P-*Cab-Cm1*	5890-7890	Promoter and leader of a chlorophyll a/b-binding (CAB) protein from *Cucumis melo* (melon), which directs transcription in plant cells (Hernandez-Garcia and Finer, 2014)
Intervening Sequence	7891-7893	Sequence used in DNA cloning
CS-C*ry1B.2*	7894-11457	Codon optimized gene fusion comprised of sequences encoding Cry1Be, Cry1Ka2 and Cry1Ab domains from *Bacillus thuringiensis* (*Bt*), which confers protection against lepidopteran insects (Chen *et al.*, 2021)
T-*Lox-Mt1*	11458-11957	3' UTR sequence from *Medicago truncatula* (barrel medic) of a lipoxygenase gene, which directs polyadenylation of the mRNA (Hunt, 1994)
Intervening Sequence	11958-12187	Sequence used in DNA cloning
B-Left Border Region	12188-12629	DNA region from *Agrobacterium tumefaciens* containing the left border sequence used for transfer of the T–DNA (Barker *et al.*, 1983)
Vector Backbone		
Intervening Sequence	12630-12666	Sequence used in DNA cloning
CS-*ble1*	12667-12818	Partial coding sequence of the bleomycin resistance gene from transposon Tn*5* that confers antibiotic resistance (Mazodier *et al.*, 1985)
Intervening Sequence	12819-12838	Sequence used in DNA cloning
CS-*nptII*	12839-13633	Coding sequence of the *neo* gene from transposon Tn*5* of *E. coli* encoding neomycin phosphotransferase II (NPT II) (Beck *et al.*, 1982) that confers neomycin and kanamycin resistance (Fraley *et al.*, 1983)

Table 1. Summary of Genetic Elements in PV-GMIR527237 (Continued)

Genetic Element	Location in Plasmid Vector	Function (Reference)
P-*rrn*	13634-13858	Promoter of the ribosomal RNA operon from *Agrobacterium tumefaciens* (Bautista-Zapanta *et al.*, 2002)
Intervening Sequence	13859-13934	Sequence used in DNA cloning
OR[5]-*ori-pBR322*	13935-14523	Origin of replication from plasmid pBR322 for maintenance of plasmid in *E. coli* (Sutcliffe, 1979)
Intervening sequence	14524-14950	Sequence used in DNA cloning
CS-*rop*	14951-15142	Coding sequence for repressor of primer protein from the ColE1 plasmid for maintenance of plasmid copy number in *E. coli* (Giza and Huang, 1989)
Intervening sequence	15143-15330	Sequence used in DNA cloning
OR-*ori-pRi*	15331-19444	Origin of replication from plasmid pRi for maintenance of plasmid in *Agrobacterium* (Ye *et al.*, 2011)
Intervening Sequence	19445-19451	Sequence used in DNA cloning
T-DNA II		
B-Left Border Region	19452-19770	DNA region from *Agrobacterium tumefaciens* containing the left border sequence used for transfer of the T-DNA (Barker *et al.*, 1983)
Intervening Sequence	19771-19802	Sequence used in DNA cloning
T-*nos*	19803-20055	3' UTR sequence of the *nopaline synthase* (*nos*) gene from *Agrobacterium tumefaciens* pTi encoding NOS that directs polyadenylation (Bevan *et al.*, 1983; Fraley *et al.*, 1983)
Intervening Sequence	20056-20071	Sequence used in DNA cloning
CS-*splA*	20072-21529	Coding sequence of the *splA* gene from *Agrobacterium tumefaciens* strain C58 encoding the sucrose phosphorylase protein that catalyzes the conversion of sucrose to fructose and glucose–1–phosphate (Piper *et al.*, 1999)
Intervening Sequence	21530-21541	Sequence used in DNA cloning
P-*Usp*	21542-22720	5' UTR leader, promoter, and enhancer sequence of a gene from *Vicia faba* (broad bean) encoding an unknown seed protein gene that is involved in regulating gene expression (Bäumlein *et al.*, 1991)
Intervening Sequence	22721-22771	Sequence used in DNA cloning
T-*E9*	22772-23414	3' UTR sequence from *Pisum sativum* (pea) *rbcS* gene family encoding the small subunit of ribulose bisphosphate carboxylase protein (Coruzzi *et al.*, 1984) that directs polyadenylation of the mRNA
Intervening Sequence	23415-23429	Sequence used in DNA cloning
aadA	23430-24221	Coding sequence for an aminoglycoside-modifying enzyme, 3"(9)-*O*-nucleotidyltransferase from the transposon Tn*7* (Fling *et al.*, 1985) that confers spectinomycin and streptomycin resistance
TS[6]-*CTP2*	24222-24449	Targeting sequence of the *ShkG* gene from *Arabidopsis thaliana* encoding the EPSPS transit peptide region that directs transport of the protein to the chloroplast (Herrmann, 1995; Klee *et al.*, 1987)

Table 1. Summary of Genetic Elements in PV-GMIR527237 (Continued)

Genetic Element	Location in Plasmid Vector	Function (Reference)
Intervening Sequence	24450-24458	Sequence used in DNA cloning
P-*EF-1*α	24459-25606	Promoter, leader, and intron sequences of the *EF–1*α gene from *Arabidopsis thaliana* encoding elongation factor EF–1α (Axelos *et al.*, 1989) that directs transcription in plant cells
Intervening Sequence	25607-25629	Sequence used in DNA cloning
E[7]-*FMV*	25630-26166	Enhancer from the 35S RNA of figwort mosaic virus (FMV) (Richins *et al.*, 1987) that enhances transcription in most plant cells (Rogers, 2000)
Intervening Sequence	26167-26212	Sequence used in DNA cloning
B-Right Border Region	26213-26543	DNA region from *Agrobacterium tumefaciens* containing the right border sequence used for transfer of the T-DNA (Depicker *et al.*, 1982; Zambryski *et al.*, 1982)
Vector Backbone		
Intervening Sequence	26544-26558	Sequence used in DNA cloning

[1] B, Border
[2] P, Promoter
[3] CS, Coding Sequence
[4] T, Transcription Termination Sequence
[5] OR, Origin of Replication
[6] TS, Targeting Sequence
[7] E, Enhancer

A.3(b)(i)(i) The *cry1A.2* coding sequence and Cry1A.2 protein

The *cry1A.2* expression cassette in MON 94637 encodes a 135 kDa Cry1A.2 protein consisting of a single polypeptide of 1189 amino acids (Figure 2). The *cry1A.2* coding sequence is the coding sequence of domain I from Cry1Ah, domain II and the C-terminal domain from Cry1Ac, and domain III from Cry1Ca from various subspecies of the soil bacterium *B. thuringiensis*. The production of the Cry1A.2 protein in soybean provides protection against lepidopteran pests.

```
1    MEIVNNQNQC VPYNCLNNPE IEILEGGRIS VGNTPIDISL SLTQFLLSEF
51   VPGAGFVLGL IDLIWGFVGP SQWDAFLAQV EQLINQRIAE AVRNTAIQEL
101  EGMARVYRTY ATAFAEWEKA PDDPELREAL RTQFTATETY ISGRISVLKI
151  QTFEVQLLSV FAQAANLHLS LLRDVVFFGQ RWGFSTTTVN NYYNDLTEGI
201  STYTDYAVRW YNTGLERVWG PDSRDWVRYN QFRRELTLTV LDIVALFPNY
251  DSRRYPIRTV SQLTREIYTN PVLENFDGSF RGSAQGIERS IRSPHLMDIL
301  NSITIYTDAH RGYYYWSGHQ IMASPVGFSG PEFTFPLYGT MGNAAPQQRI
351  VAQLGQGVYR TLSSTLYRRP FNIGINNQQL SVLDGTEFAY GTSSNLPSAV
401  YRKSGTVDSL DEIPPQNNNV PPRQGFSHRL SHVSMFRSGF SNSSVSIIRA
451  PMFSWIHRSA EFNNIIASDS INQIPLVKGF RVWGGTSVIT GPGFTGGDIL
501  RRNTFGDFVS LQVNINSPIT QRYRLRFRYA SSRDARVIVL TGAASTGVGG
551  QVSVNMPLQK TMEIGENLTS RTFRYTDFSN PFSFRANPDI IGISEQPLFG
601  AGSISSGELY IDKIEIILAD ATFEAESDLE RAQKAVNALF TSTNQLGLKT
651  NVTDYHIDQV SNLVTYLSDE FCLDEKRELS EKVKHAKRLS DERNLLQDSN
701  FKDINRQPER GWGGSTGITI QGGDDVFKEN YVTLSGTFDE CYPTYLYQKI
751  DESKLKAFTR YQLRGYIEDS QDLEIYLIRY NAKHETVNVP GTGSLWPLSA
801  QSPIGKCGEP NRCAPHLEWN PDLDCSCRDG EKCAHHSHHF SLDIDVGCTD
851  LNEDLGVWVI FKIKTQDGHA RLGNLEFLEE KPLVGEALAR VKRAEKKWRD
901  KREKLEWETN IVYKEAKESV DALFVNSQYD QLQADTNIAM IHAADKRVHS
951  IREAYLPELS VIPGVNAAIF EELEGRIFTA FSLYDARNVI KNGDFNNGLS
1001 CWNVKGHVDV EEQNNQRSVL VVPEWEAEVS QEVRVCPGRG YILRVTAYKE
1051 GYGEGCVTIH EIENNTDELK FSNCVEEEIY PNNTVTCNDY TVNQEEYGGA
1101 YTSRNRGYNE APSVPADYAS VYEEKSYTDG RRENPCEFNR GYRDYTPLPV
1151 GYVTKELEYF PETDKVWIEI GETEGTFIVD SVELLLMEE
```

Figure 2. Deduced Amino Acid Sequence of the Cry1A.2 Protein

The amino acid sequence of the MON 94637 Cry1A.2 protein was deduced from the full-length coding nucleotide sequence present in PV-GMIR527237 (See Table 1 for more details).

A.3(b)(i)(ii) The *cry1B.2* coding sequence and Cry1B.2 protein

The *cry1B.2* expression cassette in MON 94637 encodes a 135 kDa Cry1B.2 protein consisting of a single polypeptide of 1187 amino acids (Figure 3). The *cry1B.2* coding sequence is the coding sequence of domains I and II from Cry1Be, domain III from Cry1Ka2, and the C-terminal domain from Cry1Ab from various subspecies of soil bacterium *B. thuringiensis*. The production of Cry1B.2 protein in soybean provides protection against lepidopteran pests.

```
1    MTSNRKNENE IINALSIPAV SNHSAQMNLS TDARIEDSLC IAEGNNIDPF
51   VSASTVQTGI NIAGRILGVL GVPFAGQIAS FYSFLVGELW PRGRDPWEIF
101  LEHVEQLIRQ QVTENTRDTA LARLQGLGNS FRAYQQSLED WLENRDDART
151  RSVLYTQYIA LELDFLNAMP LFAIRNQEVP LLMVYAQAAN LHLLLLRDAS
201  LFGSEFGLTS QEIQRYYERQ VEKTREYSDY CARWYNTGLN NLRGTNAESW
251  LRYNQFRRDL TLGVLDLVAL FPSYDTRVYP MNTSAQLTRE IYTDPIGRTN
301  APSGFASTNW FNNNAPSFSA IEAAVIRPPH LLDFPEQLTI FSVLSRWSNT
351  QYMNYWVGHR LESRTIRGSL STSTHGNTNT SINPVTLQFT SRDVYRTESF
401  AGINILLTTP VNGVPWARFN WRNPLNSLRG SLLYTIGYTG VGTQLFDSET
451  ELPPETTERP NYESYSHRLS NIRLISGNTL RAPVYSWTHR SADRTNTISS
501  DSITQIPLVK AHTLQSGTTV VKGPGFTGGD ILRRTSGGPF AFSNVNLDFN
551  LSQRYRARIR YASTTNLRIY VTVAGERIFA GQFDKTMDAG APLTFQSFSY
601  ATINTAFTFP ERSSSLTVGA DTFSSGNEVY VDRFELIPVT ATFEAESDLE
651  RAQKAVNELF TSSNQIGLKT DVTDYHIDQV SNLVECLSDE FCLDEKKELS
701  EKVKHAKRLS DERNLLQDPN FRGINRQLDR GWRGSTDITI QGGDDVFKEN
751  YVTLLGTFDE CYPTYLYQKI DESKLKAYTR YQLRGYIEDS QDLEIYLIRY
801  NAKHETVNVP GTGSLWPLSA PSPIGKCAHH SHHFSLDIDV GCTDLNEDLG
851  VWVIFKIKTQ DGHARLGNLE FLEEKPLVGE ALARVKRAEK KWRDKREKLE
901  WETNIVYKEA KESVDALFVN SQYDRLQADT NIAMIHAADK RVHSIREAYL
951  PELSVIPGVN AAIFEELEGR IFTAFSLYDA RNVIKNGDFN NGLSCWNVKG
1001 HVDVEEQNNH RSVLVVPEWE AEVSQEVRVC PGRGYILRVT AYKEGYGEGC
1051 VTIHEIENNT DELKFSNCVE EEVYPNNTVT CNDYTATQEE YEGTYTSRNR
1101 GYDGAYESNS SVPADYASAY EEKAYTDGRR DNPCESNRGY GDYTPLPAGY
1151 VTKELEYFPE TDKVWIEIGE TEGTFIVDSV ELLLMEE
```

Figure 3. Deduced Amino Acid Sequence of the Cry1B.2 Protein

The amino acid sequence of the MON 94637 Cry1B.2 protein was deduced from the full-length coding nucleotide sequence present in PV-GMIR527237 (See Table 1 for more details).

A.3(b)(i)(iii) Regulatory Sequences

The transformation plasmid PV-GMIR527237 contains the *cry1A.2* and *cry1B.2* expression cassettes in T-DNA I, and also the expression cassettes for the *splA* and *aadA* selectable markers in T-DNA II, each with their own regulatory sequences. The regulatory sequences associated with each cassette are described in A.3(b) and Table 1.

A.3(b)(i)(iv) T-DNA Border Regions

PV-GMIR527237 contains Left and Right Border regions (Figure 4 and Table 1) that were derived from *A. tumefaciens* plasmids. The border regions each contain a nick site that is the site of DNA exchange during transformation (Barker *et al.*, 1983; Depicker *et al.*, 1982; Zambryski *et al.*, 1982). The border regions separate each T-DNA from the plasmid backbone region and are involved in the efficient transfer of T-DNA into the soybean genome.

A.3(b)(i)(v) Genetic Elements Outside the T-DNA Border Regions

Genetic elements that exist outside of the T-DNA border regions are those that are essential for the maintenance or selection of PV-GMIR527237 in bacteria and are referred to as plasmid backbone. The gene *ble1* is the partial coding sequence of the bleomycin resistance gene from transposon Tn5, which confers antibiotic resistance (Mazodier *et al.*, 1985) but is non-functional and was not used in the development of MON 94637. The selectable marker gene *nptII* is the coding sequence of the *neo* gene from transposon Tn5 of *E. coli* encoding neomycin phosphotransferase II (NPT II) (Beck *et al.*, 1982), which confers neomycin and kanamycin resistance in *E. coli* and *Agrobacterium* during molecular cloning (Fraley *et al.*, 1983). Expression of the *nptII* gene is under control of the *rrn* promoter which is the promoter of the ribosomal RNA operon from *Agrobacterium tumefaciens* (Bautista-Zapanta *et al.*, 2002). The origin of replication, *ori-pBR322*, is required for the maintenance of the plasmid in *E. coli* and is derived from the plasmid vector pBR322. Coding sequence *rop* encodes the repressor of primer protein from the ColE1 plasmid for maintenance of plasmid copy number in *E. coli* (Giza and Huang, 1989). The origin of replication, *ori-pRi*, is required for the maintenance of the plasmid in *Agrobacterium* (Ye *et al.*, 2011). Because these elements are outside the border regions, they are not expected to be transferred into the soybean genome. The absence of the plasmid backbone and other unintended plasmid sequence in MON 94637 was confirmed by sequencing and bioinformatic analyses (See Section A.3(c)).

A.3(b)(ii) A detailed map of the location and orientation of all the genetic components contained within the construct and vector, including the location of relevant restriction sites

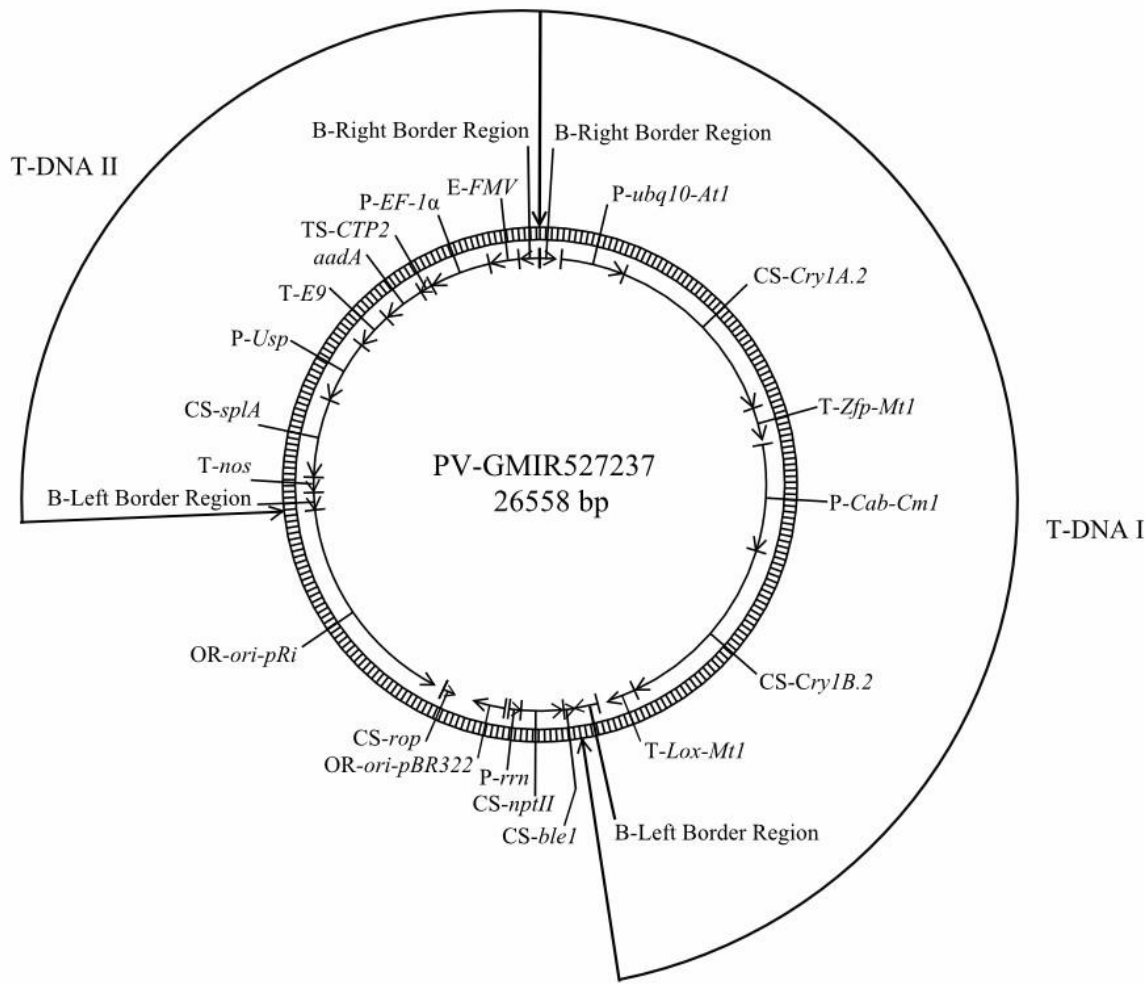

Figure 4. Circular Map of PV-GMIR527237

A circular map of PV-GMIR527237 used to develop MON 94637 is shown. PV-GMIR527237 contains two T–DNAs. Genetic elements are shown on the exterior of the map.

A.3(c) A full molecular characterisation of the genetic modification in the new organism, including:

This section describes the methods and results of a comprehensive molecular characterisation of the genetic modification present in MON 94637. It provides information on the DNA insertion(s) into the plant genome of MON 94637, and additional information regarding the arrangement and stability of the introduced genetic material. The information provided in this section addresses the relevant factors in the Codex Plant Guideline, Section 4, paragraphs 30, 31, 32, and 33 (Codex Alimentarius, 2009).

A.3(c)(i) Identification of all transferred genetic material and whether it has undergone any rearrangements

A schematic representation of the next generation sequencing (NGS) methodology and the basis of the characterisation using NGS and PCR sequencing are illustrated in Figure 5 below. Appendix **1** defines the test, control and reference substances, and provides an additional overview of these techniques, their use in DNA characterisation in soybean plants and the materials and methods.

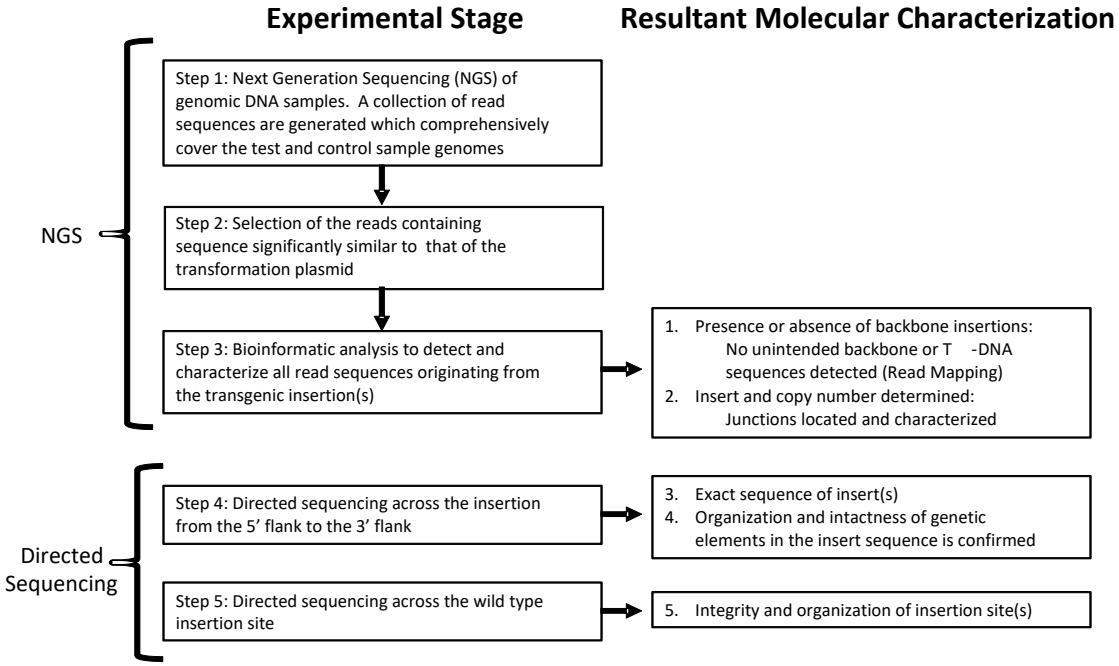

Figure 5. Molecular Characterisation Using Sequencing and Bioinformatics

Genomic DNA from MON 94637 and the conventional control were sequenced using technology that produces a set of short, randomly distributed sequence reads that comprehensively cover MON 94637 and control genomes (Step 1). Utilizing these genomic sequence reads, bioinformatics searches are conducted to identify all sequence reads that are significantly similar to the transformation plasmid (Step 2). These captured reads are then mapped and analyzed to determine the presence/absence of transformation plasmid backbone or T-DNA II sequences, identify insert junctions, and to determine the insert and copy number (Step 3). Overlapping PCR products are also produced which span any identified insert and their corresponding wild type locus (Step 4 and Step 5 respectively); these overlapping PCR products are sequenced to allow for detailed characterisation of the inserted DNA and insertion site.

The whole genome sequencing and bioinformatic strategy used to determine the number of insertion loci and the number of copies of the integrated DNA was designed to ensure that all inserted segments were identified. Genomic DNA from MON 94637 and the conventional controls were used to generate short (~150 bp), randomly distributed sequence fragments (sequencing reads) in sufficient numbers to yield comprehensive coverage of the soybean genomes. The depth of coverage (the mean number of times each base of the genome is independently sequenced) was ≥75× for each generation that was evaluated. It has previously been reported that 75× genome coverage is adequate to provide comprehensive coverage and detection of all inserted DNA (Kovalic *et al.*, 2012). In a comprehensive analysis of NGS, as a characterisation method, it has been shown that at levels of coverage as low as 11× it is possible to detect both intended transgenes as well as unintended inserted fragments as small as 25 bp in length (Cade *et al.*, 2018). This makes 75× coverage a robust level of sequencing for the accurate characterisation of both homozygous and hemizygous inserts, and is well in excess of the levels which have been demonstrated as capable of identifying unintended inserted fragments. The level of sensitivity of this method was demonstrated by detection of a positive control plasmid DNA sampled at 1 and $1/10^{th}$ copy-per-genome equivalent. This confirms the method's ability to detect any sequences derived from the transformation plasmid. Bioinformatics analysis was then used to select sequencing reads that contained sequences similar to the transformation plasmid, and these were analysed in depth to determine the number of DNA inserts. NGS was run on five breeding generations of MON 94637 and the appropriate conventional controls. Results of NGS are shown in Sections A.3(c)(ii) and A.3(c)(iii).

The DNA inserts of MON 94637 were characterised by mapping of sequencing reads to the transformation plasmid and identifying junctions and unpaired read mappings adjacent to the junctions. Examples of five types of NGS reads are shown in Figure 6. The junctions of the DNA insert and the flanking DNA are unique for each insertion (Kovalic *et al.*, 2012). Therefore, insertion sites can be recognized by analyzing for sequence reads containing such junctions.

Directed sequencing (locus-specific PCR and DNA sequencing analyses, Figure 5, step 4) complements the NGS characterisation. Sequencing of the insert and flanking DNA determines the complete sequence of the insert and flanks by evaluating if the sequence of the insert is identical to the corresponding sequence in the plasmid vector, and if each genetic element in the insert is intact. Furthermore, the genomic organization at the insertion site was assessed by comparing the insert and flanking sequence to the sequence of the insertion site in conventional soybean. Results are described in Sections A.3(c)(ii); methods are presented in Appendix **1**.

The stability of the T-DNA present in MON 94637 across multiple breeding generations was evaluated by NGS and subsequent read mapping. Sequence reads of genomic DNA from a total of five breeding generations of MON 94637 were mapped to the transformation plasmid and the number of junction signatures and sequences were determined for each as described above. This information was used to determine the number and identity of the DNA inserts. As described earlier, for a single copy T-DNA insert, two junction signatures are expected. In the case of an event where a single locus is stably inherited over multiple breeding generations, two identical junction signatures would be detected in all the breeding generations tested. Results are described in Section A.3(e)(i); methods are presented in Appendix **1**.

Segregation analysis of T-DNA I was conducted to determine the inheritance and generational stability of the insert in MON 94637. Segregation analysis corroborates the insert stability demonstrated by NGS and independently establishes the genetic behavior of the T-DNA. Results are described in Section A.3(e)(ii).

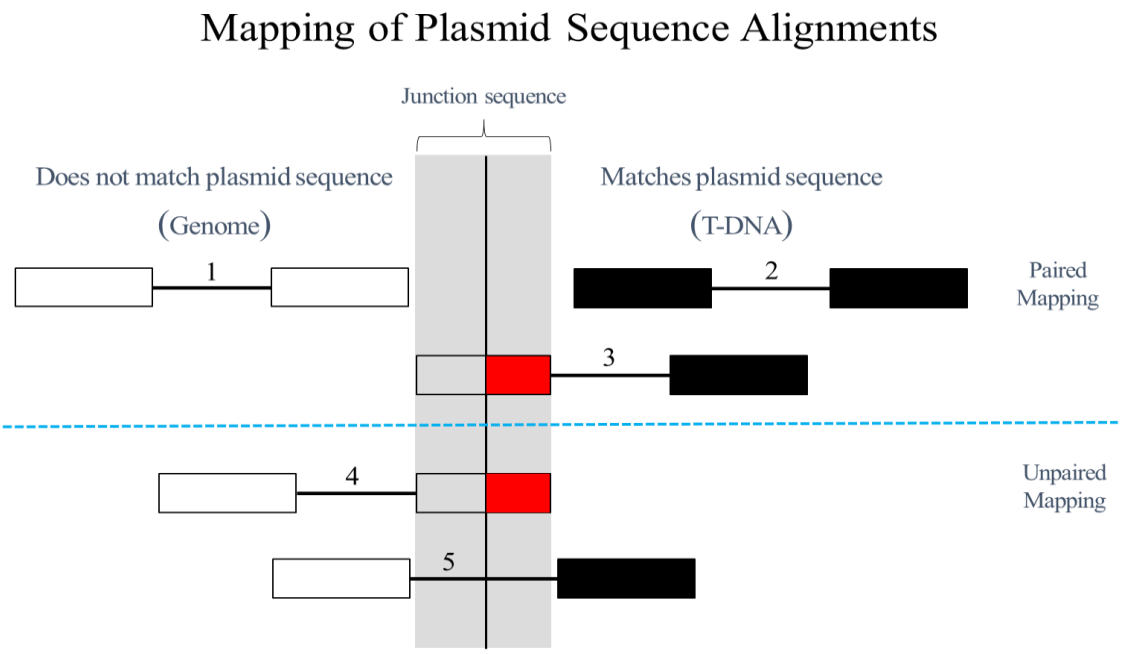

Figure 6. Five Types of NGS Reads

NGS yields data in the form of read pairs where sequence from each end of a size selected DNA fragment is returned. Depicted above are five types of sequencing reads/read pairs generated by NGS sequencing which can be found spanning or outside of junction points. Sequence boxes are color-filled if they matchwith plasmid sequence, and empty if they match with genomic sequence. Grey highlighting indicates sequence reads spanning the junction. Junctions are detected by examining the NGS data for reads having portions of plasmid sequences that span less than the full read, as well as reads mapping adjacent to the junction points where their mate pair does not map to the plasmid sequence. The five types of sequencing reads/read pairs being (1) Paired and unpaired reads mapping to genomic sequence outside of the insert, greater than 99.999% of collected reads fall into this category and are not evaluated in this analysis, (2) Paired reads mapping entirely to the transformation plasmid sequence, such reads reveal the presence of transformation sequence *in planta*, (3) Paired reads where one read maps entirely within the inserted DNA and the other read maps partially to the insert (indicating a junction point), (4) Single read mapping partially to the transformation plasmid DNA sequence (indicating a junction point) where its mate maps entirely to the genomic flanking sequence, and (5) Single read mapping entirely to the transformation plasmid DNA sequence where its mate maps entirely to genomic flanking sequence, such reads are part of the junction signature.

A.3(c)(ii) A determination of number of insertion sites, and the number of copies at each insertion site

The number of inserted DNA sequences from PV-GMIR527237 in MON 94637 was assessed by generating a comprehensive collection of reads via NGS of MON 94637 genomic DNA using the R3 generation (Figure 7). A plasmid map of PV-GMIR527237 is shown in Figure 4 and shows elements present in MON 94637 (Table 2). A schematic representation of the insert and flanking sequences in MON 94637 is shown in Figure 8. For full details on materials and methods see Appendix **1**.

Table 2. Summary of Genetic Elements in MON 94637

Genetic Element	Location in Sequence	Function (Reference)
Flanking DNA	1-1000	DNA sequence flanking the 5′ end of the insert
B[1]-Right Border Region[r1]	1001-1068	DNA region from *Agrobacterium tumefaciens* containing the right border sequence used for transfer of the T–DNA (Depicker *et al.*, 1982; Zambryski *et al.*, 1982)
Intervening Sequence	1069-1181	Sequence used in DNA cloning
P[2]-ubq10-At1	1182-2383	Promoter, leader and intron from *Arabidopsis thaliana* of the polyubiquitin gene *UBQ10* (Norris *et al.*, 1993), which directs transcription in plant cells
Intervening Sequence	2384-2392	Sequence used in DNA cloning
CS[3]-Cry1A.2	2393-5962	Codon optimized gene fusion comprised of sequences encoding Cry1Ah, Cry1Ac and Cry1Ca domains from *Bacillus thuringiensis* (*Bt*), which confers protection against lepidopteran insects (Chen *et al.*, 2021)
Intervening Sequence	5963-5970	Sequence used in DNA cloning
T[4]-Zfp-Mt1	5971-6570	3' UTR sequence from *Medicago truncatula* (barrel medic) of a gene encoding a putative zinc finger protein, which directs polyadenylation of the mRNA (Hunt, 1994)
Intervening Sequence	6571-6672	Sequence used in DNA cloning
P-Cab-Cm1	6673-8673	Promoter and leader of a chlorophyll a/b-binding (CAB) protein from *Cucumis melo* (melon), which directs transcription in plant cells (Hernandez-Garcia and Finer, 2014)
Intervening Sequence	8674-8676	Sequence used in DNA cloning
CS-Cry1B.2	8677-12240	Codon optimized gene fusion comprised of sequences encoding Cry1Be, Cry1Ka2 and Cry1Ab domains from *Bacillus thuringiensis* (*Bt*), which confers protection against lepidopteran insects (Chen *et al.*, 2021)
T-Lox-Mt1	12241-12740	3' UTR sequence from *Medicago truncatula* (barrel medic) of a lipoxygenase gene, which directs polyadenylation of the mRNA (Hunt, 1994)

Table 2. Summary of Genetic Elements in MON 94637 (Continued)

Genetic Element	Location in Sequence	Function (Reference)
Intervening Sequence	12741-12970	Sequence used in DNA cloning
B-Left Border Region[r1]	12971-13240	DNA region from *Agrobacterium tumefaciens* containing the left border sequence used for transfer of the T–DNA (Barker *et al.*, 1983)
Flanking DNA	13241-14240	DNA sequence flanking the 3′ end of the insert

[1] **B**, Border
[2] **P**, Promoter
[3] **CS**, Coding Sequence
[4] **T**, Transcription Termination Sequence
[r1] Superscript in the Left and Right Border Regions indicates that the sequence in MON 94637 was truncated compared to the sequences in PV-GMIR52723

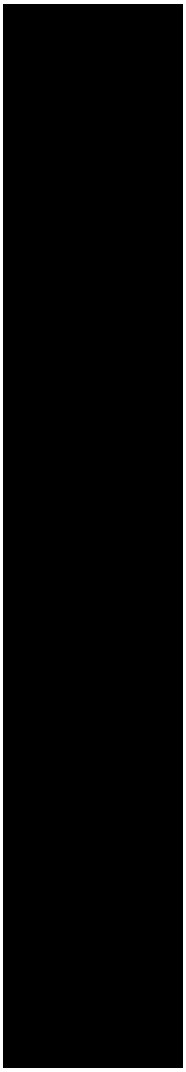

Figure 7. Breeding History of MON 94637

The generations used for molecular characterisation and insert stability analyses are indicated in bold text. R0 corresponds to the transformed plant, U designates self-pollination.
[1] Generation used for molecular characterisation
[2] Generations used to confirm insert stability
[3] Generation used for commercial development of MON 94637

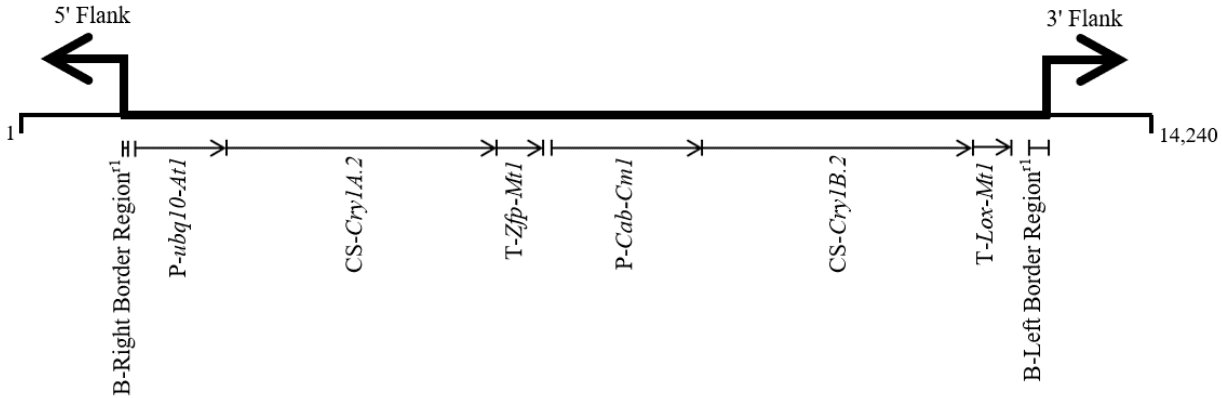

Figure 8. Schematic Representation of the Insert and Flanking Sequences in MON 94637

DNA derived from T-DNA of PV-GMIR527237 integrated in MON 94637. Right-angled arrows indicate the ends of the integrated T-DNA and the beginning of the flanking sequence. Identified on the map are genetic elements within the insert. This schematic diagram may not be drawn to scale.

[r1] Superscript in the Left and Right Border Regions indicates that the sequence in MON 94637 was truncated compared to the sequences in PV-GMIR527237.

A.3(c)(ii)(i) Next generation sequencing for MON 94637 soybean and conventional control genomic DNA

Detailed information on NGS method and interpretation of data is described in Appendix **1**. Please refer to Appendix 1 for details.

Genomic DNA from five breeding generations of MON 94637 (Figure 7) and conventional controls were isolated from seed and prepared for sequencing. For material and method details see Appendix 1. These genomic DNA libraries were used to generate short (~150 bp) randomly distributed sequencing reads of the soybean genomes (Figure 5, Step 1).

To demonstrate sufficient sequence coverage the 150 bp sequence reads were analyzed by mapping all reads to a known single-copy endogenous gene (*Glycine max* lectin (*Le1*), GenBank accession version: K00821.1). The analysis showed that the depth of coverage (*i.e.*, the mean number of times any base of the genome is expected to be independently sequenced) was 75× or greater for the five generations of MON 94637 (R3, R4, R5, R6, and R7) and the conventional control . It has previously been demonstrated that 75× coverage of the soybean genome is adequate to provide comprehensive coverage and ensure detection of inserted DNA (Kovalic *et al.*, 2012).

To demonstrate the method's ability to detect any sequences derived from the PV-GMIR527237 transformation plasmid, a sample of PV-GMIR527237 was sequenced by NGS following the same processes outlined for all samples. The resulting PV-GMIR527237 reads were randomly selected to achieve a depth of one and 1/10th genome equivalent relative to the mean coverage of the A3555 conventional control. This result demonstrates that all nucleotides of PV-GMIR527237 are observed by the sequencing and bioinformatic assessments performed and that a detection level of at least $1/10^{th}$ genome equivalent was achieved for the plasmid DNA sequence assessment.

A.3(c)(ii)(ii) Selection of sequence reads that align to PV-GMIR527237

PV-GMIR527237 was transformed into the parental variety A3555 to produce MON 94637. Consequently, any DNA inserted into MON 94637 will consist of sequences that are similar to the PV-GMIR527237 DNA sequence. Therefore, to fully characterise the DNA from PV-GMIR527237 inserted in MON 94637, it is sufficient to completely analyze only the sequence reads that have similarity to PV-GMIR527237 (Figure 5, Step 2).

Using established criteria (described in the materials and methods, in Appendix **1**), sequence reads similar to PV-GMIR527237 were selected from MON 94637 sequence datasets and were then used as input data for bioinformatic junction sequence analysis. PV-GMIR527237 sequences were also compared against the conventional control sequence dataset.

A.3(c)(ii)(iii) Determination of T-DNA I copy number and presence or absence of plasmid vector backbone and T-DNA II

Mapping sequence reads relative to the transformation plasmid allows for the identification of junction signatures, the presence or absence of plasmid backbone and T-DNA II sequences, and the number of T-DNA I insertions. For a single copy T-DNA I insert sequence at a single genomic locus, a single junction signature pair and few, if any, reads aligning with the transformation plasmid backbone sequences are expected.

When reads from the A3555 control dataset were aligned with the transformation plasmid sequence, a small number of reads mapped sporadically across the plasmid sequence. A single unpaired and paired read mapped to P-*Cab-Cm1* in T-DNA I, a single paired read mapped to P-*Usp* in T-DNA II, and a single unpaired read mapped to the CS-*rop* backbone sequence (Figure 9). The sporadic low-level detection of plasmid sequences has previously been described (Zastrow-Hayes *et al.*, 2015).

When reads from the MON 94637 (R3) dataset were aligned with the transformation plasmid sequence, large numbers of reads mapped to the intended T-DNA I sequence and no reads mapped to the transformation plasmid backbone sequences (Figure 10). A single paired read mapped to T-*E9* in T-DNA II, but the read is of low quality, lacks a junction signature, and is not indicative of DNA integration in the soybean genome. The mapping of large numbers of reads from the MON 94637 (R3) dataset to the intended T-DNA I sequence is expected and is fully consistent with the presence of the inserted DNA.

To determine the insert number in MON 94637 (R3), selected reads mapping to T-DNA I were analyzed to identify junctions. This bioinformatic analysis is used to find and classify partially matched reads characteristic of the ends of insertions. The number of unique junctions determined by this analysis are shown in Table 3.

Table 3. Unique Junction Sequence Result

Sample	Junctions Detected
MON 94637 (R3)	2
A3555	0

Detailed mapping information of the junction sequences is shown in Figure 10 The location and orientation of the junction sequences relative to the DNA insert in MON 94637 are also shown in Figure 10 (panels 1, 2, and 3). The two junctions are visualized in Figure 10 (panels 2 and 3). Both junctions contain the T-DNA I border sequence joined to flanking genomic sequence, indicating that they represent the sequences at the junctions of the intended T-DNA I insert and the soybean genome. As described earlier, no junctions were detected in the control sample (Figure 9).

Considered together, the absence of plasmid backbone and T-DNA II sequences and the presence of two junctions (joining T-DNA I borders and flanking sequences) indicate a single intended T-DNA I at a single locus in the genome of MON 94637. Both junctions originate from the same locus of the MON 94637 genome and are linked by contiguous, known and expected DNA sequence. This is demonstrated by complete coverage of the sequenced reads spanning the interval between the junctions and the directed sequencing of overlapping PCR products described in Section A.3(c)(iii).

Based on the comprehensive NGS and junction identification it is concluded that MON 94637 contains one copy of T-DNA I inserted into a single locus, as shown in Figure 8. This conclusion is confirmed by the sequencing and analysis of overlapping PCR products from this locus as described in Section A.3(c)(iii).

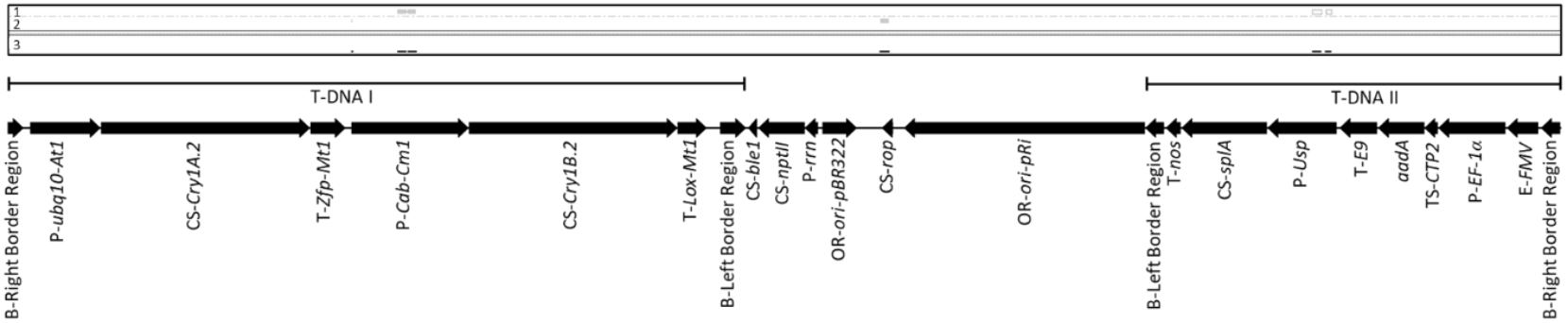

Figure 9. Read Mapping of Conventional Soybean A3555 versus PV-GMIR527237

Panel 1 shows the location of left to right oriented paired reads. Panel 2 shows unpaired reads and panel 3 is a representation of combined read depth for unpaired and paired reads with a read depth range from 0 to 1.

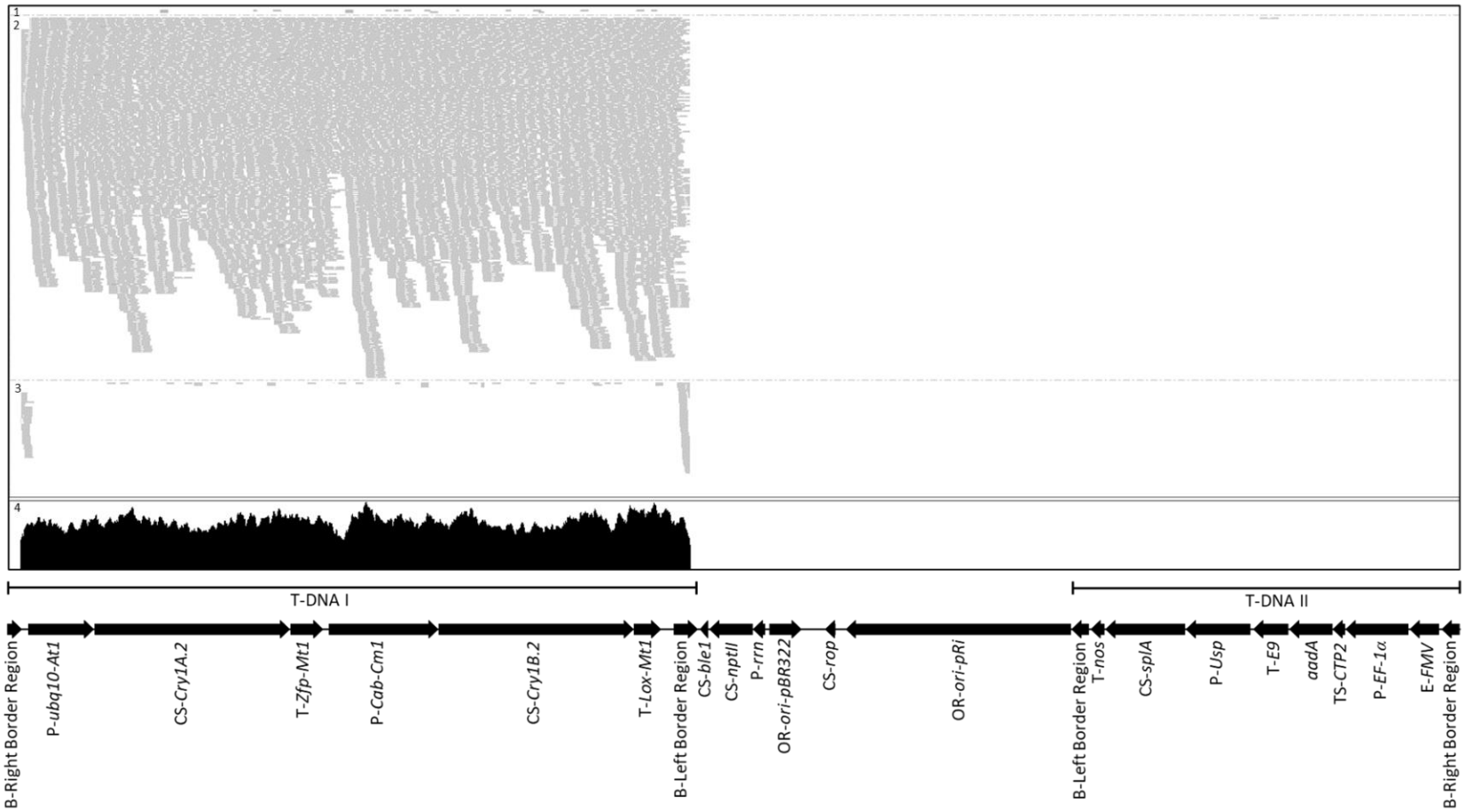

Figure 10. Read Mapping of MON 94637 (R3) versus PV-GMIR527237

Panel 1 shows the location of right to left oriented paired reads. Panel 2 shows the location of left to right oriented paired reads. Panel 3 shows unpaired reads and panel 4 is a representation of combined read depth for unpaired and paired reads with a read depth range from 0 to 193. Comparable results were observed when read mapping the R4, R5, R6, and R7 generations of MON 94637 against PV-GMIR527237 (see Table 4 for the generational stability analysis).

A.3(c)(iii) Full DNA sequence of each insertion site, including junction regions with the host DNA

A.3(c)(iii)(i) Organization and sequence of the insert and adjacent DNA in MON 94637

The organization of the elements within the DNA insert and the adjacent genomic DNA was assessed using directed DNA sequence analysis (refer to Figure 5, Step 4). PCR primers were designed to amplify two overlapping regions of the MON 94637 genomic DNA that span the entire length of the insert and the adjacent genomic DNA flanking the insert (Figure 11). The amplified PCR products were subjected to DNA sequencing analyses. The results of this analysis confirm that the MON 94637 insert is 12,240 bp and that each genetic element within T-DNA I is intact compared to PV-GMIR527237, with the exception of the border regions. The border regions both contain small terminal deletions with the remainder of the inserted border regions being identical to the sequence in PV-GMIR527237. The sequence and organization of the insert was also shown to be identical to the corresponding T-DNA I of PV-GMIR527237 as intended. This analysis also shows that only T-DNA I elements (described in Table 2) were present. In addition, 1000 base pairs flanking the 5′ end of the MON 94637 insert (Table 2 bases 1-1000) and 1000 base pairs flanking the 3′ end of the MON 94637 insert (Table 2, bases 13,241-14,240) were determined.

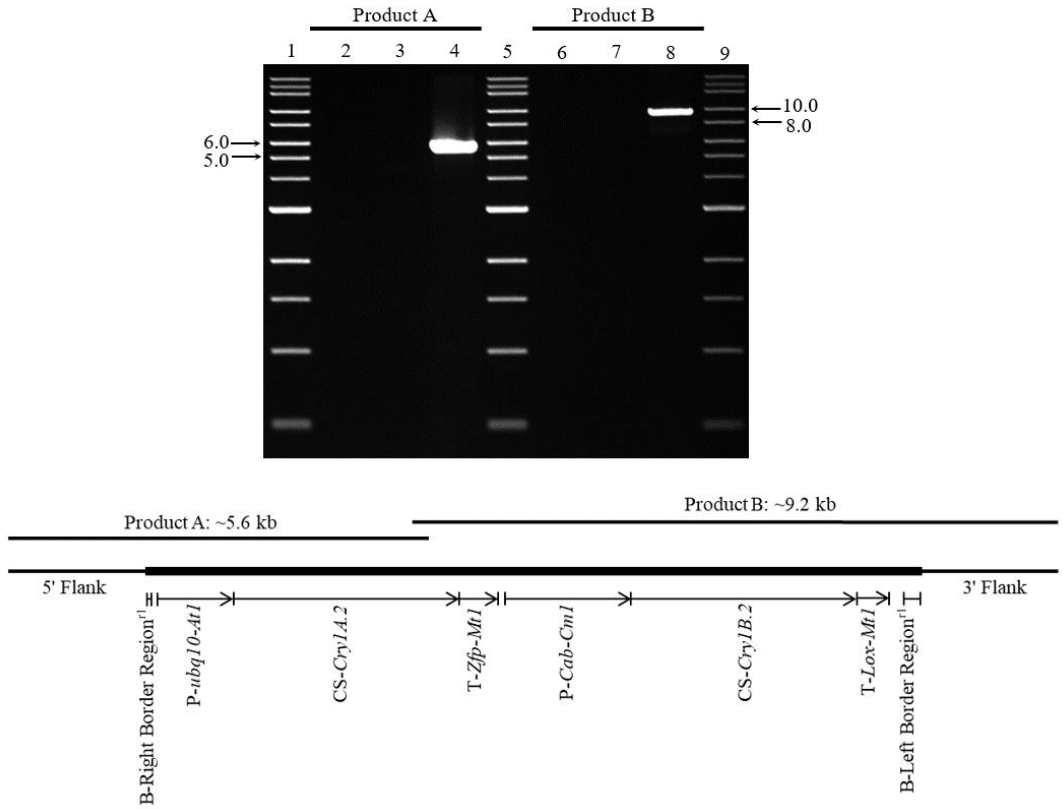

Figure 11. Analysis of Overlapping PCR Products Across the Insert in MON 94637

PCR was performed on both conventional control genomic DNA and genomic DNA of the R3 generation of MON 94637 using two pairs of primers to generate overlapping PCR fragments from MON 94637 for sequencing analysis. To verify the PCR products, 2 µl of each of the PCR reactions was loaded on the gel. The expected product size for each amplicon is provided in the illustration of the insert in MON 94637, which appears at the bottom of the figure. This figure is representative of the data generated in the study. Lane designations are as follows:

Lane	
1	1 Kb Extend DNA Ladder
2	No template control
3	A3555 Conventional Control
4	MON 94637
5	1 Kb Extend DNA Ladder
6	No template control
7	A3555 Conventional Control
8	MON 94637
9	1 Kb Extend DNA Ladder

Arrows on the agarose gel photograph denote the size of the DNA, in kilobase pairs, obtained from the 1 Kb Extend DNA Ladder (New England BioLabs) on the ethidium bromide stained gel.

[r1] Superscript in the Right and Left Border Region indicates that the sequence in MON 94637 was truncated compared to the sequences in PV-GMIR527237.

A.3(c)(iii)(ii) Sequence of the MON 94637 insertion site

PCR and sequence analysis were also performed on genomic DNA extracted from the conventional control to examine the insertion site in conventional soybean (see Figure 5, Step 5). The PCR was performed with one primer specific to the genomic DNA sequence flanking the 5′ end of the MON 94637 insert paired with a second primer specific to the genomic DNA sequence flanking the 3′ end of the insert (Figure 12). A sequence comparison between the PCR product generated from the conventional control and the sequence generated from the 5′ and 3′ flanking sequences of MON 94637 indicates that 14 bases of soybean genomic DNA were deleted during integration of the T-DNA I. Such changes are common during plant transformation (Anderson *et al.*, 2016) and these changes presumably result from double stranded break repair mechanisms in the plant during the *Agrobacterium*-mediated transformation process (Salomon and Puchta, 1998). The remainder of the evaluated soybean genomic DNA sequences flanking the insert in MON 94637 are identical to the conventional control.

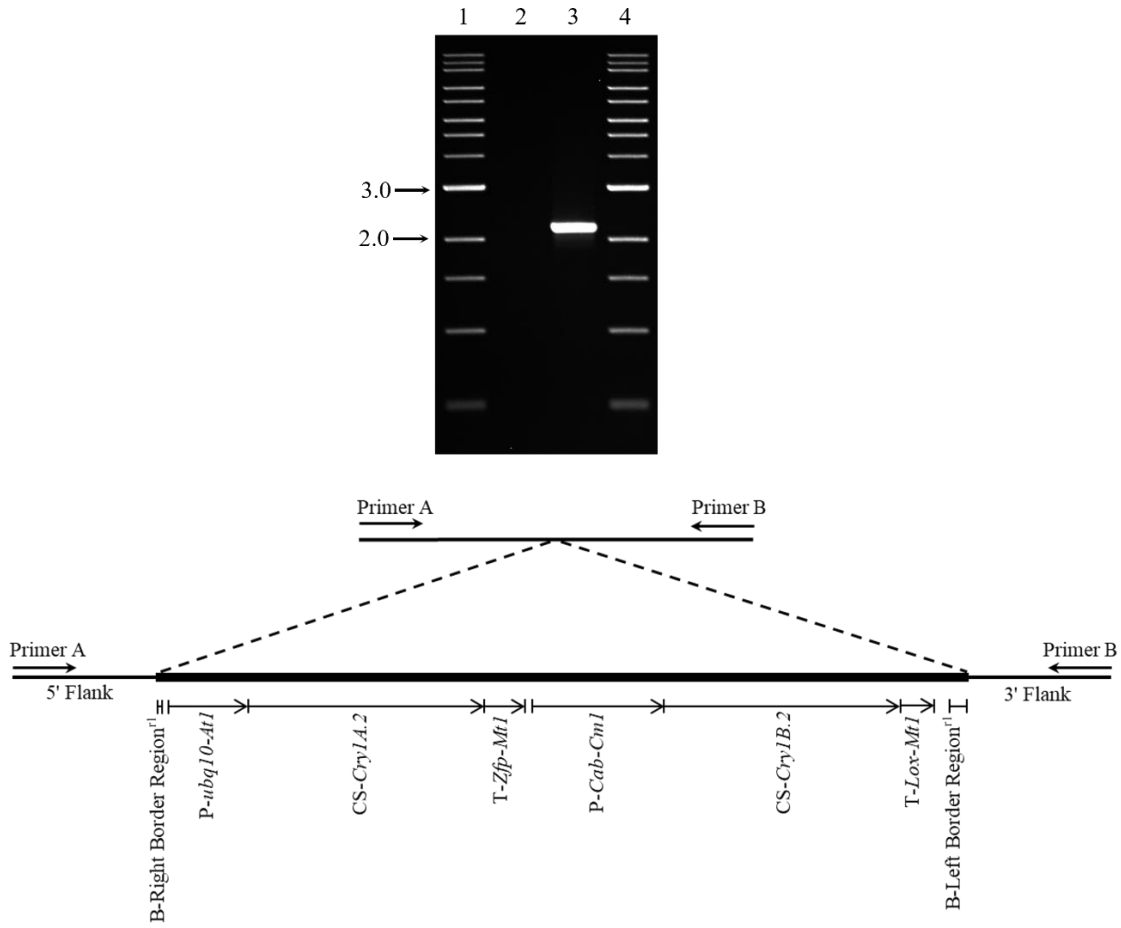

Figure 12. PCR Amplification of the MON 94637 Insertion Site

PCR analysis was performed to evaluate the insertion site. PCR was performed on conventional control DNA using Primer A, specific to the 5′ flanking sequence, and Primer B, specific to the 3′ flanking sequence of the insert in MON 94637. The expected PCR product size is ~2.2 kb. The DNA generated from the conventional control PCR was used for sequencing analysis. This illustration depicts the MON 94637 insertion site in the conventional control (upper panel) and the MON 94637 insert (lower panel). Approximately 2 µl of each of the PCR reactions were loaded on the gel. This figure is representative of the data generated in the study. Lane designations are as follows:

Lane	
1	1 Kb Extend DNA Ladder
2	No template control
3	A3555 Conventional Control
4	1 Kb Extend DNA Ladder

Arrows on the agarose gel photograph denote the size of the DNA, in kilobase pairs, obtained from the 1 Kb Extend DNA Ladder (New England BioLabs) on the ethidium bromide stained gel.

[r1] Superscript in Right and Left Border Regions indicates that the sequence in MON 94637 was truncated compared to the sequences in PV-GMIR527237.

A.3(c)(iv) A map depicting the organisation of the inserted genetic material at each insertion site

PCR and DNA sequence analyses performed on MON 94637 soybean and the conventional control determined the organisation of the genetic elements within the insert as given in Figure 12.

A.3(c)(v) Details of an analysis of the insert and junction regions for the occurrence of any open reading frames (ORFs)

Details of method and results from bioinformatics evaluation of the T-DNA insert and putative open reading frame at junction regions are described in Appendix **2** and Appendix **3**, respectively.

The 2009 Codex Alimentarius Commission guidelines for the safety assessment of food derived from biotechnology crops (Codex Alimentarius, 2009) includes an assessment element on the identification and evaluation of "*open reading frames within the inserted DNA or created by the insertion with contiguous plant genomic DNA*." These assessments examine the potential homology of any putative polypeptides or proteins that could be produced from open reading frames (ORFs) in the insert or at the plant-insert junction to known toxins or allergens. These analyses are conducted even if there is no evidence that such alternative reading frames in the insert or such ORFs at the plant-insert junction are capable of being transcribed or translated into a protein. Bioinformatic analyses were performed on the MON 94637 insert and flanking genomic DNA sequences to assess the potential for allergenicity, toxicity, or biological activity of putative polypeptides encoded by all six reading frames present in the MON 94637 insert DNA, as well as ORFs spanning the 5' and 3' insert DNA-flanking sequence junctions. The results from these bioinformatics analyses demonstrate that any putative polypeptides encoded by the MON 94637 event sequence are unlikely to exhibit allergenic, toxic or otherwise biologically adverse properties.

Bioinformatic analyses were performed on the MON 94637 insert to assess the potential for allergenicity, toxicity, or biological activity of putative polypeptides encoded by all six reading frames present in the MON 94637 insert DNA, as well as ORFs present in the 5' and 3' flanking sequence junctions. These various bioinformatic evaluations are depicted in Figure 13. ORFs spanning the 5' and 3' soybean genomic DNA-inserted DNA junctions were translated from stop codon to stop codon in all six reading frames (three forward reading frames and three reading frames in reverse orientation)[7]. Polypeptides of eight amino acids or greater from each reading frame were then compared to toxin, allergen and all proteins databases using bioinformatic tools. Similarly, the entire T-DNA sequence was translated in all six reading frames and the resulting deduced amino acid sequence was subjected to bioinformatic analyses. The data generated from these analyses confirm that even in the highly unlikely occurrence that a translation product other than MON 94637 Cry1A.2 and Cry1B.2 proteins were derived from frames one to six of the insert DNA or the ORFs spanning the insert junctions, they would not share a sufficient degree of sequence similarity with other proteins to indicate they would be potentially allergenic, toxic, or have other safety implications. Therefore, there is no

[7] An evaluation of sequence translated from stop codon to stop codon represents the most conservative approach possible for flank junction analysis as it does not take into consideration that a start codon is necessary for the production of a protein sequence.

evidence for concern regarding the relatedness of the putative polypeptides for MON 94637 to known toxins, allergens, or biologically active putative peptides.

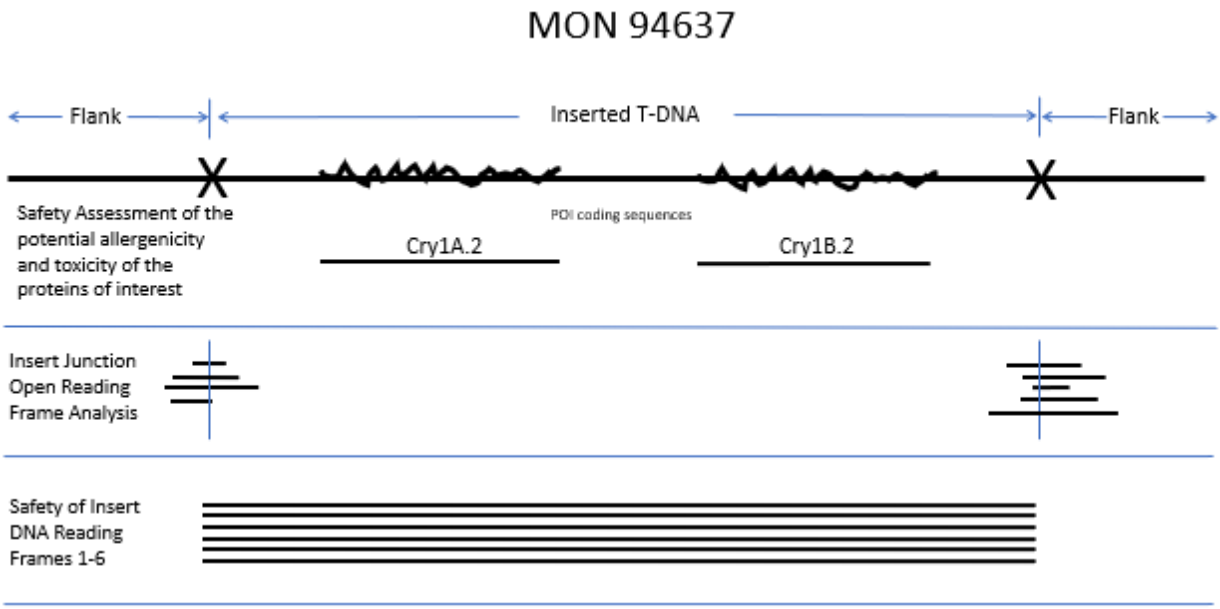

Figure 13. Schematic Summary of MON 94637 Bioinformatic Analyses

A.3(c)(v)(i) Bioinformatics evaluation of the T-DNA insert in MON 94637

Pleaes refer Appendix **2** for details on Bioinformatics evaluation of T-DNA insert.

Bioinformatic analyses were performed to assess the potential of toxicity, allergenicity or biological activity of any putative peptides encoded by translation of reading frames 1 through 6 of the inserted DNA in MON 94637 (Figure 13).

The FASTA sequence alignment tool was used to assess structural relatedness between the query sequences and any protein sequences in the AD_2023, TOX_2023, and PRT_2023 databases. Structural similarities shared between each putative polypeptide with each sequence in the database were examined. The extent of structural relatedness was evaluated by detailed visual inspection of the alignment, the calculated percent identity and alignment length to ascertain if alignments exceeded Codex (Codex Alimentarius, 2009) thresholds for FASTA searches of the AD_2023 database, and the *E*-score. Alignments having an *E*-score less than 1×10^{-5} are deemed significant because they may reflect shared structure and function among sequences. In addition to structural similarity, each putative polypeptide was screened for short polypeptide matches using a pair-wise comparison algorithm.

The results of the search comparisons showed that no relevant structural similarity to known allergens and toxins were observed for any of the putative polypeptides when compared to proteins in the allergen (AD_2023) or toxin (TOX_2023) databases. Furthermore, no short (eight amino acid) polypeptide matches were shared between any of the putative polypeptides and proteins in the allergen database.

Taken together, these data demonstrate the lack of relevant similarities between known allergens or toxins for putative peptides derived from all six reading frames from the inserted DNA sequence of MON 94637. As a result, in the unlikely event that a translation product other than Cry1A.2 and Cry1B.2 proteins were derived from reading frames 1 to 6, these putative polypeptides are not expected to be cross-reactive allergens, toxins, or display adverse biological activity.

A.3(c)(v)(ii) Bioinformatics Evaluation of the DNA Sequences Flanking the 5′ and 3′ Junctions of the MON 94637 Insert: Assessment of Putative Peptides

Pleaes refer Appendix **3** for details on Bioinformatics evaluation of putative open reading frames at junction regions.

Analyses of putative polypeptides encoded by DNA spanning the 5' and 3' genomic junctions of the MON 94637 inserted DNA were performed using a bioinformatic comparison strategy. The purpose of the assessment is to evaluate the potential for novel open reading frames (ORFs) that may have homology to known allergens, toxins, or proteins that display adverse biological activity. Sequences spanning the 5' and 3' genomic DNA-insert DNA junctions, (Figure 13) were translated from stop codon to stop codon in all six reading frames. Putative polypeptides from each reading frame, that were eight amino acids or greater in length, were compared to AD_2023, TOX_2023, and PRT_2023 databases using FASTA and to the AD_2023 database using an eight amino acid sliding window search. A total of 9 putative peptides were compared to allergen (AD_2023), toxin (TOX_2023), and all protein (PRT_2023) databases using bioinformatic tools.

The FASTA sequence alignment tool was used to assess the relatedness between the query sequences and any protein sequence in the AD_2023, TOX_2023, and PRT_2023 databases. Similarities shared between the sequence with each sequence in the database were examined. The extent of relatedness was evaluated by detailed visual inspection of the alignment, the calculated percent identity, and the *E*-score. Alignments having *E*-scores of $\leq$1e-5 (1×10^{-5}) are deemed significant because they may reflect shared structure and function among sequences. In addition to sequence similarity, sequences were screened for short peptide matches using a pair-wise comparison algorithm. In these analyses, eight contiguous and identical amino acids were defined as immunologically relevant, where eight represents the typical minimum sequence length likely to represent an immunological epitope (Silvanovich *et al.*, 2006).

The results of these data indicate that no biologically relevant sequence similarities were observed between the translated putative flank junction sequences and allergens, toxins, or biologically active proteins associated with adverse effects for human or animal health. The bioinformatic analyses performed using the putative sequences translated from junctions is theoretical. Likewise, other than translation of Cry1A.2 and Cry1B.2 no evidence exists to indicate that any other sequence from the T-DNA is translated. Rather, the results of these bioinformatic analyses indicate that in the unlikely occurrence that any of the putative flank junction sequences analyzed herein is found *in planta*, or translation of sequence other than the intended protein products was to occur, none would share significant similarity or identity to known allergens, toxins, or other biologically active proteins that could affect human or animal health.

A.3(d) A description of how the line or strain from which food is derived was obtained from the original transformant (i.e. provide a family tree or describe the breeding process) including which generations have been used for each study

Generations used for each study is shown in breeding tree (Figure 7).

MON 94637 was derived from a single plant transformant of variety A3555. The conventional soybean variety A3555, used as the recipient for the expression cassette insertion that produced MON 94637, was developed by Asgrow Seed Company. A3555 is a mid−maturity group III soybean variety.

Details about transformation and selection process is described in A.3(a). Briefly, The R0 plants generated through the transformation process were self-pollinated to produce R1 seed, the unlinked insertions of T-DNA I (containing the *cry1A.2* and *cry1B.2* expression cassettes) and T-DNA II (containing the selectable and scorable marker genes) were segregated. R1 plants homozygous for T-DNA I were selected using TaqMan-based Real-time PCR assay. Homozygous R1 progenies were subjected to further development, that included additional molecular analysis, measurement of protein expression, insect protection/efficacy test, and phenotypic assessments. After careful selection and evaluation of these events in the laboratory, greenhouse and field, MON 94637 was selected as the lead event based on superior efficacy, agronomic, phenotypic, and molecular characteristics. Studies on MON 94637 were initiated to further characterise the genetic insertion and the expressed products, and to establish the food safety and unaltered environmental risk compared to commercial soybean. The major development steps of MON 94637 are depicted in Figure 1.

A.3(e) Evidence of the stability of the genetic changes, including:

A.3(e)(i) The pattern of inheritance of the transferred gene(s) and the number of generations over which this has been monitored

For detailed method and results about the stability of inserted T-DNA I in MON 94637, please refer to Appendix **1**.

In order to demonstrate the stability of the T-DNA I present in MON 94637 through multiple breeding generations, NGS was performed using DNA obtained from five breeding generations of MON 94637. The breeding history of MON 94637 is presented in Figure 7, and the specific generations tested are indicated in the figure legend. The MON 94637 (R3) generation was used for the molecular characterisation analyses discussed in Sections A.3(c)(ii) and A.3(c)(iii). To assess stability, four additional generations were evaluated by NGS as previously described in Section A.3(c)(i), and compared to the fully characterised MON 94637 (R3) generation. The conventional control used for the generational stability analysis was A3555, which has a genetic background similar to the other generations in Table 4 and represents the original transformation line. Genomic DNA isolated from each of the selected generations of MON 94637 and conventional control was used for NGS mapping and subsequent junction identification (Table 4).

Table 4. Junction Sequence Deceted

Sample	Junction Sequence Detected
MON 94637 (R3)	2
MON 94637 (R4)	2
MON 94637 (R5)	2
MON 94637 (R6)	2
MON 94637 (R7)	2
A3555	0

As shown by alignments to the full flank/insert sequence obtained from directed sequencing, a single conserved pair of junctions linked by contiguous known and expected DNA sequence is present in MON 94637 (R3). Two identical junctions are found in each of the breeding generations (R3, R4, R5, R6, and R7; Appendix **1**), confirming the insertion of a single copy of PV-GMIR527237 T-DNA at a single locus in the genome of MON 94637. The consistency of these junctions in the mapping data across all generations tested demonstrates that this single locus is stably maintained throughout the MON 94637 breeding process.

These results demonstrate that the MON 94637 (R3) single locus of integration is found in all subsequent generations of the MON 94637 breeding history, thereby confirming the stability of the insert. Based on this comprehensive sequence data and bioinformatic analysis of NGS data, it is concluded that MON 94637 contains a single, stable inserted T-DNA I.

A.3(e)(ii) The pattern of inheritance and expression of the phenotype over several generations and, where appropriate, across different environments

A.3(e)(ii)(i) Inheritance of the genetic insert in MON 94637

For detailed methods and results of inheritance, please refer to Appendix **4**.

The MON 94637 T-DNA I resides at a single locus within the soybean genome and therefore should be inherited according to Mendelian principles of inheritance. During development of lines containing MON 94637, genotypic segregation data were recorded to assess the inheritance and stability of the MON 94637 T-DNA I using Chi square (χ^2) analysis over several generations. The χ^2 analysis is based on comparing the observed segregation ratio to the expected segregation ratio according to Mendelian principles.

The MON 94637 breeding path for generating segregation data is described in Figure 14. The transformed R0 plant was self-pollinated to generate R1 seed. An individual plant homozygous for the MON 94637 T-DNA I (homozygous positive) was identified in the R1 segregating population via a Real-Time TaqMan® PCR assay.

The homozygous positive R1 plant was self-pollinated to give rise to R2 seed, and a homozygous positive R2 plant was self-pollinated to give rise to R3 seed. The homozygous

positive R3 plants were crossed via traditional breeding techniques to a Bayer CropScience LP proprietary elite inbred parent that did not contain the T-DNA I insert to produce hemizygous F1 seed. The hemizygous F1 plants were self-pollinated to produce F2 seed. The F2 generation was tested for the presence of MON 94637 T-DNA I by Qualitative End Point TaqMan® PCR assay for the *Lox-Mt1* genetic element that is a component of T-DNA I. Qualitative End Point TaqMan® PCR assays detect the fluorescence of amplified PCR products specific to the TaqMan probe target sequence at the conclusion of PCR cycling.

The inheritance of the MON 94637 T-DNA I was assessed in the F2 generation and in subsequent F3 and F4 generations using the Qualitative End Point TaqMan® PCR *Lox-Mt1* assay as described above. In all generations, the MON 94637 T-DNA I was predicted to segregate at a 1:2:1 ratio (homozygous positive: hemizygous positive: homozygous negative) according to Mendelian inheritance principles.

A Pearson's chi-square (χ^2) analysis was used to compare the observed segregation ratios of the MON 94637 T-DNA I to the expected ratios.

The Chi-square was calculated as:

$$\chi^2 = \sum [(| o - e |)^2 / e]$$

where o = observed frequency of the genotype or phenotype and e = expected frequency of the genotype or phenotype. The level of statistical significance was predetermined to be 5% ($\alpha = 0.05$).

The results of the χ^2 analysis of the segregating progeny of MON 94637 are presented in Table 5. The χ^2 value in the F2, F3, and F4 generations indicated no statistically significant difference between the observed and expected segregation ratios of MON 94637 T-DNA I. These results support the conclusion that the MON 94637 T-DNA I resides at a single locus within the soybean genome and is inherited according to Mendelian principles of inheritance. These results are also consistent with the molecular characterisation data indicating that MON 94637 contains a single intact copy of the T-DNA I inserted at a single locus in the soybean genome (Sections A.3(c)(ii), A.3(c)(iii) and A.3(e)(i)).

.

Figure 14. Breeding Path for Generating Segregation Data on MON 94637

*An elite inbred line that did not contain the MON 94637 T-DNA coding sequences.
**Chi-square analysis was conducted on segregation data from F2, F3, and F4 generations (bolded text).
U: Self-Pollinated

Table 5. Segregation of the T-DNA During the Development of MON 94637

					1:2:1 Segregation				
Generation	Total Plants	Observed # Plant Homozygous Positive	Observed # Plant Hemizygous Positive	Observed # Plant Homozygous Negative	Expected # Plant Homozygous Positive	Expected # Plant Hemizygous Positive	Expected # Plant Homozygous Negative	χ^2	Probability
F2	380	87	192	101	95	190	95	1.07	0.585
F3	562	133	274	155	140.5	281	140.5	2.07	0.355
F4	379	107	188	84	94.75	189.5	94.75	2.82	0.245

A.3(e)(ii)(ii) Expression of the genetic insert

For detailed methods and results of generational stability of Cry1A.2 and Cry1B.2 protein expression, please refer to Appendix **5**.

In order to assess the presence of the Cry1A.2 and Cry1B.2 proteins in MON 94637 across multiple breeding generations, Western blot analysis of MON 94637 was conducted on grain tissue collected from generations R3, R4, R5, R6, and R7 of MON 94637, using grain tissue of the conventional control (A3555) as negative control.

The presence of the Cry1A.2 protein was demonstrated in five breeding generations of MON 94637 using western blot analysis. The *Bt*-produced Cry1A.2 protein reference standard (5 ng) was used as a reference for the positive identification of the Cry1A.2 protein (Figure 15, lane 3). The presence of the Cry1A.2 protein in grain tissue samples of MON 94637 was determined by visual comparison of the bands detected in five breeding generations (Figure 15, lanes 5-9) to the *Bt*-produced Cry1A.2 protein reference standard. The MON 94637-produced Cry1A.2 protein migrated indistinguishably from that of the *Bt*-produced protein standard analyzed on the same Western blot. As expected, the Cry1A.2 protein was not detected in the conventional control grain extract (Figure 15, lane 4).

The presence of the Cry1B.2 protein was demonstrated in five breeding generations of MON 94637 using Western blot analysis. The *Bt*-produced Cry1B.2 protein reference standard (5 ng) was used as a reference for the positive identification of the Cry1B.2 protein (Figure 16, lane 3). The presence of the Cry1B.2 protein in grain tissue samples of MON 94637 was determined by visual comparison of the bands detected in five breeding generations (Figure 16, lanes 5-9) to the *Bt*-produced Cry1B.2 protein reference standard. The MON 94637-produced Cry1B.2 protein migrated indistinguishably from that of the *Bt*-produced protein standard analyzed on the same Western blot. As expected, the Cry1B.2 protein was not detected in the conventional control grain extract (Figure 16, lane 4).

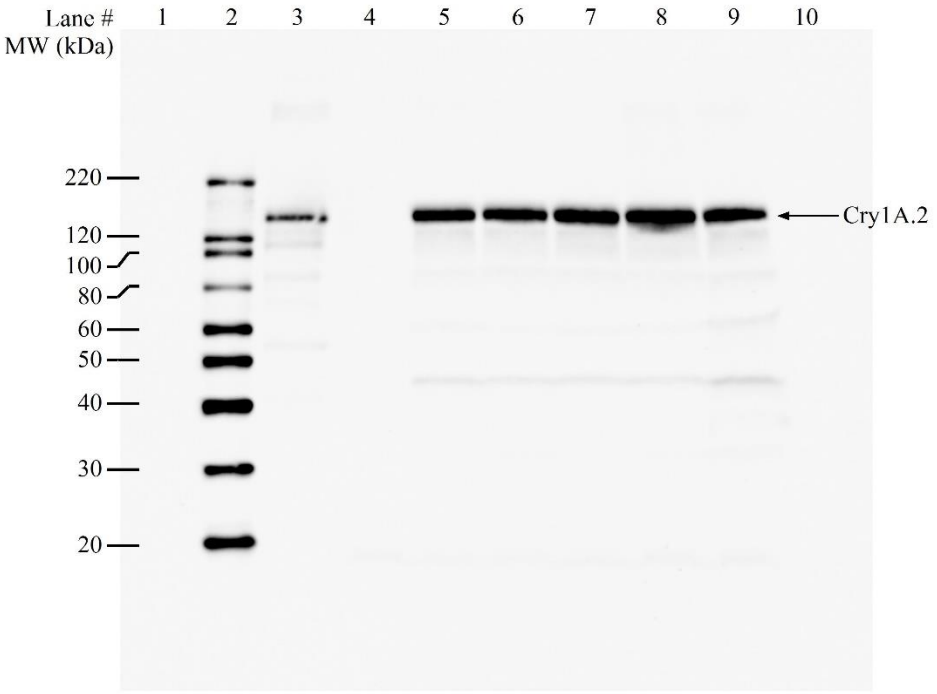

Figure 15. Presence of the Cry1A.2 Protein in Multiple Generations of MON 94637 Grain

Blot probed with a monoclonal anti-Cry1A.2 primary antibody and an HRP-conjugated anti-mouse IgG secondary antibody. The 5-second exposure image is shown. The approximate MWs (kDa) of the MagicMark XP Protein Standards are shown on the left. Lane designations are as follows:

Lane	Sample	Amount
1	Precision Plus Dual Protein Standards	5 µl
2	MagicMark XP Protein Standards	2 µl
3	*Bt*-produced Cry1A.2 protein	5 ng
4	Conventional Control, 11494217	20 µl
5	MON 94637, R3, 11511622	20 µl
6	MON 94637, R4, 11493842	20 µl
7	MON 94637, R5, 11494218	20 µl
8	MON 94637, R6, 11511512	20 µl
9	MON 94637, R7, 11511513	20 µl
10	Precision Plus Dual Protein Standards	5 µl

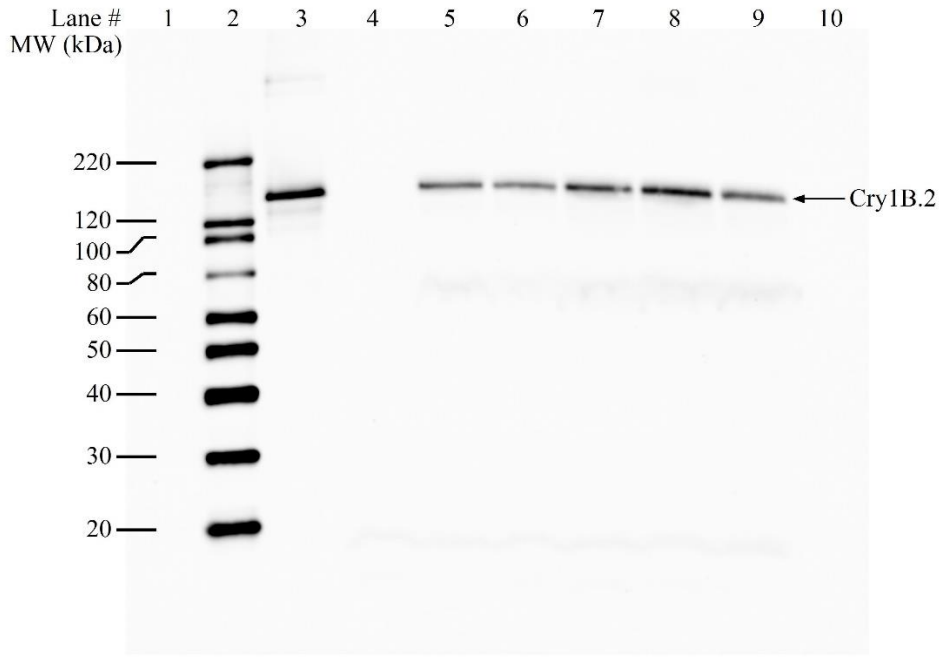

Figure 16. Presence of the Cry1B.2 Protein in Multiple Generations of MON 94637 Grain

Blot probed with a monoclonal anti-Cry1B.2 primary antibody and an HRP-conjugated anti-mouse IgG secondary antibody. The 13-second exposure image is shown. The approximate MWs (kDa) of the MagicMark XP Protein Standards are shown on the left. Lane designations are as follows:

Lane	Sample	Amount
1	Precision Plus Dual Protein Standards	5 µl
2	MagicMark XP Protein Standards	2 µl
3	*Bt*-produced Cry1B.2 protein	5 ng
4	Conventional Control, 11494217	20 µl
5	MON 94637, R3, 11511622	20 µl
6	MON 94637, R4, 11493842	20 µl
7	MON 94637, R5, 11494218	20 µl
8	MON 94637, R6, 11511512	20 µl
9	MON 94637, R7, 11511513	20 µl
10	Precision Plus Dual Protein Standards	5 µl

A.3(f) An analysis of the expressed RNA transcripts, where RNA interference has been used

Not relevant for this product.

B. CHARACTERISATION AND SAFETY ASSESSMENT OF NEW SUBSTANCES

B.1 Characterisation and Safety Assessment of New Substances

B.1(a) Full description of the biochemical function and phenotypic effects of all new substances (e.g. a protein or an untranslated RNA) that are expressed in the new GM organism, including their levels and site of accumulation, particularly in edible portions

B.1(a)(i) Description, mode-of action, and specificity of Cry1A.2 and Cry1B.2 proteins expressed in MON 94637

The MON 94637 Cry1A.2 and Cry1B.2 proteins belong to the Cry three domain family of proteins that has a well-documented mode of action (Vachon *et al.*, 2012; Gill *et al.*, 1992; OECD, 2007; Schnepf *et al.*, 1998). Ingestion of Cry proteins by the target insect pest exposes the protein to the alkaline conditions and proteases in the insect midgut, resulting in proteolytic cleavage of the protein's protoxin domain, thus solubilizing the parasporal inclusions and converting the protein to the active insecticidal toxin. Following activation, this protease-resistant core protein is comprised of three distinct structural domains that function in a step-wise mechanism of binding to specific membrane-embedded receptors, oligomerization at the membrane interface, insertion into the plasma membrane and pore formation leading to loss of cell integrity followed by delayed development or insect death (Bravo *et al.*, 2007; Deist *et al.*, 2014).

B.1(a)(i)(i) Cry1A.2 protein expressed in MON 94637

Cry1A.2 is a protein that comprises a single polypeptide of 1189 amino acids with an apparent molecular weight of approximately 135 kDa. Like other Cry proteins, Cry1A.2 is first synthesized as a prototoxin that upon exposure to the midgut of target organisms is cleaved by digestive enzymes to yield an approximately 65 kDa activated protein (Bravo *et al.*, 2007). Cry1A.2 is a chimeric three domain (3D) protein that consists of domains I from Cry1Ah (*Bacillus thuringiensis* (*Bt)*), domain II and the C-terminal protoxin domain from Cry1Ac (*Bt* subsp. *kurstaki*), and domain III from Cry1Ca *(Bt* subsp. *aizawai*) (Chen *et al.*, 2021; Crickmore *et al.*, 1998) (Figure 17). Cry1A and Cry1C proteins are from a family of insecticidal proteins derived from various subspecies of the soil bacterium *Bacillus thuringiensis* (*Bt*) which have been used extensively in formulation for commercial biopesticides (Betz *et al.*, 2000; EFSA, 2012; Bravo *et al.*, 2011). Cry1A.2 was designed using a domain exchange strategy to achieve high levels of activity against target lepidopteran insect pests. Domain exchange is a well-known mechanism in nature, resulting in diversities in Cry protein functional activity that have been described extensively in the literature (de Maagd *et al.*, 2003; de Maagd *et al.*, 2001). By utilizing modern molecular biological tools, a domain exchange strategy has previously been used successfully to switch the functional domains of Cry1 proteins to develop microbial biopesticides with improved specificity to lepidopteran insect pests (Baum, 1998; Baum *et al.*, 1999; Gao *et al.*, 2006). Similarly, by exchanging domains, Cry1A.2 has been engineered to have an enhanced specificity for southern armyworm relative to Cry1A. 107 and Cry1A.105 (Chen *et al.*, 2021) while maintaining significant efficacy on other soy pests including soybean looper (SBL), velvetbean caterpillar (VBC) and black armyworm (BLAW.) Domain I is 100% identical to the respective domain of Cry1Ah, domain II is 100% identical to domain of Cry1Ac. Domain III of Cry1A.2 is 100% identical to domain III of Cry1Ca. The C-terminal region of Cry1A.2 is 100% identical to that of Cry1Ac.

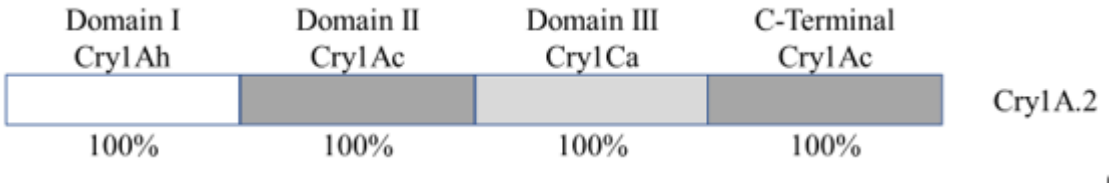

Figure 17. Schematic Representation of the Primary Domain Architecture of the Cry1A.2 Protein

The domain architecture of the chimeric Cry1A.2 protein is schematically presented. Different shades are used to differentiate the origin of domains. For simplicity, the lengths of the domains in this illustration are not in proportion to the lengths of amino acid sequence of the respective domains.

B.1(a)(i)(ii) Cry1B.2 protein expressed in MON 94637

Cry1B.2 in MON 94637 is a protein that comprises a single polypeptide of 1187 amino acids, with an apparent molecular weight of approximately 135 kDa. Like other Cry proteins, it is first synthesized as a prototoxin that upon exposure to the midgut of target organisms is cleaved by digestive enzymes to yield an approximately 65 kDa activated protein (Bravo *et al.*, 2007). Cry1B.2 is a chimeric three domain protein that consists of domains I and II from Cry1Be (*Bt*), domain III from Cry1Ka2 (*Bt* subsp. *morrisoni*), and the C-terminal protoxin domain from Cry1Ab (*Bt* subsp. *kurstaki*) (Chen *et al.*, 2021; Crickmore *et al.*, 1998)(Figure 18). Cry1A and Cry1C proteins are from a family of insecticidal proteins derived from various subspecies of the soil bacterium *Bacillus thuringiensis* (*Bt*) which have been used extensively in formulation for commercial biopesticides (Betz *et al.*, 2000; EFSA, 2012; Bravo *et al.*, 2011). Cry1B.2 was designed using a domain exchange strategy to achieve high levels of activity against target lepidopteran insect pests.As described above for Cry1A.2, domain exchange is a common mechanism for diversity generation in nature and as used in the design of Cry1B.2. By exchanging Domain III, Cry1B.2 has been engineered to have an enhanced specificity for fall armyworm relative to Cry1Be (Chen *et al.*, 2021). Domains I and II of Cry1B.2 are 100% identical to the respective domains of Cry1Be. Domain III of Cry1B.2 is 100% identical to domain III of Cry1Ka2. The C-terminal region of Cry1B.2 is 100% identical to that of Cry1Ab.

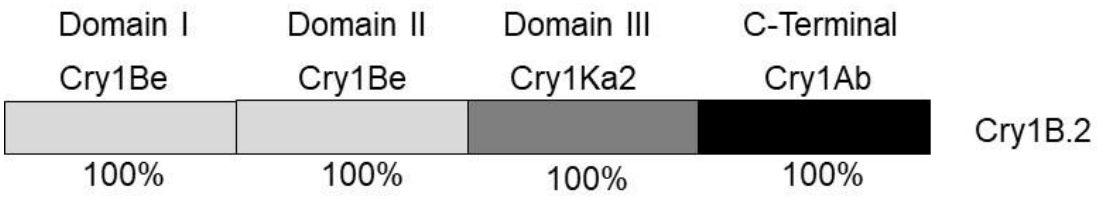

Figure 18. Schematic Representation of the Primary Domain Architecture of the Cry1B.2 Protein

The domain architecture of the chimeric Cry1B.2 protein is schematically presented. Different shades are used to differentiate the origin of domains. For simplicity, the lengths of the domains in this illustration are not in proportion to the lengths of amino acid sequence of the respective domains.

B.1(a)(ii) Characterisation of the Cry1A.2 and Cry1B.2 proteins from MON 94637

The safety assessment of crops derived through biotechnology includes characterisation of the physicochemical and functional properties of the protein(s) encoded by the inserted DNA, and confirmation of the safety of the protein(s). The expression level of Cry1A.2 and Cry1B.2 in MON 94637 is low, and insufficient for use in the subsequent safety evaluations. Therefore, recombinant Cry1A.2 and Cry1B.2 proteins were produced in a heterologous *Bt* expression system, using expression vectors with *cry1A.2* or *cry1B.2* coding sequences that matched those of the *cry1A.2* or *cry1B.2* coding sequences in MON 94637. The physicochemical and functional characteristics of the MON 94637-produced Cry1A.2 and Cry1B.2 proteins were determined and shown to be equivalent to the *Bt*-produced Cry1A.2 and Cry1B.2 proteins, respectively.

B.1(a)(ii)(i) Characterisation of the MON 94637 Cry1A.2 protein

The details of the materials and methods for the panel of analytical tests used to evaluate and compare the properties of the MON 94637-produced Cry1A.2 and *Bt*-produced Cry1A.2 proteins are described in Appendix **6**.

For the safety data generated using the *Bt*-produced Cry1A.2 protein to be applied to the MON 94637-produced Cry1A.2 protein (plant-produced Cry1A.2), the equivalence of the plant- and *Bt*-produced proteins must first be demonstrated. To assess the equivalence between the MON 94637-produced and *Bt*-produced Cry1A.2 proteins, a small quantity of the MON 94637-produced Cry1A.2 protein was purified from MON 94637 grain. The MON 94637-produced Cry1A.2 protein was characterised and the equivalence of the physicochemical characteristics and functional activity between the MON 94637-produced and *Bt*-produced Cry1A.2 proteins was assessed using a panel of analytical tests, as shown in Table 6. Taken together, these data provide a detailed characterisation of the MON 94637-produced Cry1A.2 protein and establish the equivalence of the MON 94637-produced and *Bt*-produced Cry1A.2 proteins. Based on this established equivalence, conclusions derived from digestibility, heat susceptibility, acute oral mammalian toxicology study and non-target organism studies conducted with *Bt*-produced Cry1A.2 protein are applicable to MON 94637-produced Cry1A.2 protein.

Table 6. Summary of MON 94637 Cry1A.2 Protein Identity and Equivalence

Analytical Test Assessment	Section Cross Reference	Analytical Test Outcome
N-terminal sequence	B.1(a)(ii)(i)(i)	The expected N-terminal sequence for MON 94637-produced Cry1A.2 protein was observed by Nano LC-MS/MS[1]
Nano LC-MS/MS[1]	B.1(a)(ii)(i)(ii)	Nano LC-MS/MS[1] analysis of trypsin or Asp-N digested peptides from MON 94637-produced Cry1A.2 protein yielded peptide masses consistent with expected peptide masses from the theoretical trypsin or Asp-N digest of the amino acid sequence
Western blot analysis	B.1(a)(ii)(i)(iii)	MON 94637-produced Cry1A.2 protein identity was confirmed using a western blot probed with antibodies specific for Cry1A.2 protein Immunoreactive properties of the MON 94637produced Cry1A.2 and the *Bt*produced Cry1A.2 proteins were shown to be equivalent
Apparent molecular weight (MW)	B.1(a)(ii)(i)(iv)	Electrophoretic mobility and apparent molecular weight of the MON 94637-produced Cry1A.2 and the *Bt*-produced Cry1A.2 proteins were shown to be equivalent
Glycosylation analysis	B.1(a)(ii)(i)(v)	Glycosylation status of MON 94637-produced Cry1A.2 and *Bt*-produced Cry1A.2 proteins were shown to be equivalent
Functional activity	B.1(a)(ii)(i)(vi)	Functional activity of the MON 94637-produced Cry1A.2 and the *Bt*-produced Cry1A.2 proteins were shown to be equivalent by insect bioassay

[1] Nano LC-MS/MS = Nanoscale liquid chromatography-tandem mass spectrometry

B.1(a)(ii)(i)(i) Results of the N-terminal sequencing analysis of Cry1A.2

The expected N-terminal sequence for the Cry1A.2 protein deduced from the *cry1A.2* gene present in seed of MON 94637 soybean was observed by LC-MS/MS (see Experimental Sequence, Figure 19). The N-terminal sequence for MON 94637-produced Cry1A.2 protein was consistent with the N-terminal sequence for the *Bt*-produced Cry1A.2 protein observed by LC-MS/MS (Figure 19 and Appendix **6**). Hence, the sequence information confirms the identity of the Cry1A.2 protein isolated from the seed of MON 94637 soybean.

Amino Acids Residue # from the N-terminus	→	1	2	3	4	5	6	7	8	9	10	11	12	13	14	15
Bt-produced Cry1A.2 sequence	→	M	E	I	V	N	N	Q	N	Q	C	V	P	Y	N	C
Expected Cry1A.2 Sequence	→	M	E	I	V	N	N	Q	N	Q	C	V	P	Y	N	C
MON 94637 Experimental Sequence	→	M	E	I	V	N	N	Q	N	Q	C	V	P	Y	N	C

Figure 19. N-terminal Sequence of the MON 94637-Produced Cry1A.2 Protein

The experimental sequence obtained from the MON 94637-produced Cry1A.2 protein was compared to the expected sequence deduced from the *cry1A.2* gene present in MON 94637. The *Bt*-produced Cry1A.2 protein N-terminal sequence above was derived from the reference substance COA (lot 314311). The experimentally determined sequence (initial fifteen amino acids shown) corresponds to the deduced Cry1A.2 protein beginning at the initial methionine (M) amino acid position. The single letter International Union of Pure and Applied Chemistry - International Union of Biochemistry (IUPAC-IUB) amino acid code is M, Methionine; E, Glutamic acid; I, Isoleucine; V, Valine; N, Asparagine; Q, Glutamine; C, Cysteine; P, Proline; Y, Tyrosine.

B.1(a)(ii)(i)(ii) Results of mass fingerprint analysis of Cry1A.2 protein

Peptide mass fingerprint analysis is a standard technique used for confirming the identity of proteins. The ability to identify a protein using this method is dependent upon matching a sufficient number of observed tryptic peptide fragment masses with predicted tryptic peptide fragment masses. In general, protein identification made by peptide mapping is considered to be reliable if >40% of the protein sequence was identified by matching experimental masses observed for the tryptic peptide fragments to the expected masses for the fragments (Biron *et al.*, 2006; Krause *et al.*, 1999). The identity of the MON 94637-produced Cry1A.2 protein was confirmed by LC-MS/MS analysis of peptide fragments produced by the trypsin digestion of the MON 94637-produced Cry1A.2 protein.

There were 139 unique peptides identified that corresponded to the masses expected to be produced by trypsin digestion of the MON 94637-produced Cry1A.2 protein (Table 7). The identified masses were used to assemble a coverage map of the entire Cry1A.2 protein (Figure 20). The experimentally determined coverage of the MON 94637-produced Cry1A.2 protein was 95% (Figure 20, 1135 out of 1189 amino acids). This analysis further confirms the identity of MON 94637-produced Cry1A.2 protein.

There were 113 unique peptides identified that corresponded to the masses expected to be produced by trypsin digestion of the *Bt*-produced Cry1A.2 protein (Table 8) by LC-MS/MS analysis during the protein characterisation. The identified masses were used to assemble a coverage map of the entire Cry1A.2 protein (Figure 20). The experimentally determined

coverage of the *Bt*-produced Cry1A.2 protein was 88% (Figure 20, 1057 out of 1189 amino acids).

Table 7. Summary of the Tryptic Masses Identified for the MON 94637-Produced Cry1A.2 Using LC-MS/MS[1]

Experimental Mass[2]	Calculated Mass[3]	Difference[4]	Fragment[5]	Sequence[6]
3374.5347	3374.5329	0.0018	1 - 28	MEIV...EGGR
6430.4110	6430.3821	0.0289	29 - 87	ISVG...INQR
1988.0004	1987.9996	0.0008	88 - 105	IAEA...GMAR
657.3805	657.3810	-0.0005	88 - 93	IAEAVR
1347.6438	1347.6452	-0.0014	94 - 105	NTAI...GMAR
2678.3005	2678.2976	0.0029	109 - 131	TYAT...EALR
2209.0285	2209.0327	-0.0042	109 - 127	TYAT...PELR
1315.6084	1315.6084	0.0000	109 - 119	TYAT...EWEK
1380.6995	1380.6997	-0.0002	120 - 131	APDD...EALR
911.4348	911.4348	0.0000	120 - 127	APDDPELR
487.2755	487.2754	0.0001	128 - 131	EALR
4706.5798	4706.5799	-0.0001	132 - 173	TQFT...SLLR
1473.7096	1473.7100	-0.0004	132 - 144	TQFT...ISGR
3250.8740	3250.8805	-0.0065	145 - 173	ISVL...SLLR
558.3742	558.3741	0.0001	145 - 149	ISVLK
3659.0029	3658.9988	0.0041	150 - 181	IQTF...FGQR
2710.5211	2710.5170	0.0041	150 - 173	IQTF...SLLR
966.4929	966.4923	0.0006	77 - 181	DVVFFGQR
3251.4608	3251.4571	0.0037	182 - 209	WGFS...YAVR
1037.4936	1037.4930	0.0006	210 - 217	WYNTGLER
1371.6675	1371.6684	-0.0009	218 - 228	VWGP...DWVR
815.3935	815.3926	0.0009	218 - 224	VWGPDSR
1438.7190	1438.7218	-0.0028	225 - 234	DWVR...QFRR
574.2863	574.2863	0.0000	225 - 228	DWVR
883.4302	883.4300	0.0002	229 - 234	YNQFRR
726.3448	726.3449	-0.0001	229 - 233	YNQFR
2490.3571	2490.3594	-0.0023	234 - 254	RELT...DSRR
2334.2578	2334.2583	-0.0005	234 - 253	RELT...YDSR
2334.2575	2334.2583	-0.0008	235 - 254	ELTL...DSRR
2178.1561	2178.1572	-0.0011	235 - 253	ELTL...YDSR
703.4136	703.4129	0.0007	254 - 258	RYPIR
547.3117	547.3118	-0.0001	255 - 258	YPIR
803.4500	803.4501	-0.0001	259 - 265	TVSQLTR
2698.3051	2698.2987	0.0064	266 - 289	EIYT...GIER
1899.8985	1899.9003	-0.0018	266 - 281	EIYT...GSFR
816.4087	816.4090	-0.0003	282 - 289	GSAQGIER
2212.0978	2212.0946	0.0032	293 - 311	SPHL...DAHR
4244.9207	4244.9037	0.0170	312 - 349	GYYY...PQQR

Experimental Mass[2]	Calculated Mass[3]	Difference[4]	Fragment[5]	Sequence[6]
5835.0216	5835.0020	0.0196	350 - 402	IVAQ...AVYR
2124.1664	2124.1691	-0.0027	350 - 368	IVAQ...TLYR
1202.6771	1202.6772	-0.0001	350 - 360	IVAQ...GVYR
4650.3527	4650.3354	0.0173	361 - 402	TLSS...AVYR
939.5031	939.5025	0.0006	361 - 368	TLSSTLYR
3855.9528	3855.9544	-0.0016	369 - 403	RPFN...VYRK
3728.8574	3728.8434	0.0140	369 - 402	RPFN...AVYR
2276.1397	2276.1397	0.0000	403 - 423	KSGT...VPPR
2148.0428	2148.0447	-0.0019	404 - 423	SGTV...VPPR
730.3511	730.3511	0.0000	424 - 429	QGFSHR
991.4903	991.4909	-0.0006	430 - 437	LSHVSMFR
1252.6407	1252.6412	-0.0005	438 - 449	SGFS...SIIR
3313.7028	3313.6917	0.0111	450 - 478	APMF...PLVK
1159.5584	1159.5597	-0.0013	450 - 458	APMF...WIHR
2172.1415	2172.1426	-0.0011	459 - 478	SAEF...PLVK
2349.2157	2349.2230	-0.0073	479 - 501	GFRV...DILR
2145.1327	2145.1331	-0.0004	482 - 502	VWGG...ILRR
1989.0307	1989.0320	-0.0013	482 - 501	VWGG...DILR
2405.2478	2405.2452	0.0026	502 - 522	RNTF...ITQR
2249.1449	2249.1441	0.0008	503 - 522	NTFG...ITQR
582.2763	582.2762	0.0001	529 - 533	YASSR
2686.3830	2686.3848	-0.0018	534 - 560	DARV...PLQK
3979.0563	3979.0395	0.0168	537 - 574	VIVL...RTFR
2341.2660	2341.2676	-0.0016	537 - 560	VIVL...PLQK
1265.5941	1265.5921	0.0020	561 - 571	TMEI...LTSR
1783.8316	1783.8318	-0.0002	572 - 585	TFRY...FSFR
1379.6151	1379.6146	0.0005	575 - 585	YTDF...FSFR
4906.4632	4906.4651	-0.0019	586 - 631	ANPD...DLER
2890.4593	2890.4600	-0.0007	586 - 613	ANPD...YIDK
2034.0157	2034.0157	0.0000	614 - 631	IEII...DLER
1903.0537	1903.0527	0.0010	632 - 649	AQKA...LGLK
1575.8629	1575.8620	0.0009	635 - 649	AVNA...LGLK
3373.5741	3373.5773	-0.0032	650 - 677	TNVT...DEKR
3217.4756	3217.4762	-0.0006	650 - 676	TNVT...LDEK
604.3069	604.3068	0.0001	678 - 682	ELSEK
774.3985	774.3984	0.0001	688 - 693	RLSDER
2176.0869	2176.0872	-0.0003	689 - 706	LSDE...DINR
1677.8313	1677.8322	-0.0009	689 - 702	LSDE...SNFK
618.2971	618.2973	-0.0002	689 - 693	LSDER
2087.0445	2087.0395	0.0050	694 - 710	NLLQ...QPER

Experimental Mass[2]	Calculated Mass[3]	Difference[4]	Fragment[5]	Sequence[6]
1575.7995	1575.8005	-0.0010	694 - 706	NLLQ...DINR
1077.5453	1077.5455	-0.0002	694 - 702	NLLQ...SNFK
1026.5208	1026.5206	0.0002	703 - 710	DINRQPER
516.2657	516.2656	0.0001	703 - 706	DINR
528.2657	528.2656	0.0001	707 - 710	QPER
4367.0095	4366.9893	0.0202	711 - 749	GWGG...LYQK
1793.8585	1793.8585	0.0000	711 - 728	GWGG...DVFK
2590.1573	2590.1574	-0.0001	729 - 749	ENYV...LYQK
831.4696	831.4702	-0.0006	750 - 756	IDESKLK
590.2911	590.2911	0.0000	750 - 754	IDESK
734.4439	734.4439	0.0000	755 - 760	LKAFTR
493.2649	493.2649	0.0000	757 - 760	AFTR
578.3178	578.3176	0.0002	761 - 764	YQLR
1825.9087	1825.9098	-0.0011	765 - 779	GYIE...YLIR
2850.4694	2850.4664	0.0030	780 - 806	YNAK...PIGK
494.2488	494.2489	-0.0001	780 - 783	YNAK
3087.5154	3087.5196	-0.0042	784 - 812	HETV...EPNR
2374.2271	2374.2281	-0.0010	784 - 806	HETV...PIGK
731.3021	731.3021	0.0000	807 - 812	CGEPNR
2458.0083	2458.0100	-0.0017	813 - 832	CAPH...DGEK
2028.8214	2028.8241	-0.0027	813 - 828	CAPH...CSCR
447.1966	447.1965	0.0001	829 - 832	DGEK
1024.5408	1024.5414	-0.0006	863 - 871	IKTQ...GHAR
783.3619	783.3624	-0.0005	865 - 871	TQDGHAR
2097.1463	2097.1470	-0.0007	872 - 890	LGNL...ALAR
630.3810	630.3813	-0.0003	893 - 897	RAEKK
474.2802	474.2802	0.0000	894 - 897	AEKK
1550.7982	1550.7980	0.0002	903 - 914	EKLE...IVYK
1293.6611	1293.6605	0.0006	905 - 914	LEWE...IVYK
3707.7880	3707.7737	0.0143	915 - 947	EAKE...ADKR
3379.6122	3379.5990	0.0132	918 - 947	ESVD...ADKR
3223.5130	3223.4979	0.0151	918 - 946	ESVD...AADK
766.4562	766.4562	0.0000	947 - 952	RVHSIR
610.3551	610.3551	0.0000	948 - 952	VHSIR
3901.0010	3900.9825	0.0185	953 - 987	EAYL...YDAR
2615.3512	2615.3482	0.0030	953 - 976	EAYL...LEGR
1302.6603	1302.6608	-0.0005	977 - 987	IFTA...YDAR
2079.9615	2079.9684	-0.0069	988 - 1005	NVIK...WNVK
472.3009	472.3009	0.0000	988 - 991	NVIK
1625.6816	1625.6780	0.0036	992 - 1005	NGDF...WNVK

Experimental Mass[2]	Calculated Mass[3]	Difference[4]	Fragment[5]	Sequence[6]
1423.6424	1423.6440	-0.0016	1006 - 1017	GHVD...NNQR
1955.0013	1955.0000	0.0013	1018 - 1034	SVLV...QEVR
587.2849	587.2850	-0.0001	1035 - 1039	VCPGR
620.3647	620.3646	0.0001	1040 - 1044	GYILR
2969.3574	2969.3600	-0.0026	1045 - 1070	VTAY...DELK
2407.0470	2407.0485	-0.0015	1050 - 1070	EGYG...DELK
4023.6787	4023.6687	0.0100	1071 - 1104	FSNC...YTSR
2359.0612	2359.0604	0.0008	1105 - 1125	NRGY...YEEK
2923.3229	2923.3260	-0.0031	1107 - 1132	GYNE...DGRR
2767.2207	2767.2249	-0.0042	1107 - 1131	GYNE...TDGR
2087.9312	2087.9323	-0.0011	1107 - 1125	GYNE...YEEK
853.4045	853.4042	0.0003	1126 - 1132	SYTDGRR
697.3033	697.3031	0.0002	1126 - 1131	SYTDGR
1220.5350	1220.5356	-0.0006	1132 - 1140	RENP...EFNR
1441.6053	1441.6044	0.0009	1133 - 1143	ENPC...RGYR
1064.4347	1064.4345	0.0002	1133 - 1140	ENPCEFNR
1727.8873	1727.8883	-0.0010	1141 - 1155	GYRD...YVTK
1351.7031	1351.7024	0.0007	1144 - 1155	DYTP...YVTK
4017.9252	4017.9220	0.0032	1156 - 1189	ELEY...LMEE
1269.5788	1269.5765	0.0023	1156 - 1165	ELEY...ETDK
2766.3532	2766.3561	-0.0029	1166 - 1189	VWIE...LMEE

[1] All imported values were rounded to 4 decimal places.
[2] Only experimental masses that matched calculated masses with the highest scores are listed in the table.
[3] The calculated mass is the exact molecular mass calculated from the matched peptide sequence.
[4] The calculated difference = experimental mass – calculated mass.
[5] Position refers to amino acid residues within the predicted MON 94637-produced Cry1A.2 sequence as depicted in Figure 20.
[6] For peptide matches greater than nine amino acids in length, the first 4 residues and last 4 residues are shown separated by three dots (...).

Table 8. Summary of the Tryptic Masses Identified for the *Bt*-Produced Cry1A.2 Using LC-MS/MS[1]

Experimental Mass[2]	Calculated Mass[3]	Difference[4]	Fragment[5]	Sequence[6]
3316.5265	3316.5274	-0.0009	1 – 28	MEIV...EGGR
3185.4838	3185.4870	-0.0032	2 – 28	EIVN...EGGR
657.3810	657.3810	0.0000	88 - 93	IAEAVR
1331.6507	1331.6503	0.0004	94 - 105	NTAI...GMAR
1315.6096	1315.6084	0.0012	109 - 119	TYAT...EWEK
2209.0338	2209.0327	0.0011	109 - 127	TYAT...PELR
2678.2998	2678.2976	0.0022	109 - 131	TYAT...EALR
911.4350	911.4348	0.0002	120 - 127	APDDPELR
1380.7023	1380.6997	0.0026	120 - 131	APDD...EALR
1473.7094	1473.7100	-0.0006	132 - 144	TQFT...ISGR
558.3741	558.3741	0.0000	145 - 149	ISVLK
2710.5190	2710.5170	0.0020	150 - 173	IQTF...SLLR
3659.0012	3658.9988	0.0024	150 - 181	IQTF...FGQR
966.4912	966.4923	-0.0011	77 - 181	DVVFFGQR
3250.4745	3250.4731	0.0014	182 - 209	WGFS...YAVR
1037.4936	1037.4930	0.0006	210 - 217	WYNTGLER
815.3928	815.3926	0.0002	218 - 224	VWGPDSR
1371.6670	1371.6684	-0.0014	218 - 228	VWGP...DWVR
574.2857	574.2863	-0.0006	225 - 228	DWVR
726.3449	726.3449	0.0000	229 - 233	YNQFR
2334.2611	2334.2583	0.0028	234 - 253	RELT...YDSR
2178.1576	2178.1572	0.0004	235 - 253	ELTL...YDSR
2334.2612	2334.2583	0.0029	235 - 254	ELTL...DSRR
703.4130	703.4129	0.0001	254 - 258	RYPIR
547.3119	547.3118	0.0001	255 - 258	YPIR
803.4504	803.4501	0.0003	259 - 265	TVSQLTR
1899.9001	1899.9003	-0.0002	266 - 281	EIYT...GSFR
816.4085	816.4090	-0.0005	282 - 289	GSAQGIER
2196.1014	2196.0997	0.0017	293 - 311	SPHL...DAHR
4211.9324	4211.9299	0.0025	312 - 349	GYYY...PQQR
1202.6775	1202.6772	0.0003	350 - 360	IVAQ...GVYR
939.5024	939.5025	-0.0001	361 - 368	TLSSTLYR
3727.8615	3727.8594	0.0021	369 - 402	RPFN...AVYR
3855.9597	3855.9544	0.0053	369 - 403	RPFN...VYRK
2276.1402	2276.1397	0.0005	403 - 423	KSGT...VPPR
2148.0453	2148.0447	0.0006	404 - 423	SGTV...VPPR
730.3510	730.3511	-0.0001	424 - 429	QGFSHR
975.4963	975.4960	0.0003	430 - 437	LSHVSMFR
2210.1282	2210.1266	0.0016	430 - 449	LSHV...SIIR
1252.6411	1252.6412	-0.0001	438 - 449	SGFS...SIIR
1143.5649	1143.5648	0.0001	450 - 458	APMF...WIHR
2172.1417	2172.1426	-0.0009	459 - 478	SAEF...PLVK

Experimental Mass[2]	Calculated Mass[3]	Difference[4]	Fragment[5]	Sequence[6]
2532.3361	2532.3336	0.0025	459 - 481	SAEF...KGFR
2349.2212	2349.2230	-0.0018	479 - 501	GFRV...DILR
1989.0315	1989.0320	-0.0005	482 - 501	VWGG...DILR
2145.1305	2145.1331	-0.0026	482 - 502	VWGG...ILRR
2405.2463	2405.2452	0.0011	502 - 522	RNTF...ITQR
2249.1434	2249.1441	-0.0007	503 - 522	NTFG...ITQR
2325.2740	2325.2726	0.0014	537 - 560	VIVL...PLQK
1249.5970	1249.5972	-0.0002	561 - 571	TMEI...LTSR
1379.6153	1379.6146	0.0007	575 - 585	YTDF...FSFR
2890.4630	2890.4600	0.0030	586 - 613	ANPD...YIDK
4906.4690	4906.4651	0.0039	586 - 631	ANPD...DLER
2034.0169	2034.0157	0.0012	614 - 631	IEII...DLER
1903.0503	1903.0527	-0.0024	632 - 649	AQKA...LGLK
1575.8629	1575.8620	0.0009	635 - 649	AVNA...LGLK
3217.4778	3217.4762	0.0016	650 - 676	TNVT...LDEK
3373.5796	3373.5773	0.0023	650 - 677	TNVT...DEKR
760.4073	760.4079	-0.0006	677 - 682	RELSEK
774.3984	774.3984	0.0000	688 - 693	RLSDER
1677.8318	1677.8322	-0.0004	689 - 702	LSDE...SNFK
2176.0876	2176.0872	0.0004	689 - 706	LSDE...DINR
1077.5464	1077.5455	0.0009	694 - 702	NLLQ...SNFK
1575.7999	1575.8005	-0.0006	694 - 706	NLLQ...DINR
2086.0559	2086.0555	0.0004	694 - 710	NLLQ...QPER
1026.5203	1026.5206	-0.0003	703 - 710	DINRQPER
1793.8552	1793.8585	-0.0033	711 - 728	GWGG...DVFK
4366.0098	4366.0053	0.0045	711 - 749	GWGG...LYQK
2590.1603	2590.1574	0.0029	729 - 749	ENYV...LYQK
831.4693	831.4702	-0.0009	750 - 756	IDESKLK
493.2632	493.2649	-0.0017	757 - 760	AFTR
578.3176	578.3176	0.0000	761 - 764	YQLR
1825.9106	1825.9098	0.0008	765 - 779	GYIE...YLIR
2850.4687	2850.4664	0.0023	780 - 806	YNAK...PIGK
2374.2276	2374.2281	-0.0005	784 - 806	HETV...PIGK
3087.5146	3087.5196	-0.0050	784 - 812	HETV...EPNR
2028.8260	2028.8241	0.0019	813 - 828	CAPH...CSCR
2458.0056	2458.0100	-0.0044	813 - 832	CAPH...DGEK
1024.5417	1024.5414	0.0003	863 - 871	IKTQ...GHAR
783.3623	783.3624	-0.0001	865 - 871	TQDGHAR
2097.1485	2097.1470	0.0015	872 - 890	LGNL...ALAR
502.2864	502.2863	0.0001	893 - 896	RAEK
1550.8023	1550.7980	0.0043	903 - 914	EKLE...IVYK
1293.6620	1293.6605	0.0015	905 - 914	LEWE...IVYK
3690.7924	3690.7947	-0.0023	915 - 947	EAKE...ADKR

Experimental Mass[2]	Calculated Mass[3]	Difference[4]	Fragment[5]	Sequence[6]
3206.5182	3206.5190	-0.0008	918 - 946	ESVD...AADK
3362.6200	3362.6201	-0.0001	918 - 947	ESVD...ADKR
766.4563	766.4562	0.0001	947 - 952	RVHSIR
610.3551	610.3551	0.0000	948 - 952	VHSIR
2615.3487	2615.3482	0.0005	953 - 976	EAYL...LEGR
1302.6604	1302.6608	-0.0004	977 - 987	IFTA...YDAR
1623.7109	1623.7100	0.0009	992 - 1005	NGDF...WNVK
1423.6446	1423.6440	0.0006	1006 - 1017	GHVD...NNQR
3360.6220	3360.6335	-0.0115	1006 - 1034	GHVD...QEVR
1954.9994	1955.0000	-0.0006	1018 - 1034	SVLV...QEVR
587.2849	587.2850	-0.0001	1035 - 1039	VCPGR
620.3645	620.3646	-0.0001	1040 - 1044	GYILR
2406.0657	2406.0645	0.0012	1050 - 1070	EGYG...DELK
4022.6892	4022.6847	0.0045	1071 - 1104	FSNC...YTSR
2358.0772	2358.0764	0.0008	1105 - 1125	NRGY...YEEK
2087.9303	2087.9323	-0.0020	1107 - 1125	GYNE...YEEK
2767.2270	2767.2249	0.0021	1107 - 1131	GYNE...TDGR
2923.3209	2923.3260	-0.0051	1107 - 1132	GYNE...DGRR
697.3034	697.3031	0.0003	1126 - 1131	SYTDGR
853.4041	853.4042	-0.0001	1126 - 1132	SYTDGRR
1220.5354	1220.5356	-0.0002	1132 - 1140	RENP...EFNR
1064.4327	1064.4345	-0.0018	1133 - 1140	ENPCEFNR
1440.6213	1440.6204	0.0009	1133 - 1143	ENPC...RGYR
1727.8894	1727.8883	0.0011	1141 - 1155	GYRD...YVTK
1351.7022	1351.7024	-0.0002	1144 - 1155	DYTP...YVTK
1269.5766	1269.5765	0.0001	1156 - 1165	ELEY...ETDK
4001.9270	4001.9271	-0.0001	1156 - 1189	ELEY...LMEE
2750.3618	2750.3612	0.0006	1166 - 1189	VWIE...LMEE

[1] All imported values were rounded to 4 decimal places.
[2] Only experimental masses that matched calculated masses with the highest scores are listed in table.
[3] The calculated mass is the exact molecular mass calculated from the matched peptide sequence.
[4] The calculated difference = experimental mass – calculated mass.
[5] Position refers to amino acid residues within the predicted *Bt*-produced Cry1A.2 sequence as depicted in Figure 20.
[6] For peptide matches greater than nine amino acids in length the first 4 residues and last 4 residues are shown separated by dots (…).

(A)

```
1    MEIVNNQNQC VPYNCLNNPE IEILEGGRIS VGNTPIDISL SLTQFLLSEF
51   VPGAGFVLGL IDLIWGFVGP SQWDAFLAQV EQLINQRIAE AVRNTAIQEL
101  EGMARVYRTY ATAFAEWEKA PDDPELREAL RTQFTATETY ISGRISVLKI
151  QTFEVQLLSV FAQAANLHLS LLRDVVFFGQ RWGFSTTTVN NYYNDLTEGI
201  STYTDYAVRW YNTGLERVWG PDSRDWVRYN QFRRELTLTV LDIVALFPNY
251  DSRRYPIRTV SQLTREIYTN PVLENFDGSF RGSAQGIERS IRSPHLMDIL
301  NSITIYTDAH RGYYYWSGHQ IMASPVGFSG PEFTFPLYGT MGNAAPQQRI
351  VAQLGQGVYR TLSSTLYRRP FNIGINNQQL SVLDGTEFAY GTSSNLPSAV
401  YRKSGTVDSL DEIPPQNNNV PPRQGFSHRL SHVSMFRSGF SNSSVSIIRA
451  PMFSWIHRSA EFNNIIASDS INQIPLVKGF RVWGGTSVIT GPGFTGGDIL
501  RRNTFGDFVS LQVNINSPIT QRYRLRFRYA SSRDARVIVL TGAASTGVGG
551  QVSVNMPLQK TMEIGENLTS RTFRYTDFSN PFSFRANPDI IGISEQPLFG
601  AGSISSGELY IDKIEIILAD ATFEAESDLE RAQKAVNALF TSTNQLGLKT
651  NVTDYHIDQV SNLVTYLSDE FCLDEKRELS EKVKHAKRLS DERNLLQDSN
701  FKDINRQPER GWGGSTGITI QGGDDVFKEN YVTLSGTFDE CYPTYLYQKI
751  DESKLKAFTR YQLRGYIEDS QDLEIYLIRY NAKHETVNVP GTGSLWPLSA
801  QSPIGKCGEP NRCAPHLEWN PDLDCSCRDG EKCAHHSHHF SLDIDVGCTD
851  LNEDLGVWVI FKIKTQDGHA RLGNLEFLEE KPLVGEALAR VKRAEKKWRD
901  KREKLEWETN IVYKEAKESV DALFVNSQYD QLQADTNIAM IHAADKRVHS
951  IREAYLPELS VIPGVNAAIF EELEGRIFTA FSLYDARNVI KNGDFNNGLS
1001 CWNVKGHVDV EEQNNQRSVL VVPEWEAEVS QEVRVCPGRG YILRVTAYKE
1051 GYGEGCVTIH EIENNTDELK FSNCVEEEIY PNNTVTCNDY TVNQEEYGGA
1101 YTSRNRGYNE APSVPADYAS VYEEKSYTDG RRENPCEFNR GYRDYTPLPV
1151 GYVTKELEYF PETDKVWIEI GETEGTFIVD SVELLLMEE
```

(B)

```
1    MEIVNNQNQC VPYNCLNNPE IEILEGGRIS VGNTPIDISL SLTQFLLSEF
51   VPGAGFVLGL IDLIWGFVGP SQWDAFLAQV EQLINQRIAE AVRNTAIQEL
101  EGMARVYRTY ATAFAEWEKA PDDPELREAL RTQFTATETY ISGRISVLKI
151  QTFEVQLLSV FAQAANLHLS LLRDVVFFGQ RWGFSTTTVN NYYNDLTEGI
201  STYTDYAVRW YNTGLERVWG PDSRDWVRYN QFRRELTLTV LDIVALFPNY
251  DSRRYPIRTV SQLTREIYTN PVLENFDGSF RGSAQGIERS IRSPHLMDIL
301  NSITIYTDAH RGYYYWSGHQ IMASPVGFSG PEFTFPLYGT MGNAAPQQRI
351  VAQLGQGVYR TLSSTLYRRP FNIGINNQQL SVLDGTEFAY GTSSNLPSAV
401  YRKSGTVDSL DEIPPQNNNV PPRQGFSHRL SHVSMFRSGF SNSSVSIIRA
451  PMFSWIHRSA EFNNIIASDS INQIPLVKGF RVWGGTSVIT GPGFTGGDIL
501  RRNTFGDFVS LQVNINSPIT QRYRLRFRYA SSRDARVIVL TGAASTGVGG
551  QVSVNMPLQK TMEIGENLTS RTFRYTDFSN PFSFRANPDI IGISEQPLFG
601  AGSISSGELY IDKIEIILAD ATFEAESDLE RAQKAVNALF TSTNQLGLKT
651  NVTDYHIDQV SNLVTYLSDE FCLDEKRELS EKVKHAKRLS DERNLLQDSN
701  FKDINRQPER GWGGSTGITI QGGDDVFKEN YVTLSGTFDE CYPTYLYQKI
751  DESKLKAFTR YQLRGYIEDS QDLEIYLIRY NAKHETVNVP GTGSLWPLSA
801  QSPIGKCGEP NRCAPHLEWN PDLDCSCRDG EKCAHHSHHF SLDIDVGCTD
851  LNEDLGVWVI FKIKTQDGHA RLGNLEFLEE KPLVGEALAR VKRAEKKWRD
901  KREKLEWETN IVYKEAKESV DALFVNSQYD QLQADTNIAM IHAADKRVHS
951  IREAYLPELS VIPGVNAAIF EELEGRIFTA FSLYDARNVI KNGDFNNGLS
1001 CWNVKGHVDV EEQNNQRSVL VVPEWEAEVS QEVRVCPGRG YILRVTAYKE
1051 GYGEGCVTIH EIENNTDELK FSNCVEEEIY PNNTVTCNDY TVNQEEYGGA
```

1101 YTSRNRGYNE APSVPADYAS VYEEKSYTDG RRENPCEFNR GYRDYTPLPV
1151 GYVTKELEYF PETDKVWIEI GETEGTFIVD SVELLLMEE

Figure 20. Peptide Map of the MON 94637-Produced and *Bt*-Produced Cry1A.2 Proteins

(A). The amino acid sequence of the MON 94637-produced Cry1A.2 protein was deduced from the *cry1A.2* gene present in MON 94637. Boxed regions correspond to peptides that were identified from the MON 94637-produced Cry1A.2 protein sample using LC-MS/MS. In total, 95% coverage (1135 out of 1189 amino acids) of the expected protein sequence was covered by the identified peptides.
(B). The amino acid sequence of the *Bt*-produced Cry1A.2 protein was deduced from the *cry1A.2* gene that is contained on the expression plasmid pMON144763. Boxed regions correspond to peptides that were identified from the *Bt*-produced Cry1A.2 protein sample using LC-MS/MS. In total, 88% coverage (1057 out of 1189 amino acids) of the expected protein sequence was covered by the identified peptides.

B.1(a)(ii)(i)(iii) Results of Western blot analysis of the Cry1A.2 protein isolated from the grain of MON 94367 and immunoreactivity comparison to *Bt*-produced Cry1A.2 protein

Western blot analysis was conducted using a mouse anti-Cry1A.2 monoclonal antibody as additional means to confirm the identity of the Cry1A.2 protein isolated from the seed of MON 94637 soybean and to assess the equivalence of the immunoreactivity of the MON 94637-produced and *Bt*-produced Cry1A.2 proteins.

The results showed that a major intact immunoreactive band with the same electrophoretic mobility was present in all lanes loaded with the MON 94637-produced and *Bt*-produced Cry1A.2 proteins as well as a few minor bands above ~70 kDa were also present in all lanes loaded with *Bt*-produced Cry1A.2 proteins (Figure 21). These minor bands above ~70 kDa could be due to degradation that occurred during the protein extraction, purification process, storage and/or sample preparation for western analysis. For each amount loaded, comparable signal intensity was observed between the MON 94637-produced and *Bt*-produced Cry1A.2 protein bands. As expected, the signal intensity increased with increasing load amounts of the MON 94637-produced and *Bt*-produced Cry1A.2 proteins, thus supporting identification of MON 94637-produced Cry1A.2 protein. One other band migrating at >220 kDa was also observed. This band was observed in lanes with higher load amounts of both protein samples and, therefore, may represent an aggregation of the Cry1A.2 occurring during sample preparation.

To compare the immunoreactivity of the MON 94637-produced and *Bt*-produced Cry1A.2 proteins, densitometric analysis was conducted on the bands that migrated at the expected apparent MW for the intact Cry1A.2 proteins (~ 125 kDa) for MON 94637-produced Cry1A.2 proteins as well as for the intact Cry1A.2 proteins (~125 kDa) and additional minor bands at ~120, ~110, ~87, and ~70 kDa of the *Bt*-produced Cry1A.2 proteins. The signal intensity (reported in OD) of the bands of interest in lanes loaded with MON 94637-produced and *Bt*-produced Cry1A.2 proteins were measured (Table 9). Because the mean signal intensity of the MON 94637-produced Cry1A.2 protein was within 35% of the mean signal intensity summation of the immunoreactive signal of the intact band (~125 kDa) and all minor bands above ~70 kDa of the reference substance, the MON 94637-produced Cry1A.2 and *Bt*-produced Cry1A.2 proteins were determined to have equivalent immunoreactivity.

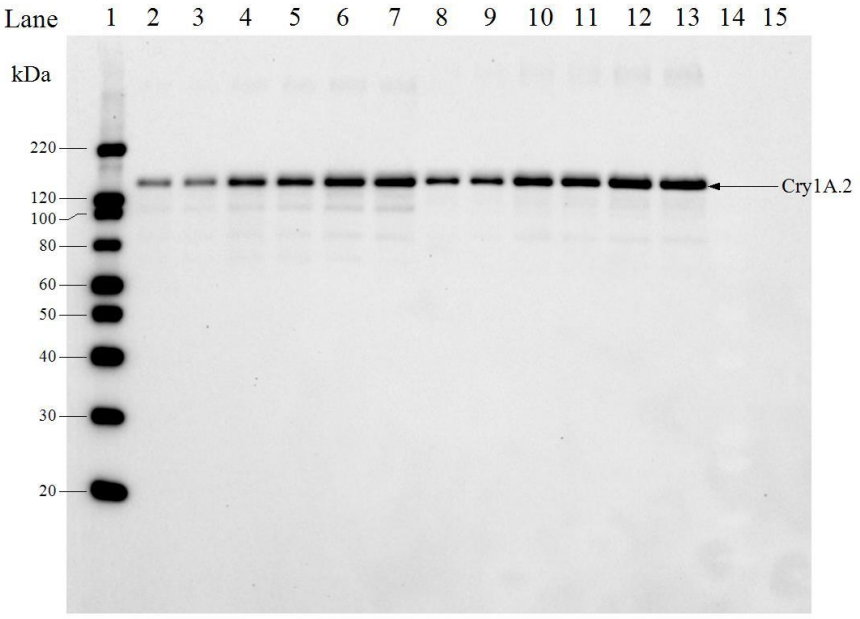

Figure 21. Western Blot Analysis and Immunoreactivity of MON 94637-Produced and *Bt*-Produced Cry1A.2 Proteins

Aliquots of the MON 94637-produced and *Bt*-produced Cry1A.2 proteins were subjected to SDS-PAGE and electrotransferred to a nitrocellulose membrane. Proteins were detected using mouse anti-Cry1A.2 monoclonal antibody as the primary antibody. Immunoreactive bands were visualized using HRP-conjugated secondary antibodies and an ECL system. The 33-second exposure is shown. The approximate MW (kDa) of the standards are shown on the left. Lane designations are as follows:

Lane	Sample	Amount (ng)
1	MagicMark XP™ Western Protein Standards	-
2	*Bt*-produced Cry1A.2	5
3	*Bt*-produced Cry1A.2	5
4	*Bt*-produced Cry1A.2	10
5	*Bt*-produced Cry1A.2	10
6	*Bt*-produced Cry1A.2	20
7	*Bt*-produced Cry1A.2	20
8	MON 94637-produced Cry1A.2	5
9	MON 94637-produced Cry1A.2	5
10	MON 94637-produced Cry1A.2	10
11	MON 94637-produced Cry1A.2	10
12	MON 94637-produced Cry1A.2	20
13	MON 94637-produced Cry1A.2	20
14	Precision Plus Protein™ Standards	-
15	Blank	-

Table 9. Immunoreactivity of the MON 94367-Produced and *Bt*-Produced Cry1A.2 Proteins

Mean Signal Intensity from MON 94637-Produced Cry1A.2 [1] (OD)	Mean Signal Intensity from *Bt*-produced Cry1A.2 [1] (OD)	Acceptance Limits [2] (OD)
5,670,726.83	4,303,588.83	2,797,332.74 – 5,809,844.92

[1] Each value represents the mean of six values (n = 6).
[2] The acceptance limits are for the MON 94637-produced Cry1A.2 protein and are based on the interval between -35% (4,303,588.83 x 0.65 = 2,797,332.74) and +35 % (4,303,588.83 x 1.35 = 5,809,844.92) of the mean of the *Bt*-produced Cry1A.2 signal intensity across all loads.

B.1(a)(ii)(i)(iv) Results of the Cry1A.2 protein molecular weight and purity analysis

For apparent MW and purity determination, the MON 94637-produced Cry1A.2 and the *Bt*-produced Cry1A.2 proteins were subjected to SDS-PAGE. Following electrophoresis, the gel was stained with Brilliant Blue G-Colloidal stain and analyzed by densitometry. The MON 94637-produced Cry1A.2 protein (Figure 22, lanes 3-8) migrated to the same position on the gel as the *Bt*-produced Cry1A.2 protein ((Figure 22, lane 2) and the apparent MW was calculated to be 124.2 kDa (Table 10). Because the experimentally determined apparent MW of the MON 94637-produced Cry1A.2 protein was within the acceptance limits (115.3 kDa to 133.5 kDa) for equivalence (Table 11), the MON 94637-produced Cry1A.2 and *Bt*-produced Cry1A.2 proteins were determined to have equivalent apparent molecular weights.

The purity of the MON 94637-produced Cry1A.2 protein was calculated based on the six lanes loaded on the gel ((Figure 22, lanes 3-8). The average purity was determined to be 98% (Table 10).

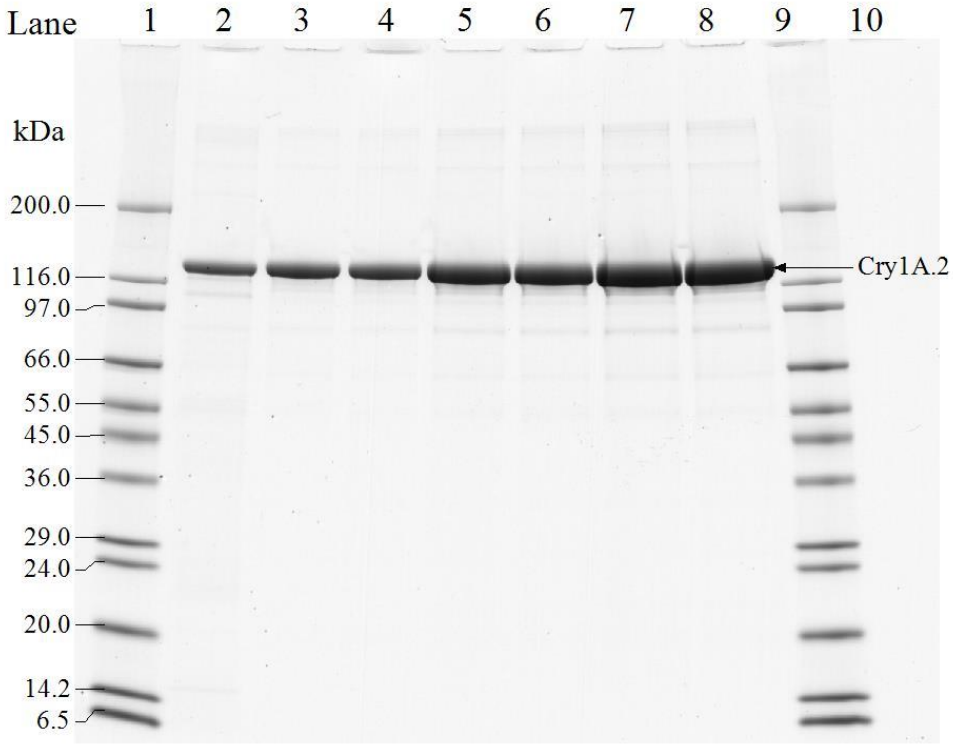

Figure 22. Purity and Apparent Molecular Weight Analysis of the MON 94637-Produced Cry1A.2 Proteins

Aliquots of the MON 94637-produced and the *Bt*-produced Cry1A.2 proteins were subjected to SDS-PAGE and the gel was stained with Brilliant Blue G-Colloidal stain. The MWs (kDa) are shown on the left and correspond to the standards loaded in lanes 1 and 9. The Cry1A.2 protein is indicated with an arrow in the image. Lane designations are as follows:

Lane	Sample	Amount (µg)
1	SigmaMarker™ Wide Range	N/A
2	*Bt*-produced Cry1A.2	1.0
3	MON 94637-produced Cry1A.2	1.0
4	MON 94637-produced Cry1A.2	1.0
5	MON 94637-produced Cry1A.2	2.0
6	MON 94637-produced Cry1A.2	2.0
7	MON 94637-produced Cry1A.2	3.0
8	MON 94637-produced Cry1A.2	3.0
9	SigmaMarker™ Wide Range	N/A
10	Blank	

Table 10. Apparent Molecular Weight and Purity Analysis of the MON 94637-Produced Cry1A.2 Protein

	Apparent MW[1] (kDa)	Purity[2] (%)
Average (n=6)	124.2	98

[1]Final MW was rounded to one decimal place.
[2]Average % purity was rounded to the nearest whole number.

Table 11. Apparent Molecular Weight Comparison Between the MON 94367- and *Bt*-Produced Cry1A.2 Proteins

Apparent MW of MON 94637-Produced Cry1A.2 Protein (kDa)	Apparent MW of Bt-produced Cry1A.2 Protein[1] (kDa)	Acceptance Limits[2] (kDa)
124.2	124.4	115.3 – 133.5

[1] As reported on the COA of the *Bt*-produced Cry1A.2 protein.
[2] Data obtained for the *Bt*-produced Cry1A.2 protein was used to generate the prediction interval (Appendix 6).

B.1(a)(ii)(i)(v) Cry1A.2 glycosylation analysis

Some eukaryotic proteins are post-translationally modified by the addition of carbohydrate moieties (Rademacher *et al.*, 1988). To test whether the Cry1A.2 protein was glycosylated when expressed in the seed of MON 94637 soybean, the MON 94637-produced Cry1A.2 protein was analyzed using an ECL™ glycoprotein detection method. Transferrin, a glycosylated protein, was used as a positive control in the assay. To assess equivalence of the MON 94637-produced and *Bt*-produced Cry1A.2 proteins, the *Bt*-produced Cry1A.2 protein was also analyzed.

A clear glycosylation signal was observed at the expected molecular weight (~80 kDa) in the lanes containing the positive control (transferrin) and the band intensity increased with increasing concentration (Figure 23A). In contrast, no glycosylation signal was observed in the lanes containing the *Bt*-produced Cry1A.2 protein or MON 94637-produced Cry1A.2 protein (Figure 23A).

To confirm that MON 94637-produced Cry1A.2 and *Bt*-produced Cry1A.2 proteins were appropriately loaded for glycosylation analysis, a second membrane with identical loadings and transfer time was stained with Coomassie Blue R250 for protein detection. Both the MON 94637-produced and *Bt*-produced Cry1A.2 proteins were detected (Figure 23B). These data indicate that the glycosylation status of MON 94637-produced Cry1A.2 protein is equivalent to that of the *Bt*-produced Cry1A.2 protein and that neither is glycosylated.

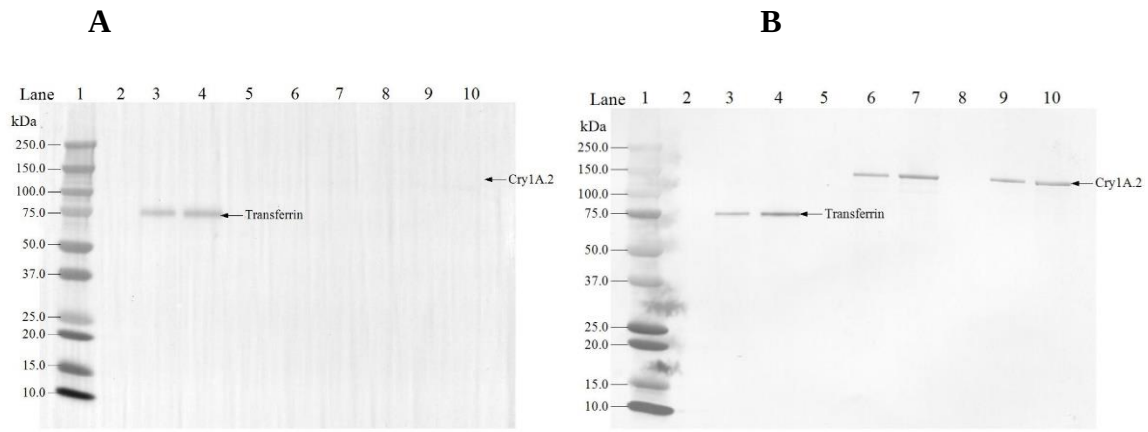

Figure 23. Glycosylation Analysis of the MON 94367-Produced and *Bt*-produced Cry1A.2 Proteins

Aliquots of the transferrin (positive control), *Bt*-produced Cry1A.2 and MON 94637-produced Cry1A.2 proteins were subjected to SDS-PAGE and electrotransferred to a PVDF membrane. The MWs (kDa) correspond to the Precision Plus Protein™ Standards. The arrows show the expected migration of the MON 94637-produced and *Bt*-produced Cry1A.2 proteins and transferrin. (A) Where present, the labeled carbohydrate moieties were detected by using ECL reagents and blot images were captured using a Bio-Rad ChemiDoc Imager. The 30-second exposure is shown. (B) An equivalent blot was stained with Coomassie Blue R250 to confirm the presence of proteins. Lane designations are as follows:

Lane	Sample	Amount (ng)
1	Precision Plus Protein™ Standards	N/A
2	Blank	-
3	Transferrin (positive control)	100
4	Transferrin (positive control)	200
5	Blank	-
6	*Bt*-produced Cry1A.2	100
7	*Bt*-produced Cry1A.2	200
8	Blank	-
9	MON 94637-produced Cry1A.2	100
10	MON 94637-produced Cry1A.2	200

B.1(a)(ii)(i)(vi) Cry1A.2 functional activity

The MON 94637-produced Cry1A.2 and *Bt*-produced Cry1A.2 proteins were considered to have equivalent functional activity if the functional activity of both proteins (EC_{50}) were not significantly different, when compared using a t-test.

The experimentally determined functional activity for the MON 94637-produced and *Bt*-produced Cry1A.2 proteins are presented in Table 12. EC_{50} values were determined as the concentration of Cry1A.2 (µg/ml diet) that resulted in 50% insect mass reduction relative to the control treatment in a European corn borer insect bioassay. The mean EC_{50} of MON 94637-produced and *Bt*-produced Cry1A.2 proteins, were 0.13 and 0.10 µg of Cry1A.2 protein/ml diet, respectively. Because no significant difference for the mean EC_{50} values of both proteins was observed with a two-sided t-test ($p > 0.05$) (Table 12), the MON 94637-produced Cry1A.2 protein was considered to have equivalent functional activity to that of the *Bt*-produced Cry1A.2 protein.

Table 12. Functional Activity of the MON 94637-Produced and *Bt*-Produced Cry1A.2 Proteins

Replicates [1]	MON 94637-Produced Cry1A.2 (µg protein/ml diet)	*Bt*-produced Cry1A.2 (µg protein/ml diet)	t-test [3] (p-value)
1	0.19	0.13	
2	0.07	0.10	
5	0.14	0.09	
Mean[2]	0.13	0.10	0.4076

[1] Replicates 3 and 4 were rejected because they failed to meet the pre-set assay acceptance criteria.
[2] Value refers to mean calculated based on three independent assays (n=3).
[3] No significant difference is based on a=0.05.

B.1(a)(ii)(i)(vii) Cry1A.2 protein identity and equivalence conclusion

The MON 94637-produced Cry1A.2 protein purified from MON 94637 grain was characterised, and a comparison of the physicochemical and functional properties between the MON 94637-produced and the *Bt*-produced Cry1A.2 proteins was conducted following a panel of analytical tests: 1) N-terminal sequence analysis established the same identity for the MON 94637-produced and the *Bt*-produced Cry1A.2 proteins; 2) Nano LC-MS/MS analysis yielded peptide masses consistent with the expected peptide masses from the theoretical trypsin digest of the *cry1A.2* gene product present in MON 94637; 3) the MON 94637-produced and the *Bt*-produced Cry1A.2 proteins were both detected on a western blot probed with antibodies specific for Cry1A.2 protein and the immunoreactive properties of both proteins was shown to be equivalent; 4) the electrophoretic mobility and apparent molecular weight of the MON 94637-produced and the *Bt*-produced Cry1A.2 proteins were shown to be equivalent; 5) the glycosylation status of MON 94637-produced and the *Bt*-produced Cry1A.2 proteins was determined to be equivalent; and 6) the functional activity of the MON 94637-produced and the *Bt*-produced Cry1A.2 was demonstrated to be functionally not different These results demonstrate that the MON 94637-produced and the *Bt*-produced Cry1A.2 protein are equivalent. This demonstration of protein equivalence confirms that the *Bt*-produced Cry1A.2 protein is appropriate for use in the evaluation of the safety of the MON 94637-produced Cry1A.2 protein.

B.1(a)(ii)(ii) Characterisation of the Cry1B.2 protein

The details of the materials and methods for the panel of analytical tests used to evaluate and compare the properties of the MON 94637-produced Cry1B.2 and *Bt*-produced Cry1B.2 proteins are described at the end of Appendix **7**.

For the safety data generated using the *Bt*-produced Cry1B.2 protein to be applied to the MON 94637-produced Cry1B.2 protein (plant-produced Cry1B.2), the equivalence of the plant- and *Bt*-produced proteins must first be demonstrated. To assess the equivalence between the MON 94637-produced and *Bt*-produced Cry1B.2 proteins, a small quantity of the MON 94637-produced Cry1B.2 protein was purified from MON 94637 grain. The MON 94637-produced Cry1B.2 protein was characterised and the equivalence of the physicochemical characteristics and functional activity between the MON 94637-produced and *Bt*-produced Cry1B.2 proteins was assessed using a panel of analytical tests,as shown in Table 13. Taken together, these data provide a detailed characterisation of the MON 94637-produced Cry1B.2 protein and establish the equivalence of the MON 94637-produced and *Bt*-produced Cry1B.2 proteins.

Table 13. Summary of MON 94637 Cry1B.2 Protein Identity and Equivalence

Analytical Test Assessment	Section Cross Reference	Analytical Test Outcome
N-terminal sequence	B.1(a)(ii)(ii)(i)	The expected N-terminal sequence for MON 94637-produced Cry1B.2 protein was observed by Nano LC-MS/MS[1]
Nano LC-MS/MS[1]	B.1(a)(ii)(ii)(ii)	Nano LC-MS/MS[1] analysis of trypsin digested peptides from MON 94637-produced Cry1B.2 protein yielded peptide masses consistent with expected peptide masses from the theoretical trypsin digest of the amino acid sequence
Western blot analysis	B.1(a)(ii)(ii)(iii)	MON 94637-produced Cry1B.2 protein identity was confirmed using a western blot probed with antibodies specific for Cry1B.2 protein Immunoreactive properties of the MON 94637-produced Cry1B.2 and the *Bt*-produced Cry1B.2 proteins were shown to be equivalent
Apparent molecular weight (MW)	B.1(a)(ii)(ii)(iv)	Electrophoretic mobility and apparent molecular weight of the MON 94637-produced Cry1B.2 and the *Bt*-produced Cry1B.2 proteins were shown to be equivalent
Glycosylation analysis	B.1(a)(ii)(ii)(v)	Glycosylation status of MON 94637-produced Cry1B.2 and *Bt*-produced Cry1B.2 proteins were shown to be equivalent
Functional activity	B.1(a)(ii)(ii)(vi)	Functional activity of the MON 94637-produced Cry1B.2 and the *Bt*-produced Cry1B.2 proteins were shown to be functionally equivalent by insect bioassay

[1] Nano LC-MS/MS = Nanoscale liquid chromatography-tandem mass spectrometry

B.1(a)(ii)(ii)(i) Results of the N-terminal sequencing analysis

The expected N-terminal sequence for the Cry1B.2 protein deduced from the *cry1B.2* gene present in seed of MON 94637 soybean was observed by LC-MS/MS (see Experimental Sequence, Figure 24), except that the N-terminal methionine was cleaved *in vivo* from MON 94637-produced Cry1B.2 by methionine aminopeptidase or other aminopeptidases (see Experimental Sequence, Figure 24). The cleavage of the N-terminal methionine from proteins *in vivo* by methionine aminopeptidase is common in many organisms (Bradshaw *et al.*, 1998; Giglione *et al.*, 2004; Wingfield, 2017). The N-terminal sequence for MON 94637-produced Cry1B.2 protein was consistent with the N-terminal sequence for the *Bt*-produced Cry1B.2 protein observed by LC-MS/MS (Figure 24 and Appendix 7). Hence, the sequence information confirms the identity of the Cry1B.2 protein isolated from the seed of MON 94637 soybean.

Amino Acids Residue # from the N-terminus	→	1	2	3	4	5	6	7	8	9	10	11	12	13	14	15
Bt-produced Cry1B.2 sequence	→	X	T	S	N	R	K	N	E	N	E	I	I	N	A	L
Expected Cry1B.2 Sequence	→	M	T	S	N	R	K	N	E	N	E	I	I	N	A	L
MON 94637 Experimental Sequence	→	X	T	S	N	R	K	N	E	N	E	I	I	N	A	L

Figure 24. N-Terminal Sequence of the MON 94637-Produced Cry1B.2 Protein

The experimental sequence obtained from the MON 94637-produced Cry1B.2 protein was compared to the expected sequence deduced from the *cry1B.2* gene present in MON 94637. *Bt*-produced Cry1B.2 protein sequence above was derived from the reference substance COA (lot 7917). The experimentally determined sequence (initial fifteen amino acids shown) corresponds to the deduced Cry1B.2 protein beginning at the second amino acid position, threonine. The single letter International Union of Pure and Applied Chemistry - International Union of Biochemistry (IUPAC-IUB) amino acid code is M, Methionine; T, Threonine; S: Serine, N, Asparagine, R, Arginine, K, lysine, E, Glutamic acid; I, Isoleucine; A, alanine, L, leucine, 'X' indicates the residue was not observed.

B.1(a)(ii)(ii)(ii) Results of mass fingerprint analysis

Peptide mass fingerprint analysis is a standard technique used for confirming the identity of proteins. The ability to identify a protein using this method is dependent upon matching a sufficient number of observed tryptic peptide fragment masses with predicted tryptic peptide fragment masses. In general, protein identification made by peptide mapping is considered to be reliable if >40% of the protein sequence was identified by matching experimental masses observed for the tryptic peptide fragments to the expected masses for the fragments (Biron *et al.*, 2006; Krause *et al.*, 1999). The identity of the MON 94637-produced Cry1B.2 protein was confirmed by LC-MS/MS analysis of peptide fragments produced by the trypsin digestion of the MON 94637-produced Cry1B.2 protein.

There were 115 unique peptides identified that corresponded to the masses expected to be produced by trypsin digestion of the MON 94637-produced Cry1B.2 protein (Table 14). The identified masses were used to assemble a coverage map of the entire Cry1B.2 protein (Figure 25). The experimentally determined coverage of the MON 94637-produced Cry1B.2 protein

was 92% (Figure 25, 1097 out of 1187 amino acids). This analysis further confirms the identity of MON 94637-produced Cry1B.2 protein.

There were 89 unique peptides identified that corresponded to the masses expected to be produced by trypsin digestion of the *Bt*-produced Cry1B.2 protein (Table 15) by LC-MS/MS analysis during the protein characterisation. The identified masses were used to assemble a coverage map of the entire Cry1B.2 protein (Figure 25B). The experimentally determined coverage of the *Bt*-produced Cry1B.2 protein was 66% (Figure 25B, 792 out of 1187 amino acids).

Table 14. Summary of the Tryptic Masses Identified for MON 94637-Produced Cry1B.2 Protein Using Nano LC-MS/MS[1]

Experimental Mass[2]	Calculated Mass[3]	Diff[4]	Fragment[5]	Sequence[6]
646.3404	646.3398	0.0006	2 - 6	TSNRK
3136.5606	3136.5571	0.0035	6 - 34	KNEN...TDAR
3260.5962	3260.5983	- 0.0021	35 - 65	IEDS...IAGR
2935.5966	2935.6000	- 0.0034	66 - 92	ILGV...LWPR
2136.1122	2136.1116	0.0006	93 - 109	GRDP...QLIR
1602.7967	1602.7961	0.0006	110 - 123	QQVT...ALAR
974.4770	974.4781	- 0.0011	110 - 117	QQVTENTR
3251.6008	3251.5959	0.0049	118 - 145	DTAL...LENR
645.3448	645.3446	0.0002	118 - 123	DTALAR
990.5249	990.5247	0.0002	124 - 132	LQGL...NSFR
2107.9574	2107.9559	0.0015	133 - 149	AYQQ...DDAR
1650.7625	1650.7638	- 0.0013	133 - 145	AYQQ...LENR
2800.4849	2800.4873	- 0.0024	152 - 175	SVLY...FAIR
2518.4049	2518.4093	- 0.0044	176 - 197	NQEV...LLLR
1983.9535	1983.9538	- 0.0003	198 - 215	DASL...EIQR
629.2812	629.2809	0.0003	216 - 219	YYER
760.4117	760.4079	0.0038	220 - 225	QVEKTR
502.2752	502.2751	0.0001	220 - 223	QVEK
1319.5558	1319.5564	- 0.0006	224 - 233	TREY...YCAR
1062.4067	1062.4076	- 0.0009	226 - 233	EYSDYCAR
1249.6197	1249.6203	- 0.0006	234 - 243	WYNT...NNLR
1032.4989	1032.4988	0.0001	244 - 252	GTNA...SWLR
883.4298	883.4300	- 0.0002	253 - 258	YNQFRR
726.3451	726.3449	0.0002	253 - 257	YNQFR
2263.2216	2263.2212	0.0004	258 - 277	RDLT...YDTR
2107.1197	2107.1201	- 0.0004	259 - 277	DLTL...YDTR
1379.6858	1379.6867	- 0.0009	278 - 289	VYPM...QLTR
1062.5348	1062.5346	0.0002	290 - 298	EIYT...PIGR
5244.6467	5244.6309	0.0158	299 - 346	TNAP...VLSR
2326.0695	2326.0701	- 0.0006	347 - 364	WSNT...LESR
1840.8083	1840.8104	- 0.0021	347 - 360	WSNT...VGHR
503.2705	503.2703	0.0002	361 - 364	LESR
2619.2904	2619.2889	0.0015	368 - 392	GSLS...FTSR
2888.5173	2888.5185	- 0.0012	393 - 418	DVYR...PWAR
551.2704	551.2704	0.0000	393 - 396	DVYR
2356.2447	2356.2427	0.0020	397 - 418	TESF...PWAR
1416.7239	1416.7262	- 0.0023	419 - 429	FNWR...NSLR
621.3022	621.3023	- 0.0001	419 - 422	FNWR
812.4497	812.4504	- 0.0007	423 - 429	NPLNSLR
4408.0764	4408.0659	0.0105	430 - 468	GSLL...YSHR
601.3544	601.3547	- 0.0003	469 - 473	LSNIR
872.5079	872.5080	- 0.0001	474 - 481	LISGNTLR

1115.5514	1115.5512	0.0002	482 - 490	APVY...WTHR
2145.1280	2145.1277	0.0003	491 - 510	SADR...PLVK
447.2079	447.2077	0.0002	491 - 494	SADR
2939.5931	2939.5815	0.0116	495 - 522	TNTI...TVVK
1715.9270	1715.9305	- 0.0035	495 - 510	TNTI...PLVK
2311.2284	2311.2285	- 0.0001	511 - 533	AHTL...DILR
1240.6770	1240.6776	- 0.0006	511 - 522	AHTL...TVVK
1244.6622	1244.6626	- 0.0004	523 - 534	GPGF...ILRR
1088.5617	1088.5615	0.0002	523 - 533	GPGF...DILR
2326.1418	2326.1454	- 0.0036	534 - 554	RTSG...LSQR
2170.0411	2170.0443	- 0.0032	535 - 554	TSGG...LSQR
1193.6521	1193.6516	0.0005	559 - 568	IRYA...TNLR
924.4662	924.4665	- 0.0003	561 - 568	YASTTNLR
1006.5452	1006.5447	0.0005	569 - 577	IYVT...AGER
924.4713	924.4705	0.0008	578 - 585	IFAGQFDK
2983.4069	2983.4062	0.0007	586 - 612	TMDA...FPER
4238.0134	4238.0179	- 0.0045	613 - 651	SSSL...DLER
2190.0094	2190.0077	0.0017	613 - 633	SSSL...YVDR
2066.0201	2066.0208	- 0.0007	634 - 651	FELI...DLER
1619.8531	1619.8519	0.0012	655 - 669	AVNE...IGLK
732.4020	732.4017	0.0003	697 - 702	KELSEK
604.3069	604.3068	0.0001	698 - 702	ELSEK
774.3983	774.3984	- 0.0001	708 - 713	RLSDER
1715.8590	1715.8591	- 0.0001	709 - 722	LSDE...PNFR
618.2970	618.2973	- 0.0003	709 - 713	LSDER
1115.5724	1115.5723	0.0001	714 - 722	NLLQ...PNFR
458.2602	458.2601	0.0001	723 - 726	GINR
530.2814	530.2813	0.0001	727 - 730	QLDR
4150.9367	4150.9245	0.0122	734 - 769	GSTD...LYQK
1551.7434	1551.7417	0.0017	734 - 748	GSTD...DVFK
831.4701	831.4702	- 0.0001	770 - 776	IDESKLK
590.2911	590.2911	0.0000	770 - 774	IDESK
750.4380	750.4388	- 0.0008	775 - 780	LKAYTR
509.2598	509.2598	0.0000	777 - 780	AYTR
578.3185	578.3176	0.0009	781 - 784	YQLR
1825.9112	1825.9098	0.0014	785 - 799	GYIE...YLIR
2820.4499	2820.4446	0.0053	800 - 826	YNAK...PIGK
494.2488	494.2489	- 0.0001	800 - 803	YNAK
2343.2220	2343.2223	- 0.0003	804 - 826	HETV...PIGK
1024.5406	1024.5414	- 0.0008	857 - 865	IKTQ...GHAR
783.3625	783.3624	0.0001	859 - 865	TQDGHAR
2097.1512	2097.1470	0.0042	866 - 884	LGNL...ALAR
1550.7994	1550.7980	0.0014	897 - 908	EKLE...IVYK
1293.6600	1293.6605	- 0.0005	899 - 908	LEWE...IVYK
1969.9412	1969.9381	0.0031	909 - 925	EAKE...QYDR
1641.7635	1641.7635	0.0000	912 - 925	ESVD...QYDR

1766.9122	1766.9097	0.0025	926 - 941	LQAD...ADKR
1610.8094	1610.8086	0.0008	926 - 940	LQAD...AADK
610.3551	610.3551	0.0000	942 - 946	VHSIR
2615.3465	2615.3482	- 0.0017	947 - 970	EAYL...LEGR
1757.9400	1757.9352	0.0048	971 - 985	IFTA...NVIK
1302.6615	1302.6608	0.0007	971 - 981	IFTA...YDAR
2078.9813	2078.9844	- 0.0031	982 - 999	NVIK...WNVK
472.3004	472.3009	- 0.0005	982 - 985	NVIK
1625.6767	1625.6780	- 0.0013	986 - 999	NGDF...WNVK
1433.6279	1433.6284	- 0.0005	1000 - 1011	GHVD...NNHR
1954.9999	1955.0000	- 0.0001	1012 - 1028	SVLV...QEVR
587.2844	587.2850	- 0.0006	1029 - 1033	VCPGR
620.3648	620.3646	0.0002	1034 - 1038	GYILR
2969.3697	2969.3600	0.0097	1039 - 1064	VTAY...DELK
580.3216	580.3221	- 0.0005	1039 - 1043	VTAYK
2407.0504	2407.0485	0.0019	1044 - 1064	EGYG...DELK
4070.6713	4070.6582	0.0131	1065 - 1098	FSNC...YTSR
2743.1504	2743.1521	- 0.0017	1099 - 1123	NRGY...YEEK
2472.0218	2472.0241	- 0.0023	1101 - 1123	GYDG...YEEK
837.4094	837.4093	0.0001	1124 - 1130	AYTDGRR
681.3072	681.3082	- 0.0010	1124 - 1129	AYTDGR
1146.4842	1146.4836	0.0006	1130 - 1138	RDNP...ESNR
2574.1292	2574.1333	- 0.0041	1131 - 1153	DNPC...YVTK
990.3822	990.3825	- 0.0003	1131 - 1138	DNPCESNR
1600.7767	1600.7773	- 0.0006	1139 - 1153	GYGD...YVTK
4001.9284	4001.9271	0.0013	1154 - 1187	ELEY...LMEE
1269.5757	1269.5765	- 0.0008	1154 - 1163	ELEY...ETDK

[1] All imported values were rounded to 4 decimal places.
[2] Only experimental masses that matched calculated masses with the highest scores are listed in the table.
[3] The calculated mass is the exact molecular mass calculated from the matched peptide sequence.
[4] The calculated difference = experimental mass – calculated mass.
[5] Position refers to amino acid residues within the predicted MON 94637-produced Cry1B.2 sequence as depicted in Figure 25A.
[6] For peptide matches greater than nine amino acids in length the first 4 residues and last 4 residues are shown separated by dots (…).

Table 15. Summary of the Tryptic Masses Identified for the *Bt*-Produced Cry1B.2 Protein Using LC-MS/MS[1]

Experimental Mass[2]	Calculated Mass[3]	Diff[4]	Fragment[5]	Sequence[6]
3836.9108	3836.9074	0.0034	2 - 36	TSNR...ARIE
3252.6106	3252.6156	- 0.0050	2 - 31	TSNR...NLST
1789.8169	1789.8152	0.0017	32 - 47	DARI...GNNI
602.3023	602.3024	- 0.0001	32 - 36	DARIE
1205.5249	1205.5234	0.0015	37 - 47	DSLC...GNNI
3365.6394	3365.6388	0.0006	118 - 146	DTAL...ENRD
3250.6145	3250.6119	0.0026	118 - 145	DTAL...LENR
2437.2354	2437.2350	0.0004	118 - 139	DTAL...QSLE
946.4151	946.4144	0.0007	140 - 146	DWLENRD
831.3882	831.3875	0.0007	140 - 145	DWLENR
2126.1042	2126.1008	0.0034	146 - 163	DDAR...ALEL
5511.7247	5511.7211	0.0036	229 - 274	DYCA...FPSY
3794.7759	3794.7872	- 0.0113	229 - 258	DYCA...QFRR
1734.9479	1734.9444	0.0035	259 - 274	DLTL...FPSY
3263.6237	3263.6172	0.0065	266 - 293	DLVA...EIYT
1023.5278	1023.5277	0.0001	266 - 274	DLVA...FPSY
6389.1763	6389.1716	0.0047	275 - 332	DTRV...PHLL
2274.0955	2274.0950	0.0005	275 - 293	DTRV...EIYT
4149.0837	4149.0820	0.0017	294 - 332	DPIG...PHLL
6057.1731	6057.1694	0.0037	393 - 446	DVYR...TQLF
5329.6200	5329.6140	0.0060	447 - 492	DSET...HRSA
5727.9946	5727.9973	- 0.0027	493 - 547	DRTN...NVNL
3782.9809	3782.9803	0.0006	493 - 529	DRTN...FTGG
892.4245	892.4250	- 0.0005	493 - 500	DRTNTISS
4853.5861	4853.5829	0.0032	501 - 547	DSIT...NVNL
2908.5672	2908.5659	0.0013	501 - 529	DSIT...FTGG
1963.0246	1963.0276	- 0.0030	530 - 547	DILR...NVNL
3928.8854	3928.8830	0.0024	584 - 620	DKTM...TVGA
3453.6740	3453.6729	0.0011	588 - 620	DAGA...TVGA
5565.7479	5565.7427	0.0052	621 - 670	DTFS...GLKT
3022.4095	3022.4084	0.0011	621 - 647	DTFS...EAES
1216.5249	1216.5248	0.0001	621 - 631	DTFS...EVYV
4682.3688	4682.3715	- 0.0027	632 - 673	DRFE...TDVT
1823.8944	1823.8941	0.0003	632 - 647	DRFE...EAES
2876.4875	2876.4879	- 0.0004	648 - 673	DLER...TDVT
2561.3464	2561.3449	0.0015	648 - 670	DLER...GLKT
2106.9430	2106.9416	0.0014	671 - 688	DVTD...ECLS
861.3865	861.3869	- 0.0004	671 - 677	DVTDYHI
2457.0328	2457.0352	- 0.0024	674 - 693	DYHI...EFCL
1791.8023	1791.7985	0.0038	674 - 688	DYHI...ECLS
1263.5656	1263.5653	0.0003	678 - 688	DQVS...ECLS
3557.8215	3557.8147	0.0068	689 - 717	DEFC...NLLQ

2689.3762	2689.3745	0.0017	689 - 710	DEFC...KRLS
4203.2658	4203.2624	0.0034	694 - 728	DEKK...NRQL
2892.5781	2892.5780	0.0001	694 - 717	DEKK...NLLQ
2024.1394	2024.1378	0.0016	694 - 710	DEKK...KRLS
2197.1364	2197.1352	0.0012	711 - 728	DERN...NRQL
886.4510	886.4508	0.0002	711 - 717	DERNLLQ
1328.6951	1328.6949	0.0002	718 - 728	DPNF...NRQL
1732.8149	1732.8129	0.0020	729 - 744	DRGW...QGGD
1617.7862	1617.7860	0.0002	729 - 743	DRGW...IQGG
933.4414	933.4417	- 0.0003	729 - 736	DRGWRGST
2444.2150	2444.2112	0.0038	737 - 758	DITI...LGTF
1759.8664	1759.8669	- 0.0005	744 - 758	DDVF...LGTF
1644.8404	1644.8399	0.0005	745 - 758	DVFK...LGTF
3806.8630	3806.8501	0.0129	759 - 788	DECY...GYIE
1592.7081	1592.7068	0.0013	759 - 770	DECY...YQKI
2232.1567	2232.1538	0.0029	771 - 788	DESK...GYIE
2593.3396	2593.3387	0.0009	894 - 914	DKRE...KESV
2692.2909	2692.2915	- 0.0006	915 - 938	DALF...IHAA
1638.8008	1638.8002	0.0006	915 - 928	DALF...RLQA
1055.4912	1055.4924	- 0.0012	915 - 923	DALF...NSQY
6170.2115	6170.2051	0.0064	924 - 978	DRLQ...FSLY
1654.8103	1654.8097	0.0006	924 - 938	DRLQ...IHAA
601.3182	601.3184	- 0.0002	924 - 928	DRLQA
5586.8984	5586.8973	0.0011	929 - 978	DTNI...FSLY
1055.5071	1055.5070	0.0001	929 - 938	DTNI...IHAA
985.5300	985.5305	- 0.0005	979 - 987	DARN...IKNG
1746.7798	1746.7784	0.0014	988 - 1002	DFNN...KGHV
5047.1179	5047.1196	- 0.0017	1061 - 1102	DELK...NRGY
2662.1059	2662.1051	0.0008	1061 - 1082	DELK...VTCN
4972.0881	4972.1019	- 0.0138	1083 - 1126	DYTA...KAYT
3580.5148	3580.5138	0.0010	1083 - 1114	DYTA...SVPA
2403.0247	2403.0251	- 0.0004	1083 - 1102	DYTA...NRGY
3071.3393	3071.3380	0.0013	1103 - 1130	DGAY...DGRR
2587.0890	2587.0874	0.0016	1103 - 1126	DGAY...KAYT
1195.4999	1195.4993	0.0006	1103 - 1114	DGAY...SVPA
3144.3107	3144.3115	- 0.0008	1115 - 1141	DYAS...RGYG
1893.8518	1893.8493	0.0025	1115 - 1130	DYAS...DGRR
1409.5990	1409.5986	0.0004	1115 - 1126	DYAS...KAYT
4066.8190	4066.8279	- 0.0089	1127 - 1161	DGRR...FPET
1752.7260	1752.7234	0.0026	1127 - 1141	DGRR...RGYG
3582.5802	3582.5773	0.0029	1131 - 1161	DNPC...FPET
1268.4729	1268.4728	0.0001	1131 - 1141	DNPC...RGYG
5307.5969	5307.5876	0.0093	1142 - 1187	DYTP...LMEE
2332.1182	2332.1151	0.0031	1142 - 1161	DYTP...FPET
2993.4860	2993.4831	0.0029	1162 - 1187	DKVW...LMEE
1834.9355	1834.9353	0.0002	1162 - 1177	DKVW...TFIV

1176.5589	1176.5584	0.0005	1178 - 1187	DSVE...LMEE

[1] All imported values were rounded to 4 decimal places.
[2] Only experimental masses that matched calculated masses with the highest score are listed in the table.
[3] The calculated mass is the exact molecular mass calculated from the matched peptide sequence.
[4] The calculated difference = experimental mass – calculated mass.
[5] Fragment numbering is based on the expected N-terminal sequence from the expression plasmid.
[6] For peptide matches greater than nine amino acids in length the first 4 residues and last 4 residues are shown separated by dots (…).

(A)

```
1    MTSNRKNENE IINALSIPAV SNHSAQMNLS TDARIEDSLC IAEGNNIDPF
51   VSASTVQTGI NIAGRILGVL GVPFAGQIAS FYSFLVGELW PRGRDPWEIF
101  LEHVEQLIRQ QVTENTRDTA LARLQGLGNS FRAYQQSLED WLENRDDART
151  RSVLYTQYIA LELDFLNAMP LFAIRNQEVP LLMVYAQAAN LHLLLLRDAS
201  LFGSEFGLTS QEIQRYYERQ VEKTREYSDY CARWYNTGLN NLRGTNAESW
251  LRYNQFRRDL TLGVLDLVAL FPSYDTRVYP MNTSAQLTRE IYTDPIGRTN
301  APSGFASTNW FNNNAPSFSA IEAAVIRPPH LLDFPEQLTI FSVLSRWSNT
351  QYMNYWVGHR LESRTIRGSL STSTHGNTNT SINPVTLQFT SRDVYRTESF
401  AGINILLTTP VNGVPWARFN WRNPLNSLRG SLLYTIGYTG VGTQLFDSET
451  ELPPETTERP NYESYSHRLS NIRLISGNTL RAPVYSWTHR SADRTNTISS
501  DSITQIPLVK AHTLQSGTTV VKGPGFTGGD ILRRTSGGPF AFSNVNLDFN
551  LSQRYRARIR YASTTNLRIY VTVAGERIFA GQFDKTMDAG APLTFQSFSY
601  ATINTAFTFP ERSSSLTVGA DTFSSGNEVY VDRFELIPVT ATFEAESDLE
651  RAQKAVNELF TSSNQIGLKT DVTDYHIDQV SNLVECLSDE FCLDEKKELS
701  EKVKHAKRLS DERNLLQDPN FRGINRQLDR GWRGSTDITI QGGDDVFKEN
751  YVTLLGTFDE CYPTYLYQKI DESKLKAYTR YQLRGYIEDS QDLEIYLIRY
801  NAKHETVNVP GTGSLWPLSA PSPIGKCAHH SHHFSLDIDV GCTDLNEDLG
851  VWVIFKIKTQ DGHARLGNLE FLEEKPLVGE ALARVKRAEK KWRDKREKLE
901  WETNIVYKEA KESVDALFVN SQYDRLQADT NIAMIHAADK RVHSIREAYL
951  PELSVIPGVN AAIFEELEGR IFTAFSLYDA RNVIKNGDFN NGLSCWNVKG
1001 HVDVEEQNNH RSVLVVPEWE AEVSQEVRVC PGRGYILRVT AYKEGYGEGC
1051 VTIHEIENNT DELKFSNCVE EEVYPNNTVT CNDYTATQEE YEGTYTSRNR
1101 GYDGAYESNS SVPADYASAY EEKAYTDGRR DNPCESNRGY GDYTPLPAGY
1151 VTKELEYFPE TDKVWIEIGE TEGTFIVDSV ELLLMEE
```

(B)

```
1    MTSNRKNENE IINALSIPAV SNHSAQMNLS TDARIEDSLC IAEGNNIDPF
51   VSASTVQTGI NIAGRILGVL GVPFAGQIAS FYSFLVGELW PRGRDPWEIF
101  LEHVEQLIRQ QVTENTRDTA LARLQGLGNS FRAYQQSLED WLENRDDART
151  RSVLYTQYIA LELDFLNAMP LFAIRNQEVP LLMVYAQAAN LHLLLLRDAS
201  LFGSEFGLTS QEIQRYYERQ VEKTREYSDY CARWYNTGLN NLRGTNAESW
251  LRYNQFRRDL TLGVLDLVAL FPSYDTRVYP MNTSAQLTRE IYTDPIGRTN
301  APSGFASTNW FNNNAPSFSA IEAAVIRPPH LLDFPEQLTI FSVLSRWSNT
```

351 QYMNYWVGHR LESRTIRGSL STSTHGNTNT SINPVTLQFT SRDVYRTESF

401 AGINILLTTP VNGVPWARFN WRNPLNSLRG SLLYTIGYTG VGTQLFDSET

451 ELPPETTERP NYESYSHRLS NIRLISGNTL RAPVYSWTHR SADRTNTISS

501 DSITQIPLVK AHTLQSGTTV VKGPGFTGGD ILRRTSGGPF AFSNVNLDFN

551 LSQRYRARIR YASTTNLRIY VTVAGERIFA GQFDKTMDAG APLTFQSFSY

601 ATINTAFTFP ERSSSLTVGA DTFSSGNEVY VDRFELIPVT ATFEAESDLE

651 RAQKAVNELF TSSNQIGLKT DVTDYHIDQV SNLVECLSDE FCLDEKKELS

701 EKVKHAKRLS DERNLLQDPN FRGINRQLDR GWRGSTDITI QGGDDVFKEN

751 YVTLLGTFDE CYPTYLYQKI DESKLKAYTR YQLRGYIEDS QDLEIYLIRY

801 NAKHETVNVP GTGSLWPLSA PSPIGKCAHH SHHFSLDIDV GCTDLNEDLG

851 VWVIFKIKTQ DGHARLGNLE FLEEKPLVGE ALARVKRAEK KWRDKREKLE

901 WETNIVYKEA KESVDALFVN SQYDRLQADT NIAMIHAADK RVHSIREAYL

951 PELSVIPGVN AAIFEELEGR IFTAFSLYDA RNVIKNGDFN NGLSCWNVKG

1001HVDVEEQNNH RSVLVVPEWE AEVSQEVRVC PGRGYILRVT AYKEGYGEGC

1051VTIHEIENNT DELKFSNCVE EEVYPNNTVT CNDYTATQEE YEGTYTSRNR

1101GYDGAYESNS SVPADYASAY EEKAYTDGRR DNPCESNRGY GDYTPLPAGY

1151VTKELEYFPE TDKVWIEIGE TEGTFIVDSV ELLLMEE

Figure 25. Peptide Map of the MON 94637-Produced Cry1B.2 and *Bt*-Produced Cry1B.2 Proteins

(A). The amino acid sequence of the MON 94637-produced Cry1B.2 protein was deduced from the *cry1B.2* gene present in MON 94637. Boxed regions correspond to peptides that were identified from the MON 94637-produced Cry1B.2 protein sample using LC-MS/MS. In total, 92% coverage (1097 out of 1187 amino acids) of the expected protein sequence was covered by the identified peptides.
(B). The amino acid sequence of the *Bt*-produced Cry1B.2 protein was deduced from the *cry1B.2* gene that is contained on the expression plasmid pMON236926. Boxed regions correspond to peptides that were identified from the *Bt*-produced Cry1B.2 protein sample using LC-MS/MS. In total, 66% coverage (792 out of 1187 amino acids) of the expected protein sequence was covered by the identified peptides.

B.1(a)(ii)(ii)(iii) Results of Western blot analysis of the Cry1B.2 protein isolated from the grain of MON 94637 and immunoreactivity comparison to *Bt*-produced Cry1B.2 protein

Western blot analysis was conducted using mouse anti-Cry1B.2 monoclonal antibody as additional means to confirm the identity of the Cry1B.2 protein isolated from the seed of MON 94637 soybean and to assess the equivalence of the immunoreactivity of the MON 94637-produced and *Bt*-produced Cry1B.2 proteins (Figure 26).

The results showed that an intact immunoreactive band with the same electrophoretic mobility was present in all lanes loaded with the MON 94637-produced and *Bt*-produced Cry1B.2 proteins. For each amount loaded, comparable signal intensity was observed between the MON 94637-produced and *Bt*-produced Cry1B.2 protein bands. As expected, the signal intensity increased with increasing load amounts of the MON 94637-produced and *Bt*-produced Cry1B.2 proteins, thus supporting identification of MON 94637-produced Cry1B.2 protein. One other band migrating at >220 kDa was also observed. This band was observed in lanes with higher load amounts of both protein samples and, therefore, may represent an aggregation of the Cry1B.2 occurring during sample preparation. Additionally, a minor band at ~28 kDa was detected in lanes loaded with the MON 94637-produced Cry1B.2 protein sample. Most likely this is a soybean endogenous cross-reacting protein copurified during processing the MON 94637-produced Cry1B.2 protein.

To compare the immunoreactivity of the MON 94637-produced and *Bt*-produced Cry1B.2 proteins, densitometric analysis was conducted on the bands that migrated at the expected apparent MW for the intact Cry1B.2 protein (~132.6 kDa). The signal intensity (reported in OD) of the bands of interest in lanes loaded with MON 94637-produced and *Bt*-produced Cry1B.2 proteins were measured (Table 16). Because the mean signal intensity of the MON 94637-produced Cry1B.2 protein was within 35% of the mean signal intensity of the immunoreactive signal of the intact band (~132.6 kDa) of the reference substance, the MON 94637-produced Cry1B.2 and *Bt*-produced Cry1B.2 proteins were determined to have equivalent immunoreactivity.

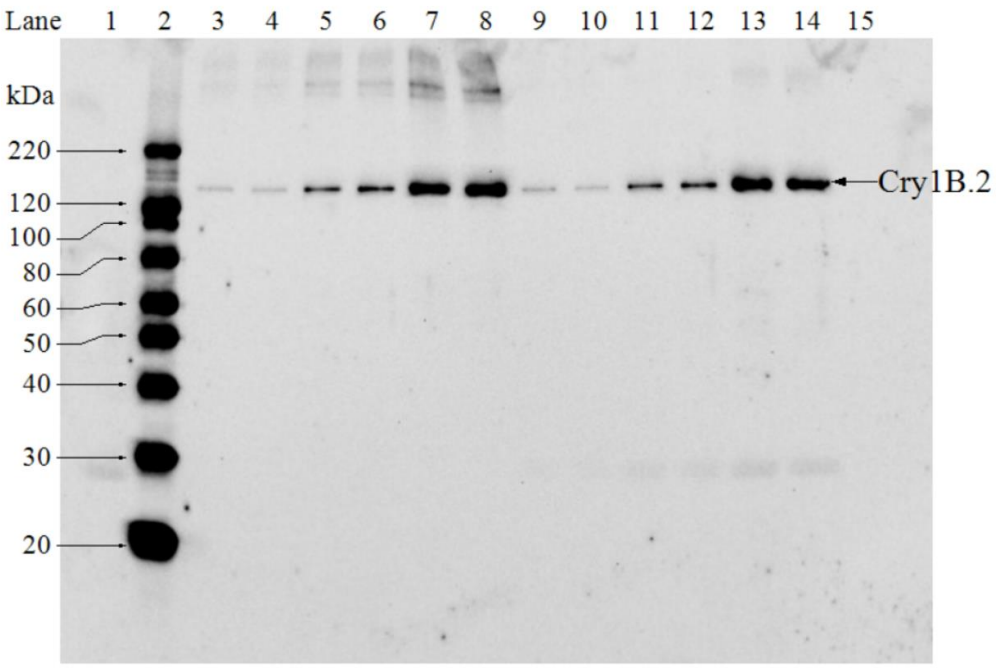

Figure 26. Western Blot Analysis and Immunoreactivity of the MON 94367-Produced and *Bt*-Produced Cry1B.2 Proteins

Aliquots of the MON 94637-produced and *Bt*-produced Cry1B.2 proteins were subjected to SDS-PAGE and electrotransferred to a nitrocellulose membrane. Proteins were detected using mouse anti-Cry1B.2 monoclonal antibody as the primary antibody. Immunoreactive bands were visualized using HRP-conjugated secondary antibodies and an ECL system. The 300-second exposure is shown. The approximate MW (kDa) of the standards are shown on the left. Lane designations are as follows:

Lane	Sample	Amount (ng)
1	Precision Plus Protein™ Standards	-
2	MagicMark XP™ Western Protein Standards	-
3	*Bt*-produced Cry1B.2	5
4	*Bt*-produced Cry1B.2	5
5	*Bt*-produced Cry1B.2	10
6	*Bt*-produced Cry1B.2	10
7	*Bt*-produced Cry1B.2	20
8	*Bt*-produced Cry1B.2	20
9	MON 94637-produced Cry1B.2	5
10	MON 94637-produced Cry1B.2	5
11	MON 94637-produced Cry1B.2	10
12	MON 94637-produced Cry1B.2	10
13	MON 94637-produced Cry1B.2	20
14	MON 94637-produced Cry1B.2	20
15	Empty	-

Table 16. Immunoreactivity of the MON 94367-Produced and *Bt*-Produced Cry1B.2 Proteins

Mean Signal Intensity from MON 94637-Produced Cry1B.2 [1] (OD)	Mean Signal Intensity from *Bt*-produced Cry1B.2 [1] (OD)	Acceptance Limits[2] (OD)
941,461.22	984,062.38	639,640.55 – 1,328,484.21

[1] Each value represents the mean of six values (n = 6).
[2] The acceptance limits are for the MON 94637-produced Cry1B.2 protein and are based on the interval between -35% (984,062.38 x 0.65 = 639,640.55) and +35 % (984,062.38 x 1.35 = 1,328,484.21) of the mean of the *Bt*-produced Cry1B.2 signal intensity across all loads.

B.1(a)(ii)(ii)(iv) Results of the Cry1B.2 protein molecular weight and purity analysis

For apparent MW and purity determination, the MON 94637-produced Cry1B.2 and the *Bt*-produced Cry1B.2 proteins were subjected to SDS-PAGE. Following electrophoresis, the gel was stained with Brilliant Blue G-Colloidal stain and analyzed by densitometry. The MON 94637-produced Cry1B.2 protein (Figure 27, lanes 3-8) migrated to the same position on the gel as the *Bt*-produced Cry1B.2 protein (Figure 27, lane 2) and the apparent MW was calculated to be 135.5 kDa (Table 17). Because the experimentally determined apparent MW of the MON 94637-produced Cry1B.2 protein was within the acceptance limits (126.2 kDa – 138.9 kDa) for equivalence (Table 18), the MON 94637-produced Cry1B.2 and *Bt*-produced Cry1B.2 proteins were determined to have equivalent apparent molecular weights.

The purity of the MON 94637-produced Cry1B.2 protein was calculated based on the six lanes loaded on the gel (Figure 27, lanes 3-8). The average purity was determined to be 77% (Table 17).

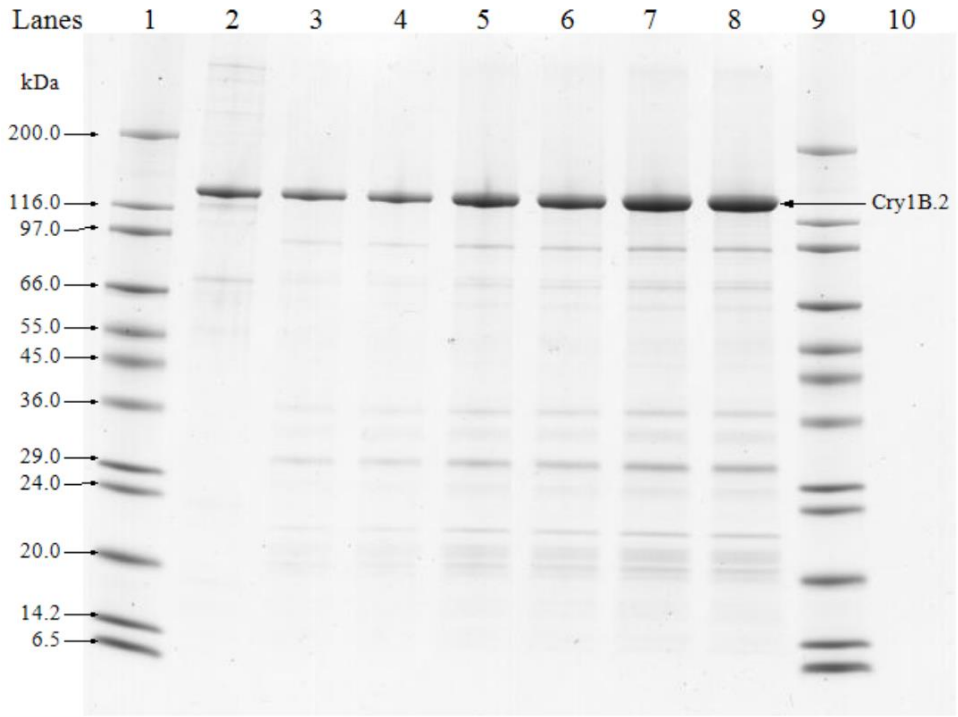

Figure 27. Purity and Apparent Molecular Weight Analysis of the MON 94367-Produced Cry1B.2 Protein

Aliquots of the MON 94637-produced and the *Bt*-produced Cry1B.2 proteins were subjected to SDS-PAGE and the gel was stained with Brilliant Blue G-Colloidal stain. The MWs (kDa) are shown on the left and correspond to the standards loaded in lanes 1 and 9. The Cry1B.2 protein is indicated with an arrow in the image. Lane designations are as follows:

Lane	Sample	Amount (µg)
1	SigmaMarker™ Wide Range	N/A
2	*Bt*-produced Cry1B.2	1.0
3	MON 94637-produced Cry1B.2	1.0
4	MON 94637-produced Cry1B.2	1.0
5	MON 94637-produced Cry1B.2	2.0
6	MON 94637-produced Cry1B.2	2.0
7	MON 94637-produced Cry1B.2	3.0
8	MON 94637-produced Cry1B.2	3.0
9	SigmaMarker™ Wide Range	N/A
10	Blank	

Table 17. Apparent Molecular Weight and Purity Analysis of the MON 94367-Produced Cry1B.2 Protein

	Apparent MW[1] (kDa)	Purity[2] (%)
Average (n=6)	135.5	77

[1]Final MW was rounded to one decimal place.
[2]Average % purity was rounded to the nearest whole number.

Table 18. Apparent Molecular Weight Comparison Between the MON 94367-Produced Cry1B.2 and *Bt*-Produced Cry1B.2 Proteins

Apparent MW of MON 94637-Produced Cry1B.2 Protein (kDa)	Apparent MW of Bt-produced Cry1B.2 Protein[1] (kDa)	Acceptance Limits[2] (kDa)
135.5	132.6	126.2 – 138.9

[1] As reported on the COA of the *Bt*-produced Cry1B.2 protein.
[2] Data obtained for the *Bt*-produced Cry1B.2 protein was used to generate the prediction interval (Appendix 7).

B.1(a)(ii)(ii)(v) Cry1B.2 glycosylation analysis

Some eukaryotic proteins are post-translationally modified by the addition of carbohydrate moieties (Rademacher *et al.*, 1988). To test whether the Cry1B.2 protein was glycosylated when expressed in the seed of MON 94637 soybean, the MON 94637-produced Cry1B.2 protein was analyzed using an ECL™ glycoprotein detection method. Transferrin, a glycosylated protein, was used as a positive control in the assay. To assess equivalence of the MON 94637-produced and *Bt*-produced Cry1B.2 proteins, the *Bt*-produced Cry1B.2 protein was also analyzed.

A clear glycosylation signal was observed at the expected molecular weight (~80 kDa) in the lanes containing the positive control (transferrin) and the band intensity increased with increasing concentration (Figure 28A). In contrast, no glycosylation signal was observed in the lanes containing the *Bt*-produced Cry1B.2 protein or MON 94637-produced Cry1B.2 protein (Figure 28A).

To confirm that MON 94637-produced Cry1B.2 and *Bt*-produced Cry1B.2 proteins were appropriately loaded for glycosylation analysis, a second membrane with identical loadings and transfer time was stained with Coomassie Blue R250 for protein detection. Both the MON 94637-produced and *Bt*-produced Cry1B.2 proteins were detected, along with the positive control protein (transferrin) (Figure 28B). These data indicate that the glycosylation status of MON 94637-produced Cry1B.2 protein is equivalent to that of the *Bt*-produced Cry1B.2 protein and that neither is glycosylated.

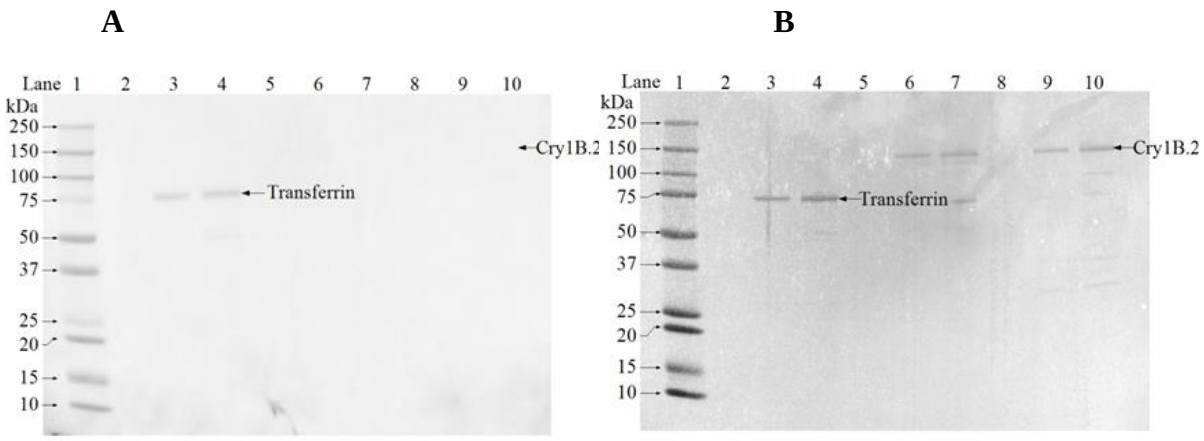

Figure 28. Glycosylation Analysis of the MON 94367-Produced and *Bt*-Produced Cry1B.2 Proteins

Aliquots of the transferrin (positive control), *Bt*-produced Cry1B.2 and MON 94637-produced Cry1B.2 proteins were subjected to SDS-PAGE and electrotransferred to a PVDF membrane. The MWs (kDa) correspond to the Precision Plus Protein™ Standards. The arrows show the expected migration of the MON 94637-produced and *Bt*-produced Cry1B.2 proteins and transferrin. (A) Where present, the labeled carbohydrate moieties were detected by using ECL reagents and blot images were captured using a Bio-Rad ChemiDoc Imager. The 120-second exposure is shown. (B) An equivalent blot was stained with Coomassie Blue R250 to confirm the presence of proteins. Lane designations are as follows:

Lane	Sample	Amount (ng)
1	Precision Plus Protein™ Standards	-
2	Blank	-
3	Transferrin (positive control)	100
4	Transferrin (positive control)	200
5	Blank	-
6	*Bt*-produced Cry1B.2	100
7	*Bt*-produced Cry1B.2	200
8	Blank	-
9	MON 94637-produced Cry1B.2	100
10	MON 94637-produced Cry1B.2	200

B.1(a)(ii)(ii)(vi) Cry1B.2 functional activity

The MON 94637-produced Cry1B.2 and *Bt*-produced Cry1B.2 proteins were considered to have equivalent functional activity if the functional activity of both proteins (EC_{50}) were not significantly different when compared using a two-sided t-test.

The experimentally determined functional activity for the MON 94637-produced and *Bt*-produced Cry1B.2 proteins are presented in Table 19. EC_{50} values were determined as the concentration of Cry1B.2 (µg/ml diet) that resulted in 50% insect mass reduction relative to the control treatment in a European corn borer insect bioassay. The mean EC_{50} of MON 94637-produced and *Bt*-produced Cry1B.2 proteins were 0.61 and 0.71 µg of Cry1B.2 protein/ml diet, respectively. Because no significant difference for the mean EC_{50} values of both proteins was observed by t-test ($p > 0.05$) (Table 19), the MON 94637-produced Cry1B.2 protein was considered to have equivalent functional activity to that of the *Bt*-produced Cry1B.2 protein.

Table 19. Functional Activity of the MON 94367-Produced and *Bt*-Produced Cry1B.2 Proteins

Replicates	MON 94637 Produced Cry1B.2 [1] (µg protein/ml diet)	*Bt*-produced Cry1B.2 [1] (µg protein/ml diet)	t-test [2] (p-value)
1	0.64	0.62	
2	0.62	0.77	
3	0.57	0.74	
Mean[1]	0.61	0.71	0.1200

[1] Value refers to mean calculated based on three independent assays (n=3).
[2] No significant difference is based on □=0.05.

B.1(a)(ii)(ii)(vii) MON 94367 Cry1B.2 protein identity and equivalence - Conclusion

The MON 94637-produced Cry1B.2 protein purified from MON 94637 grain was characterised, and a comparison of the physicochemical and functional properties between the MON 94637-produced and the *Bt*-produced Cry1B.2 proteins was conducted following a panel of analytical tests: 1) N-terminal sequence analysis established the same identity for the MON 94637-produced and the *Bt*-produced Cry1B.2 proteins; 2) Nano LC-MS/MS analysis yielded peptide masses consistent with the expected peptide masses from the theoretical trypsin digest of the *cry1B.2* gene product present in MON 94637; 3) the MON 94637-produced and the *Bt*-produced Cry1B.2 proteins were both detected on a Western blot probed with antibodies specific for Cry1B.2 protein and the immunoreactive properties of both proteins was shown to be equivalent; 4) the electrophoretic mobility and apparent molecular weight of the MON 94637-produced and the *Bt*-produced Cry1B.2 proteins were shown to be equivalent; 5) the glycosylation status of MON 94637-produced and the *Bt*-produced Cry1B.2 proteins was determined to be equivalent; and 6) the functional activity of the MON 94637-produced and the *Bt*-produced Cry1B.2was demonstrated to be equivalent. These results demonstrate that the MON 94637-produced and the *Bt*-produced Cry1B.2 proteins are equivalent. This demonstration of protein equivalence confirms that the *Bt*-produced Cry1B.2 protein is appropriate for use in the evaluation of the safety of the MON 94637-produced Cry1B.2 protein.

B.1(a)(iii) Expression levels of Cry1A.2 and Cry1B.2 proteins in MON 94367

Methods and results of protein expression analysis of Cry1A.2 and Cry1B.2 proteinss are described in Appendix **8**.

The expression levels of Cry1A.2 and Cry1B.2 proteins were determined by validated enzyme linked immunosorbent assays (ELISAs).

Protein levels in flower, forage, grain, over season leaf 1 (OSL1), and root tissues were calculated on a nanogram per milliliter (ng/ml) basis. The protein levels (ng/ml) for the test substance greater than or equal to the assay LOQ were converted to microgram per gram (µg/g) dry weight (dw) values using the tissue-to-buffer ratio(s), dilution factor(s) and extraction efficiency conversion factor (EECF). The arithmetic mean, standard error (SE), and range were determined for all protein levels for each tissue type across all sites.

Samples were collected at the following growth stages:

Tissue type	Growth Stage
Flower	R1-R2
Forage	R6
Grain	R8
OSL1	V3-V4
Root	R6

B.1(a)(iii)(i) Expression levels of Cry1A.2 protein

Cry1A.2 protein levels were determined in flower, forage, grain, leaf, and root tissues. The results obtained from the ELISA are summarized in Table 20. The expression of Cry1A.2 in MON 94637 soybean was determined and reported on a dry weight basis.

The mean Cry1A.2 protein level in MON 94637 across all sites was the highest in flower at 260 µg/g dw and lowest in root at 9.8 µg/g dw. The mean Cry1A.2 protein level in MON 94637 grain was 24 µg/g dw.

Table 20. Summary of Cry1A.2 Protein Levels in Soybean Tissues Collected from MON 94637 Produced in United States Field Trials in 2021

Tissue Type[1]	Development Stage[2]	Mean (SE) Range (µg/g dw)[3]	LOQ/LOD (µg/g dw)[4]
Flower	R1-R2	260 (24) 110- 610	0.156/0.086
Forage	R6	84 (3.4) 59 - 120	0.156/0.098
Grain	R8	24 (2.2) 7.0 - 43	0.078/0.059
OSL1	V3-V4	230 (9.4) 180 - 380	0.156/0.109
Root	R6	9.8 (3.3) 1.1 - 49	0.156/0.125

[1]OSL = over season leaf
[2]The crop development stage at which each tissue was collected.
[3]Protein levels are expressed as the arithmetic mean and standard error (SE) as microgram (µg) of protein per gram (g) of tissue on a dry weight basis (dw). The means, SE, and ranges (minimum and maximum values) were calculated for each tissue across all five sites (n=20).
[4]LOQ=limit of quantitation, LOD=limit of detection.

B.1(a)(iii)(ii) Expression levels of Cry1B.2 protein

Cry1B.2 protein levels were determined in flower, forage,grain, leaf, and root tissues. The results obtained from the ELISA are summarized in Table 21.. The expression of Cry1B.2 in MON 94637 soybean was determined and reported on a dry weight basis.

The mean Cry1B.2 protein level in MON 94637 across all sites was the highest in OSL1 at 420 µg/g dw and lowest in root at <LOQ µg/g dw. The mean Cry1B.2 protein level in MON 94637 grain was 12 µg/g dw.

Table 21. Summary of Cry1B.2 Protein Levels in Soybean Tissues Collected from MON 94367 Produced in United States Field Trials in 2021

Tissue Type[1]	Development Stage[2]	Mean (SE) Range (µg/g dw)[3]	LOQ/LOD (µg/g dw)[4]
Flower	R1-R2	180 (9.8) 130 - 300	0.625/0.129
Forage	R6	55 (3.3) 36 - 96	0.625/0.137
Grain	R8	12 (0.75) 7.1 - 20	0.313/0.095
OSL1	V3-V4	420 (17) 270 - 550	0.625/0.171
Root	R6	<LOQ (NA[5]) NA-NA	0.313/0.102

[1]OSL = over season leaf
[2]The crop development stage at which each tissue was collected.
[3]Protein levels are expressed as the arithmetic mean and standard error (SE) as microgram (µg) of protein per gram (g) of tissue on a dry weight basis (dw). The means, SE, and ranges (minimum and maximum values) were calculated for each tissue across all five sites (n=20 for all tissues except root). In root, 17 samples were<LOQ and three samples expressed >LOQ with an average of 0.43 µg/g dw.
[4]LOQ=limit of quantitation, LOD=limit of detection.
[5]NA= Not applicable

B.1(b) Information about prior history of human consumption of the new substances, if any, or their similarity to substances previously consumed in food.

Refer to Section A.2(a)(i) and A.2(a)(ii).

B.1(c) Information on whether any new protein has undergone any unexpected post-translational modification in the new host

Refer to Sections B.1(a)(ii)(i)(v) and B.1(a)(ii)(ii)(v).

B.1(d) Where any ORFs have been identified (in subparagraph A.3(c)(v) of this guideline (3.5.1)), bioinformatics analysis to indicate the potential for allergenicity and toxicity of the ORFs

Refer to Section A.3(c)(v).

B.2 New Proteins

B.2(a) Information on the potential toxicity of any new proteins, including:

B.2(a)(i) A bioinformatic comparison of the amino acid sequence of each of the new proteins to know protein toxins and anti-nutrients (e.g. protease inhibitors, lectins)

For details about the bioinformatics data and results to compare amino acid sequence of Cry1A.2 and Cry1B.2 proteins to known protein toxins and anti-nutrients, please refer to Appendix **9**.

The assessment of the potential for protein toxicity includes bioinformatic analysis of the amino acid sequence of the introduced protein. The goal of the bioinformatic analysis is to ensure that the introduced protein does not share homology to known toxins or anti-nutritional proteins associated with adverse health effects.

Potential structural similarities shared between the MON 94637 Cry1A.2 and Cry1B.2 proteins with sequences in a protein database were evaluated using the FASTA sequence alignment tool. The FASTA program directly compares amino acid sequences (*i.e.*, primary, linear protein structure) and the alignment data may be used to infer shared higher order structural similarities between two sequences (*i.e.*, secondary and tertiary protein structures). Proteins that share a high degree of similarity throughout the entire sequence are often homologous. Homologous proteins often have common secondary structures, common three-dimensional configuration, and, consequently, may share similar functions (Caetano-Anollés *et al.*, 2009; Illergård *et al.*, 2009).

FASTA bioinformatic alignment searches using the MON 946379 Cry1A.2 amino acid sequence and Cry1B.2 amino acid sequence were performed with a toxin database to identify possible homology with proteins that may be harmful to human and animal health. Periodically, the databases used to evaluate proteins are updated. Since the most recent reports were completed, the toxin (TOX_2023) and protein (PRT_2023) databases have been revised and updated. In order to determine if proteins share significant sequence similarity to new sequences contained in the updated toxin database they were used as queries for a FASTA searches of the TOX_2023 database. The toxin database, TOX_2023, is a subset of sequences derived from the Swiss-Prot database (found at https://www.uniprot.org) that was selected using a keyword search and filtered to remove likely non-toxin proteins. The TOX_2023 database contains 7,227 sequences and has been curated to remove *Bt* insecticidal Cry proteins. The results of the bioinformatic analyses demonstrated that no structurally relevant similarity exists between the Cry1A.2 and Cry1B.2 proteins and any sequence in the TOX_2023 database.

Using MON 94637 Cry1A.2 and Cry1B.2 as the query sequences, no alignment with an *E*-score of ≤1e-5 was observed using the TOX_2023 database to run a FASTA search.

.

B.2(a)(ii) Information on the stability of the proteins to proteolysis in appropriate gastrointestinal model systems

B.2(a)(ii)(i) Digestive fate of the Cry1A.2 protein

Please refer Appendix **10** for detailed methods and results of assessment of susceptibility of Cry1A.2 protein to pepsin and pancreatin degradation.

B.2(a)(ii)(i)(i) Degradation of the MON 94637 Cry1A.2 protein by pepsin

Degradation of the *Bt*-produced Cry1A.2 protein by pepsin was evaluated over time by analyzing digestion mixtures incubated for targeted time intervals following a standardized protocol validated in an international, multi-laboratory ring study (Thomas *et al.*, 2004) collected at targeted incubation time points. The susceptibility of the Cry1A.2 protein to pepsin degradation was assessed by visual analysis of a Brilliant Blue G Colloidal stained SDS-PAGE gel and by visual analysis of a western blot probed with an polyclonal anti-Cry1A.2 antibody. Both visualization methods were run concurrently with separate SDS-PAGE and western blot analyses to estimate the limit of detection (LOD) of the Cry1A.2 protein for each method.

For SDS-PAGE analysis of the digestibility of the Cry1A.2 protein in pepsin, the gel was loaded with 1 µg of total test protein (based on pre-digestion protein concentrations) for each of the digestion samples (Figure 29, Panel A). The SDS-PAGE gel for the digestibility assessment was run concurrently with a separate SDS-PAGE gel to estimate the LOD of the Cry1A.2 protein (Figure 29, Panel B). The LOD of intact Cry1A.2 protein was approximately 6.25 ng (Figure 29, Panel B, lane 7). Visual examination of SDS-PAGE data showed that the intact Cry1A.2 protein was digested within 0.5 min of incubation in pepsin (Figure 29, Panel A, lane 5). Therefore, based on the LOD, more than 99.4% (100% - 0.6% = 99.4%) of the intact Cry1A.2 protein was digested within 0.5 min of incubation in pepsin. Peptide fragments between 3.5 to 6 kDa were observed through 60 min of the pepsin digestion.

No change in the Cry1A.2 protein band intensity was observed in the absence of pepsin in the 0 min No Pepsin Control and 60 min No Pepsin Control (Figure 29, Panel A, lanes 3 and 12). This indicates that the degradation of the Cry1A.2 protein was due to the proteolytic activity of pepsin and not due to instability of the protein while incubated in 10 mM HCl, 2 mg/ml NaCl, pH 1.2 for 60 min. The 0 min No Test Protein Control and 60 min No Test Protein Control (Figure 29, Panel A, lanes 2 and 13) demonstrated that the pepsin is stable throughout the experimental phase.

A **B**

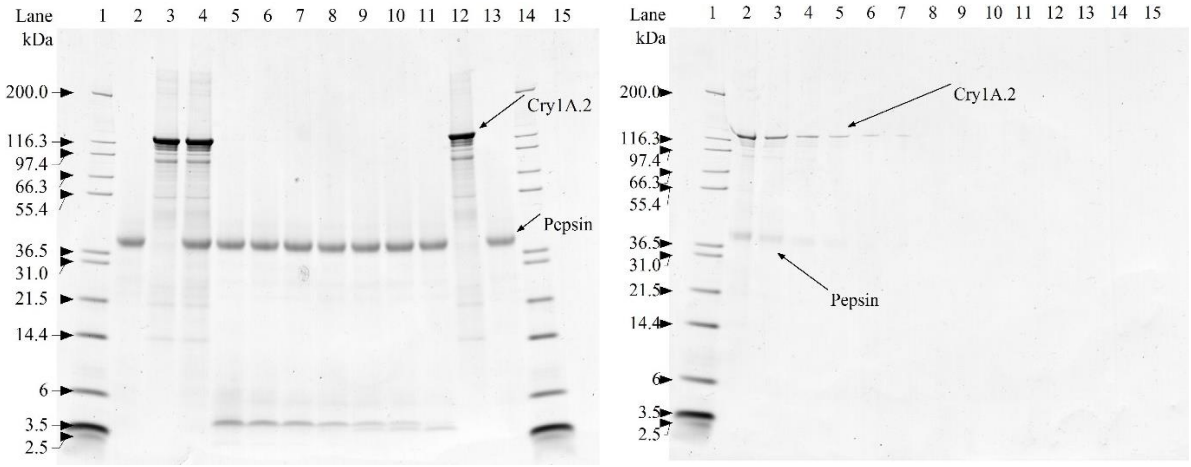

Figure 29. SDS-PAGE Analysis of the Degradation of Cry1A.2 Protein in Pepsin

Colloidal Brilliant Blue G stained SDS-PAGE gels were used to assess the degradation of Cry1A.2 protein by pepsin. Molecular weights (kDa) are shown on the left of each gel and correspond to the markers loaded. In each gel, the Cry1A.2 protein migrated to approximately 124.4 kDa and pepsin to approximately 38 kDa.

A: Cry1A.2 protein degradation in the presence of pepsin. Based on pre-reaction protein concentrations, 1 µg of test protein was loaded in each lane containing Cry1A.2 protein.

B: LOD determination. Indicated amounts of the test protein from the Pepsin Treated T0 sample were loaded to estimate the LOD of the Cry1A.2 protein.

Lane	Sample	Incubation Time (min)
1	Mark12™ MWM	-
2	0 min No Test Protein Control	0
3	0 min No Pepsin Control	0
4	Pepsin Treated T0	0
5	Pepsin Treated T1	0.5
6	Pepsin Treated T2	2
7	Pepsin Treated T3	5
8	Pepsin Treated T4	10
9	Pepsin Treated T5	20
10	Pepsin Treated T6	30
11	Pepsin Treated T7	60
12	60 min No Pepsin Control	60
13	60 min No Test Protein Control	60
14	Mark12 ™ MWM	-
15	Empty	-

Lane	Sample	Amount (ng)
1	Mark12 ™ MWM	-
2	Pepsin Treated T0	200
3	Pepsin Treated T0	100
4	Pepsin Treated T0	50
5	Pepsin Treated T0	25
6	Pepsin Treated T0	12.5
7	Pepsin Treated T0	6.25
8	Pepsin Treated T0	3.1
9	Pepsin Treated T0	1.6
10	Pepsin Treated T0	0.8
11	Pepsin Treated T0	0.4
12	Mark12 ™ MWM	-
13	Empty	-
14	Empty	-
15	Empty	-

For western blot analysis of Cry1A.2 pepsin susceptibility, the Cry1A.2 protein was loaded with approximately 10 ng per lane of total protein (based on pre-reaction total protein concentrations) for each reaction time point examined. The western blot used to assess Cry1A.2 protein to pepsin degradation (Figure 30, Panel A) was run concurrently with the western blot used to estimate the LOD (Figure 30, Panel B). The LOD of the Cry1A.2 protein was approximately 1 ng (Figure 30, Panel B, Lane 6). Western blot analysis demonstrated that the intact Cry1A.2 protein was degraded below the LOD within 0.5 min of incubation in the presence of pepsin (Figure 30, Panel A, Lane 6). Based on the western blot LOD for the Cry1A.2 protein, more than 90% (100% - 10% = 90%) of the intact Cry1A.2 protein was degraded within 0.5 min. No peptide fragments were detected at the 0.5 min and beyond time points in the western blot analysis.

No change in the intact Cry1A.2 protein band intensity was observed in the absence of pepsin in the 0 min No Pepsin Control and 60 min No Pepsin Control (Figure 30, Panel A, lanes 4 and 13). This indicates that the degradation of the Cry1A.2 protein was due to the proteolytic activity of pepsin and not due to instability of the protein while incubated in 2 mg/ml NaCl, 10 mM HCl, pH 1.2 for 60 min.

No immunoreactive bands were observed in 0 min No Protein Control and 60 min No Protein Control (Figure 30A, lanes 3 and 14). This result indicates that there was no non-specific interaction between the pepsin solution and the Cry1A.2-specific antibody under these experimental conditions.

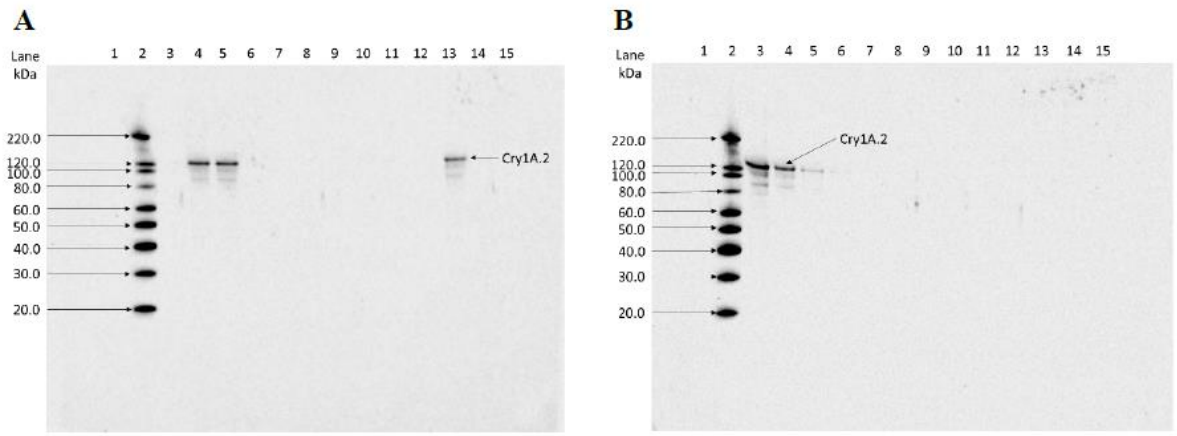

Figure 30. Western Blot Analysis of the Degradation of Cry1A.2 Protein by Pepsin

Western blots probed with an anti-Cry1A.2 antibody were used to assess the degradation of Cry1A.2 by pepsin. Molecular weights (kDa) are shown on the left of each gel and correspond to the MagicMark™ molecular weight marker. A 48 sec exposure is shown.
A: Cry1A.2 protein degradation by pepsin. Based on pre-reaction protein concentrations, 10 ng of test protein was loaded in each lane containing Cry1A.2 protein.
B: LOD determination. Indicated amounts of the test protein from the Pepsin Treated T0 sample were loaded to estimate the LOD of the Cry1A.2 protein.

Lane	Sample	Incubation Time (min)
1	Precision Plus MWM	-
2	MagicMark ™ MWM	-
3	0 min No Test Protein Control	0
4	0 min No Pepsin Control	0
5	Pepsin Treated T0	0
6	Pepsin Treated T1	0.5
7	Pepsin Treated T2	2
8	Pepsin Treated T3	5
9	Pepsin Treated T4	10
10	Pepsin Treated T5	20
11	Pepsin Treated T6	30
12	Pepsin Treated T7	60
13	60 min No Pepsin Control	60
14	60 min No Test Protein Control	60
15	Precision Plus MWM	-

Lane	Sample	Amount (ng)
1	Precision Plus MWM	-
2	MagicMark ™ MWM	-
3	Pepsin Treated T0	10
4	Pepsin Treated T0	5
5	Pepsin Treated T0	2
6	Pepsin Treated T0	1
7	Pepsin Treated T0	0.5
8	Pepsin Treated T0	0.25
9	Pepsin Treated T0	0.13
10	Pepsin Treated T0	0.063
11	Pepsin Treated T0	0.032
12	Pepsin Treated T0	0.016
13	Pepsin Treated T0	0.008
14	Pepsin Treated T0	0.004
15	Pepsin Treated T0	0.002

B.2(a)(ii)(i)(ii) Degradation of MON 94637 Cry1A.2 protein by pancreatin

The degradation of Cry1A.2 protein by pancreatin was assessed by western blot analysis (Figure 31). The Cry1A.2 protein was loaded with approximately 10 ng per lane of total protein (based on pre-reaction total protein concentrations) for each reaction time point examined. The western blot used to assess the Cry1A.2 protein degradation (Figure 31A) was run concurrently with the western blot used to estimate the LOD (Figure 31B) of the Cry1A.2 protein. The LOD of the Cry1A.2 protein was observed at approximately 1 ng protein loading (Figure 31A, lane 6). Based on the LOD for the Cry1A.2 protein, more than 90% (100% - 10% = 90%) of the intact Cry1A.2 protein was degraded within 5 min.

The majority of Cry1A.2 maintained its integrity with a small amount of Cry1A.2 reduced to a size above 75 kDa in the absence of pancreatin in the 24 hour No Pancreatin Control (Figure 31A, lanes 3 and 13). However, the fragments are larger than what was generated by pancreatin. This indicates that the degradation of all immunoreactive forms of the Cry1A.2 protein in the time point samples was due to the proteolytic activity of pancreatin and not due to instability of the protein when incubated in 50 mM KH_2PO_4, pH 7.5 over the course of the experiment.

No immunoreactive bands were observed in the 0 min No Test Protein Control and 24 hour No Test Protein Control (Figure 31A, lanes 2 and 14), demonstrating the absence of non-specific antibody interactions with the pancreatin solution.

A **B**

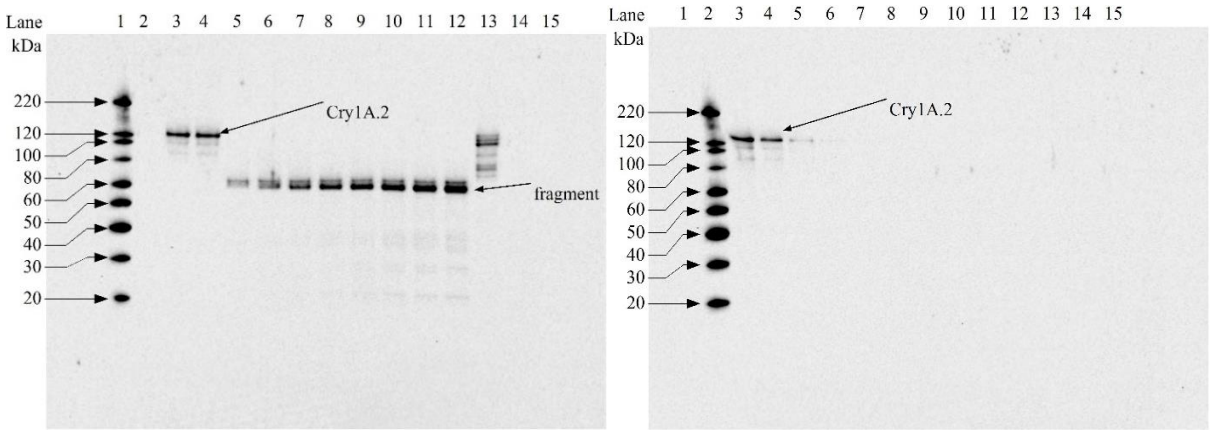

Figure 31. Western Blot Analysis of the Degradation of Cry1A.2 Protein by Pancreatin

Western blots probed with an anti-Cry1A.2 antibody were used to assess the degradation of Cry1A.2 by pancreatin. Molecular weights (kDa) are shown on the left of each gel and correspond to the MagicMark™ molecular weight marker. A 43 sec exposure is shown.
A: Cry1A.2 protein degradation by pancreatin. Based on pre-reaction protein concentrations, 10 ng of test protein was loaded in each lane containing Cry1A.2 protein.
B: LOD determination. Indicated amounts of the test protein from the Pancreatin Treated T0 sample were loaded to estimate the LOD of the Cry1A.2 protein.

Lane	Sample	Incubation Time
1	MagicMark ™ MWM	-
2	0 min No Test Protein Control	0
3	0 min No Pancreatin Control	0
4	Pancreatin Treated T0	0
5	Pancreatin Treated T1	5 min
6	Pancreatin Treated T2	15 min
7	Pancreatin Treated T3	30 min
8	Pancreatin Treated T4	1 h
9	Pancreatin Treated T5	2 h
10	Pancreatin Treated T6	4 h
11	Pancreatin Treated T7	8 h
12	Pancreatin Treated T8	24 h
13	24 h No Pancreatin Control	24 h
14	24 h No Test Protein Control	24 h
15	Precision Plus MWM	-

Lane	Sample	Amount (ng)
1	Precision Plus MWM	-
2	MagicMark ™ MWM	-
3	Pancreatin Treated T0	10
4	Pancreatin Treated T0	5
5	Pancreatin Treated T0	2
6	Pancreatin Treated T0	1
7	Pancreatin Treated T0	0.5
8	Pancreatin Treated T0	0.25
9	Pancreatin Treated T0	0.13
10	Pancreatin Treated T0	0.063
11	Pancreatin Treated T0	0.032
12	Pancreatin Treated T0	0.016
13	Pancreatin Treated T0	0.008
14	Pancreatin Treated T0	0.004
15	Pancreatin Treated T0	0.002

B.2(a)(ii)(i)(iii) Degradation of Cry1A.2 protein by pepsin followed by pancreatin

The degradation of the Cry1A.2 protein by pepsin followed by pancreatin (sequential digestion) were analyzed using SDS-PAGE and Colloidal Brilliant Blue G staining (Figure 32). The gel used to assess the digestibility of the Cry1A.2 protein in pepsin followed by pancreatin was loaded with 1 µg of total test protein (based on pre-digestion protein concentrations) for each of the digestion samples. Examination of SDS-PAGE data showed that the intact Cry1A.2 protein was digested within 2 min of incubation in pepsin (Figure 32, lane 3). and the small Cry1A.2 transient fragments between 3.5 and 6kDa was completely digested within 0.5 min of pancreatin exposure (Figure 32 lane 7).

No change in the Cry1A.2 protein band intensity was observed in the absence of pancreatin in the 0 min No Pancreatin Control and 120 minutes No Pancreatin Control (Figure 32, lanes 5 and 14). This indicates that the degradation of the Cry1A.2 protein was due to the proteolytic activity of pancreatin and not due to instability of the protein while incubated in 10 mM HCl, 2 mg/ml NaCl, pH 1.2 and 50 mM KH_2PO_4, pH 7.5 for 2 hr.

The SEQ 0 min No Test Protein Control and SEQ120 minutes No Test Protein Control (Figure 32, lanes 4 and 15) demonstrated the integrity of the pancreatin over the course of the experiment. The intensity of some pancreatin bands decreased during the course of the experiment, most likely due to auto-digestion. This is not expected to adversely impact the pancreatin degradation results, as the small Cry1A.2 transient fragments between 3.5 and 6 kDa were digested within 0.5 min of exposure to pancreatin.

The sequential digestion of the Cry1A.2 protein was also assessed by western blot (Figure 32, Panel B), with 10 ng of the test protein (based on total protein pre-digestion concentrations) loaded per lane. No bands were detected in the 2 min Pepsin Treated sample (Figure 32, Panel B, lane 3).

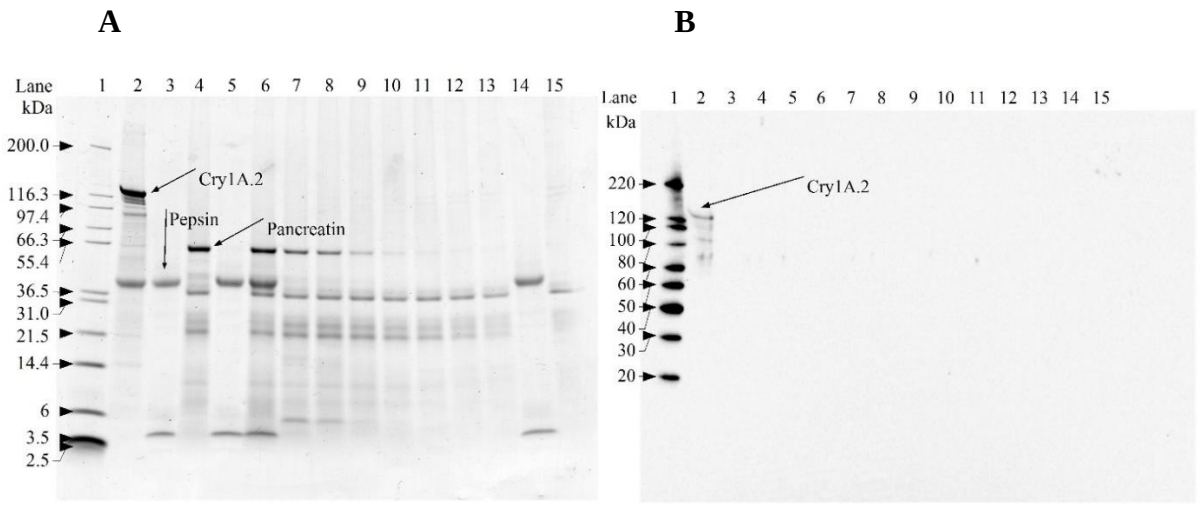

Figure 32. SDS-PAGE and Western Blot Analysis of the Degradation of Cry1A.2 Protein by Pepsin followed by Pancreatin

Colloidal Brilliant Blue G stained SDS-PAGE gel and western blot were used to assess the degradation of Cry1A.2 protein by pepsin followed by pancreatin. Molecular weights (kDa) are shown on the left of the gel and correspond to the markers loaded. In the gel, the Cry1A.2 protein migrated to approximately 124.4 kDa and pepsin to approximately 38 kDa.

A: SDS-PAGE analysis of Cry1A.2 protein degradation in the presence of pepsin followed by pancreatin. Based on pre-reaction protein concentrations, 1 µg of test protein was loaded in each lane containing Cry1A.2 protein.

B: Western blot probed with anti-Cry1A.2 antibody was used to assess the degradation of Cry1A.2 protein degradation by pepsin followed by pancreatin. Based on pre-reaction protein concentrations, 10 ng of test protein was loaded in each lane containing Cry1A.2 protein. A 45 sec exposure is shown.

Lane	Sample	Incubation Time
1	Mark12 ™ MWM	-
2	0 min Pepsin Treated (S0)	0 min
3	2 min Pepsin treated (S2)	2 min
4	SEQ 0 min No Test Protein Control	0 min
5	SEQ 0 min No Pancreatin Control	0 min
6	SEQ Pancreatin Treated T0	0 min
7	SEQ Pancreatin Treated T1	0.5 min
8	SEQ Pancreatin Treated T2	2 min
9	SEQ Pancreatin Treated T3	5 min
10	SEQ Pancreatin Treated T4	10 min
11	SEQ Pancreatin Treated T5	30 min
12	SEQ Pancreatin Treated T6	1 h
13	SEQ Pancreatin Treated T7	2 h
14	SEQ 120 min No Pancreatin Control	2 h
15	SEQ 120 min No Test Protein Control	2 h

Lane	Sample
1	MagicMark ™ MWM
2	0 min Pepsin Treated (S0)
3	2 min Pepsin treated (S2)
4	SEQ 0 min No Test Protein Control
5	SEQ 0 min No Pancreatin Control
6	SEQ Pancreatin Treated T0
7	SEQ Pancreatin Treated T1
8	SEQ Pancreatin Treated T2
9	SEQ Pancreatin Treated T3
10	SEQ Pancreatin Treated T4
11	SEQ Pancreatin Treated T5
12	SEQ Pancreatin Treated T6
13	SEQ Pancreatin Treated T7
14	SEQ 120 min No Pancreatin Control
15	SEQ 120 min No Test Protein Control

B.2(a)(ii)(i)(iv) Digestive fate of the Cry1A.2 protein conclusions

The ability of Cry1A.2 protein to be degraded by pepsin and by pancreatin and by pepsin followed by pancreatin was evaluated in this study. The results showed that at least 99.4% of the intact Cry1A.2 protein was degraded by pepsin within 0.5 min when analyzed by SDS-PAGE and 90% of the intact Cry1A.2 was degraded by pepsin within 0.5 min when analyzed by western blot using a Cry1A.2-specific antibody. SDS-PAGE analysis showed that peptide fragments between 3.5 and 6 kDA were observed throughout the 60 min of the pepsin digestion. The small Cry1A.2 transient fragments between 3.5 and 6 kDA were digested within 0.5 min when incubated with pepsin followed by pancreatin. At least 90% of the intact Cry1A.2 protein was degraded by pancreatin within 5 min when analyzed by western blot. These results show that the full-length Cry1A.2 is rapidly degraded by pepsin and pancreatin. The small Cry1A.2 transient fragments between 3.5 and 6 kDa were rapidly degraded by sequential digestion. Rapid and complete degradation of the Cry1A.2 protein by pepsin or pancreatin alone and pepsin followed by pancreatin indicates that the Cry1A.2 protein is highly unlikely to pose any safety concern to human health.

B.2(a)(ii)(ii) Digestive fate of the Cry1B.2 protein

Please refer Appendix **11** for detailed methods and results of assessment of susceptibility of Cry1B.2 protein to pepsin and pancreatin degradation.

B.2(a)(ii)(ii)(i) Degradation of MON 94637 Cry1B.2 protein by pepsin

Degradation of the *Bt*-produced Cry1B.2 protein by pepsin was evaluated over time by analyzing digestion mixtures incubated for targeted time intervals following a standardized protocol validated in an international, multi-laboratory ring study (Thomas *et al.*, 2004) collected at targeted incubation time points. The susceptibility of Cry1B.2 protein to pepsin degradation was assessed by visual analysis of a Brilliant Blue G Colloidal stained SDS-PAGE gel and by visual analysis of a western blot probed with an anti-Cry1B.2 polyclonal antibody. Both visualization methods were run concurrently with separate SDS-PAGE and western blot analyses to estimate the limit of detection (LOD) of the Cry1B.2 protein for each method.

For SDS-PAGE analysis of the digestibility of the Cry1B.2 protein in pepsin, the gel was loaded with 1 µg of total test protein (based on pre-digestion protein concentrations) for each of the digestion samples (Figure 33, Panel A). The SDS-PAGE gel for the digestibility assessment was run concurrently with a separate SDS-PAGE gel to estimate the LOD of the Cry1B.2 protein (Figure 33, Panel B). The LOD of intact Cry1B.2 protein was approximately 6.25 ng (Figure 33, Panel B, lane 8). Visual examination of SDS-PAGE data showed that the intact Cry1B.2 protein was digested within 0.5 min of incubation in pepsin (Figure 33, Panel A, lane 5). Therefore, based on the LOD, more than 99.4% (100% - 0.6% = 99.4%) of the intact Cry1B.2 protein was digested within 0.5 min of incubation in pepsin. Peptide fragments ~4 kDa were observed through 60 min of the pepsin digestion.

No change in the Cry1B.27 protein band intensity was observed in the absence of pepsin in the 0 min No Pepsin Control and 60 min No Pepsin Control (Figure 33A, lanes 3 and 12). This indicates that the degradation of the Cry1B.2 protein was due to the proteolytic activity of pepsin and not due to instability of the protein while incubated in 10 mM HCl, 2 mg/ml NaCl, pH 1.2 for 60 min. The 0 min No Test Protein Control and 60 min No Test Protein Control (Figure 33A, lanes 2 and 13) demonstrated that the pepsin is stable throughout the experimental phase.

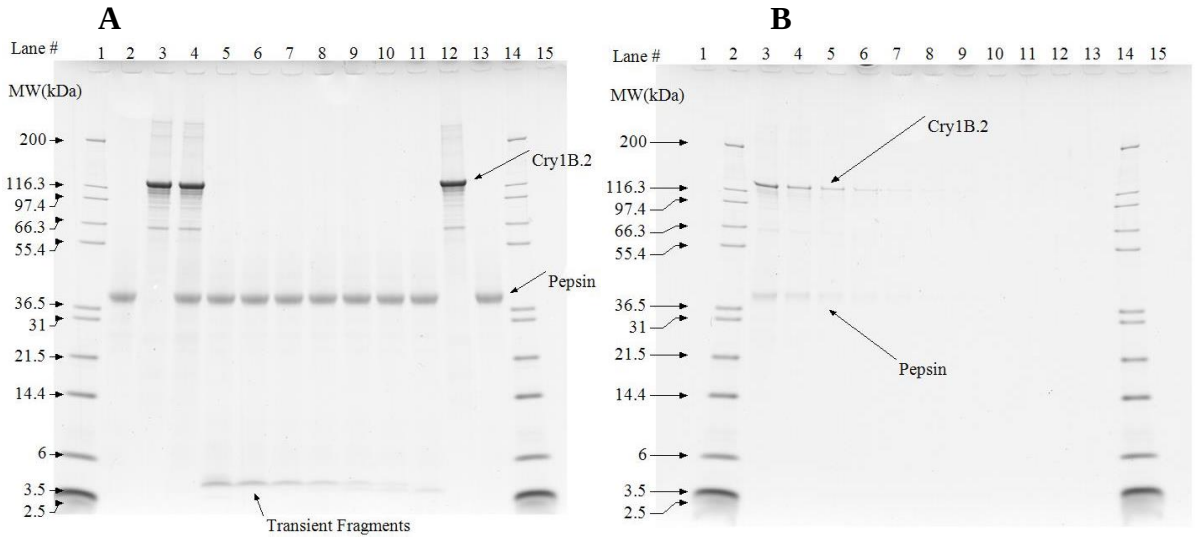

Figure 33. SDS-PAGE Analysis of the Degradation of Cry1B.2 Protein by Pepsin

Colloidal Brilliant Blue G stained SDS-PAGE gels were used to assess the degradation of Cry1B.2 protein by pepsin. Molecular weights (kDa) are shown on the left of each gel and correspond to the markers loaded. In each gel, the Cry1B.2 protein migrated to 132.6 kDa and pepsin to approximately 38 kDa.

A: Cry1B.2 protein degradation in the presence of pepsin. Based on pre-reaction protein concentrations, 1 µg of test protein was loaded in each lane containing Cry1B.2 protein.

B: LOD determination. Indicated amounts of the test protein from the Pepsin Treated T0 sample were loaded to estimate the LOD of the Cry1B.2 protein.

Lane	Sample	Incubation Time (min)
1	Mark12™ MWM	-
2	0 min No Test Protein Control	0
3	0 min No Pepsin Control	0
4	Pepsin Treated T0	0
5	Pepsin Treated T1	0.5
6	Pepsin Treated T2	2
7	Pepsin Treated T3	5
8	Pepsin Treated T4	10
9	Pepsin Treated T5	20
10	Pepsin Treated T6	30
11	Pepsin Treated T7	60
12	60 min No Pepsin Control	60
13	60 min No Test Protein Control	60
14	Mark12™ MWM	-
15	Empty	-

Lane	Sample	Amount (ng)
1	Empty	-
2	Mark12™ MWM	-
3	Pepsin Treated T0	200
4	Pepsin Treated T0	100
5	Pepsin Treated T0	50
6	Pepsin Treated T0	25
7	Pepsin Treated T0	12.5
8	Pepsin Treated T0	6.25
9	Pepsin Treated T0	3.125
10	Pepsin Treated T0	1.55
11	Pepsin Treated T0	0.8
12	Pepsin Treated T0	0.4
13	Pepsin Treated T0	0.2
14	Mark12™ MWM	-
15	Empty	-

For western blot analysis of Cry1B.2 pepsin susceptibility, the Cry1B.2 protein was loaded with approximately 10 ng per lane of total protein (based on pre-reaction total protein concentrations) for each reaction time point examined. The western blot used to assess Cry1B.2 protein degradation (Figure 34, Panel A) was run concurrently with the western blot used to estimate the LOD (Figure 34, Panel B). The LOD of the Cry1B.2 protein was approximately 1.25 ng (Figure 34, Panel B, Lane 7). Western blot analysis demonstrated that the intact Cry1B.2 protein was degraded below the LOD within 0.5 min of incubation in the presence of pepsin (Figure 34, Panel A, Lane 6). Based on the western blot LOD for the Cry1B.2 protein, more than 87.5% (100% - 12.5% = 87.5%) of the intact Cry1B.2 protein was degraded within 0.5 min. No peptide fragments were detected at the 0.5 min and beyond time points in the western blot analysis.

No change in the Cry1B.2 protein band intensity was observed in the absence of pepsin in the 0 min No Pepsin Control and 60 min No Pepsin Control (Figure 34A, lanes 4 and 13). This indicates that the degradation of the Cry1B.2 protein was due to the proteolytic activity of pepsin and not due to instability of the protein while incubated in 2 mg/ml NaCl, 10 mM HCl, pH 1.2 for 60 min.

No immunoreactive bands were observed in 0 min No Protein Control and 60 min No Protein Control (Figure 34A, lanes 3 and 14). This result indicates that there was no non-specific interaction between the pepsin solution and the Cry1B.2-specific antibody under these experimental conditions.

A **B**

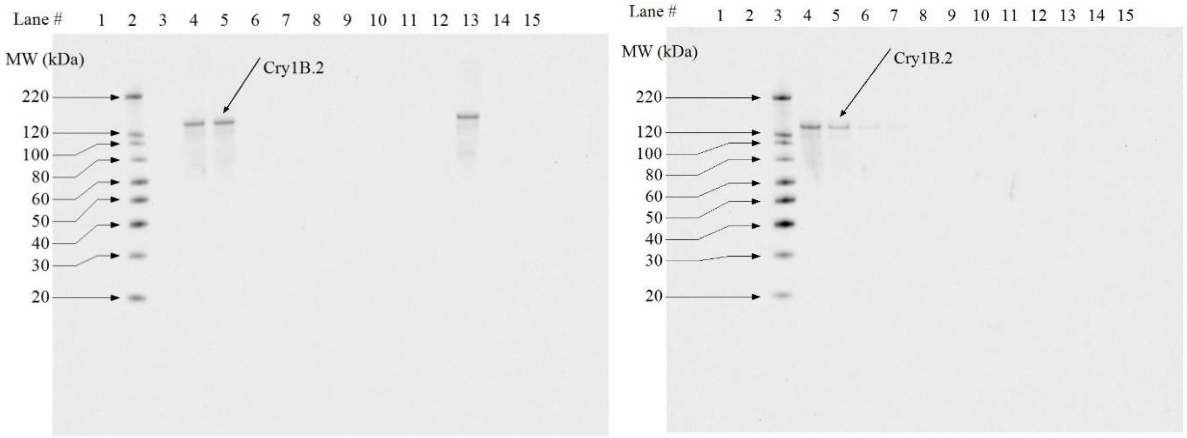

Figure 34. Western Blot Analysis of the Degradation of Cry1B.2 Protein by Pepsin

Western blots probed with an anti-Cry1B.2 antibody were used to assess the degradation of Cry1B.2 by pepsin. Molecular weights (kDa) are shown on the left of each blot and correspond to the MagicMark™ molecular weight marker. A 6 sec exposure is shown.
A: Cry1B.2 protein degradation by pepsin. Based on pre-reaction protein concentrations, 10 ng of test protein was loaded in each lane containing Cry1B.2 protein.
B: LOD determination. Indicated amounts of the test protein from the Pepsin Treated T0 sample were loaded to estimate the LOD of the Cry1B.2 protein.

Lane	Sample	Incubation Time (min)
1	Empty	-
2	MagicMark™ MWM	-
3	0 min No Test Protein Control	0
4	0 min No Pepsin Control	0
5	Pepsin Treated T0	0
6	Pepsin Treated T1	0.5
7	Pepsin Treated T2	2
8	Pepsin Treated T3	5
9	Pepsin Treated T4	10
10	Pepsin Treated T5	20
11	Pepsin Treated T6	30
12	Pepsin Treated T7	60
13	60 min No Pepsin Control	60
14	60 min No Test Protein Control	60
15	Precision Plus™ MWM	-

Lane	Sample	Amount (ng)
1	Empty	-
2	Precision Plus™ MWM	-
3	MagicMark™ MWM	-
4	Pepsin Treated T0	10
5	Pepsin Treated T0	5
6	Pepsin Treated T0	2.5
7	Pepsin Treated T0	1.25
8	Pepsin Treated T0	0.625
9	Pepsin Treated T0	0.3125
10	Pepsin Treated T0	0.156
11	Pepsin Treated T0	0.078
12	Pepsin Treated T0	0.039
13	Pepsin Treated T0	0.0195
14	Pepsin Treated T0	0.00975
15	Empty	-

B.2(a)(ii)(ii)(ii) Degradation of MON 94637 Cry1B.2 protein by pancreatin

The degradation of the Cry1B.2 protein by pancreatin was assessed by western blot analysis (Figure 35). The Cry1B.2 protein was loaded with approximately 10 ng per lane of total protein (based on pre-reaction total protein concentrations) for each reaction time point examined. The western blot used to assess the Cry1B.2 protein degradation (Figure 35A) was run concurrently with the western blot used to estimate the LOD (Figure 35B) of the Cry1B.2 protein. The LOD of the Cry1B.2 protein was observed at approximately the 1.25 ng protein loading (Figure 35A, lane 8). Based on the LOD for the Cry1B.2 protein, more than 87.5% (100% - 12.5% = 87.5%) of the intact Cry1B.2 protein was degraded within 5 min.

Instability of Cry1B.2 was observed in the absence of pancreatin in the 24 hour No Pancreatin Control (Figure 35A lane 13). The protein was truncated to a size at or above 75 kDa, which are larger than what was generated by pancreatin. This indicates that the degradation of all immunoreactive forms of the Cry1B.2 protein in the time point samples was due to the proteolytic activity of pancreatin and not due to instability of the protein when incubated in 50 mM KH_2PO_4, pH 7.5 over the course of the experiment.

No immunoreactive bands were observed in the 0 min No Test Protein Control and 24 hour No Test Protein Control (Figure 35A, lanes 2 and 14), demonstrating the absence of non-specific antibody interactions with the pancreatin solution.

A **B**

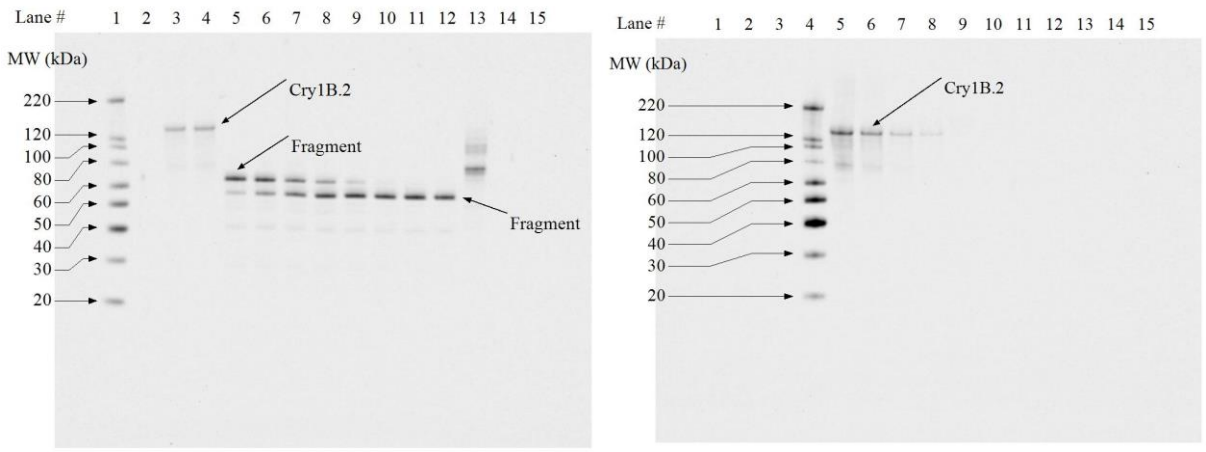

Figure 35. Western Blot Analysis of the Degradation of Cry1B.2 Protein by Pancreatin

Western blots probed with an anti-Cry1B.2 antibody were used to assess the degradation of Cry1B.2 by pancreatin. Molecular weights (kDa) are shown on the left of each blot and correspond to the MagicMark™ molecular weight marker. A 6 sec exposure is shown.
A: Cry1B.2 protein degradation by pancreatin. Based on pre-reaction protein concentrations, 10 ng of test protein was loaded in each lane containing Cry1B.2 protein.
B: LOD determination. Indicated amounts of the test protein from the Pancreatin Treated T0 sample were loaded to estimate the LOD of the Cry1B.2 protein.

Lane	Sample	Incubation Time
1	MagicMark™ MWM	-
2	0 min No Test Protein Control	0
3	0 min No Pancreatin Control	0
4	Pancreatin Treated T0	0
5	Pancreatin Treated T1	5 min
6	Pancreatin Treated T2	15 min
7	Pancreatin Treated T3	30 min
8	Pancreatin Treated T4	1 h
9	Pancreatin Treated T5	2 h
10	Pancreatin Treated T6	4 h
11	Pancreatin Treated T7	8 h
12	Pancreatin Treated T8	24 h
13	24 h No Pancreatin Control	24 h
14	24 h No Test Protein Control	24 h
15	Precision Plus™ MWM	-

Lane	Sample	Amount (ng)
1	Empty	-
2	Empty	-
3	Precision Plus™ MWM	-
4	MagicMark™ MWM	-
5	Pancreatin Treated T0	10
6	Pancreatin Treated T0	5
7	Pancreatin Treated T0	2.5
8	Pancreatin Treated T0	1.25
9	Pancreatin Treated T0	0.625
10	Pancreatin Treated T0	0.3125
11	Pancreatin Treated T0	0.156
12	Pancreatin Treated T0	0.078
13	Empty	-
14	Empty	-
15	Empty	-

B.2(a)(ii)(ii)(iii) Degradation of Cry1B.2 protein by pepsin followed by pancreatin

The degradation of the Cry1B.2 protein by pepsin followed by pancreatin (sequential digestion) was analyzed using SDS-PAGE and Colloidal Brilliant Blue G staining (Figure 36). The gel used to assess the sequential digestion of Cry1B.2 protein was loaded with 1 µg of total test protein (based on pre-digestion protein concentrations) for each of the digestion samples. Examination of SDS-PAGE data showed that the intact Cry1B.2 protein was digested within 2 min of incubation in pepsin (Figure 36A, lane 3) and the small transient fragments at ~4 kDa were completely digested within 0.5 min of pancreatin exposure (Figure 36A, lane 7).

No change in the Cry1B.2 fragments band intensity was observed in the absence of pancreatin in the 0 min No Pancreatin Control and120 minutes No Pancreatin Control (Figure 36A, lanes 5 and 14). This indicates that the degradation of the Cry1B.2 fragments were due to the proteolytic activity of pancreatin and not due to instability of the fragments while incubated in 50 mM KH_2PO_4, pH 7.5 for 2 hr.

The SEQ 0 min No Test Protein Control and SEQ 120 minutes No Test Protein Control (Figure 36A, lanes 4 and 15) demonstrated the integrity of the pancreatin over the course of the experiment. The intensity of some pancreatin bands decreased during the course of the experiment, most likely due to auto-digestion. This is not expected to adversely impact the pancreatin degradation results, as the fragments (~4 kDa) were digested within 0.5 min of exposure to pancreatin.

The sequential digestion of the Cry1B.2 protein was also assessed by western blot (Figure 36B), with 10 ng of the test protein (based on total protein pre-digestion concentrations) loaded per lane. No bands were detected in the 2 min Pepsin Treated sample (Figure 36, Panel B, lane 3).

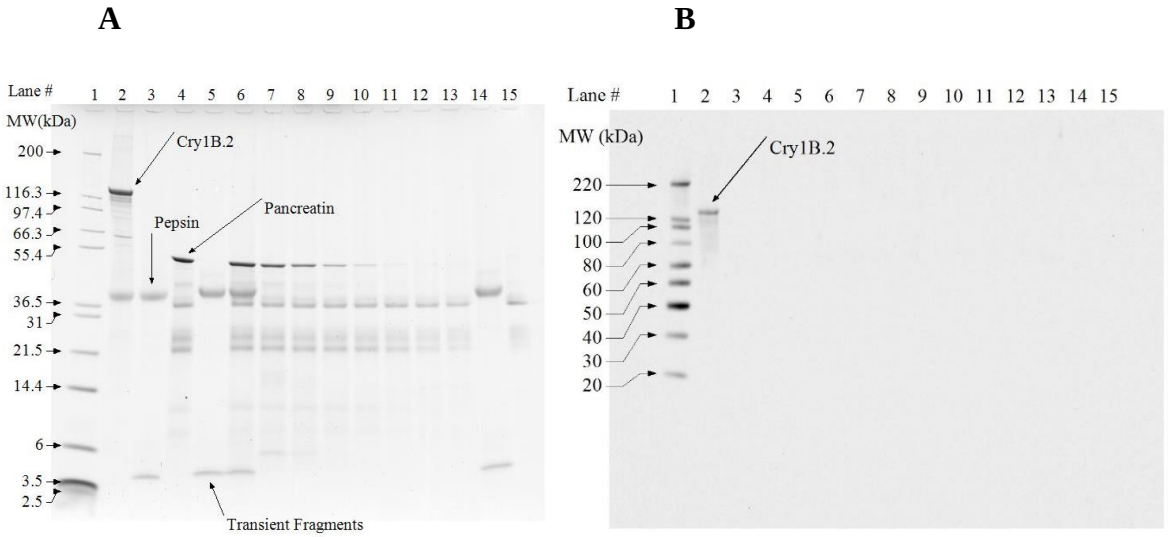

Figure 36. SDS-PAGE and Western Blot Analysis of the Degradation of Cry1B.2 Protein by Pepsin followed by Pancreatin

Colloidal Brilliant Blue G stained SDS-PAGE gel and a western blot probed with an anti-Cry1B.2 antibody were used to assess the degradation of Cry1B.2 protein by pepsin followed by pancreatin. Molecular weights (kDa) are shown on the left of the figures and correspond to the markers loaded.
A: SDS-PAGE analysis of Cry1B.2 protein degradation in the presence of pepsin followed by pancreatin. Based on pre-reaction protein concentrations, 1 µg of test protein was loaded in each lane containing Cry1B.2 protein. In the gel, the Cry1B.2 protein migrated to 132.6 kDa and pepsin to approximately 38 kDa.
B: Western blot probed with an anti-Cry1B.2 antibody was used to assess the degradation of Cry1B.2 by pepsin followed by pancreatin. Based on pre-reaction protein concentrations, 10 ng of test protein was loaded in each lane containing Cry1B.2 protein. A 6 sec exposure is shown.

Lane	Sample	Incubation Time
1	Mark12™ MWM	-
2	0 min Pepsin Treated (S0)	0 min
3	2 min Pepsin treated (S2)	2 min
4	SEQ 0 min No Test Protein Control	0 min
5	SEQ 0 min No Pancreatin Control	0 min
6	SEQ Pancreatin Treated T0	0 min
7	SEQ Pancreatin Treated T1	0.5 min
8	SEQ Pancreatin Treated T2	2 min
9	SEQ Pancreatin Treated T3	5 min
10	SEQ Pancreatin Treated T4	10 min
11	SEQ Pancreatin Treated T5	30 min
12	SEQ Pancreatin Treated T6	1 h
13	SEQ Pancreatin Treated T7	2 h
14	SEQ 120 min No Pancreatin Control	2 h
15	SEQ 120 min No Test Protein Control	2 h

Lane	Sample
1	MagicMark™ MWM
2	0 min Pepsin Treated (S0)
3	2 min Pepsin treated (S2)
4	SEQ 0 min No Test Protein Control
5	SEQ 0 min No Pancreatin Control
6	SEQ Pancreatin Treated T0
7	SEQ Pancreatin Treated T1
8	SEQ Pancreatin Treated T2
9	SEQ Pancreatin Treated T3
10	SEQ Pancreatin Treated T4
11	SEQ Pancreatin Treated T5
12	SEQ Pancreatin Treated T6
13	SEQ Pancreatin Treated T7
14	SEQ 120 min No Pancreatin Control
15	SEQ 120 min No Test Protein Control

B.2(a)(ii)(ii)(iv) Digestive fate of the Cry1B.2 protein conclusions

The ability of Cry1B.2 protein to be degraded by pepsin and by pancreatin was evaluated in this study. The results showed that at least 99.4% of the intact Cry1B.2 protein was degraded by pepsin within 0.5 min when analyzed by SDS-PAGE and 87.5% of the intact Cry1B.2 was degraded by pepsin within 0.5 min when analyzed by western blot using a Cry1B.2-specific antibody. SDS-PAGE analysis showed that transient peptide fragments at ~4 kDa were observed through the 60 min of the pepsin digestion. At least 87.5% of the intact Cry1B.2 protein was degraded by pancreatin within 5 min when analyzed by western blot. The fragments of Cry1B.2 were digested within 0.5 min when incubated with pepsin followed by pancreatin.These results show that the full-length Cry1B.2 is rapidly degraded by pepsin and pancreatin, and that the Cry1B.2 fragments are also quickly degraded by pepsin followed by pancreatin.Rapid degradation of the intact Cry1B.2 protein by pepsin or pancreatin alone and rapid degradation of the Cry1B.2 fragments by pepsin followed by pancreatin indicates that the Cry1B.2 protein is highly unlikely to pose any safety concern to human health.

B.2(a)(iii) An animal toxicity study if the bioinformatic comparison and biochemical studies indicate either a relationship with known protein toxins/anti-nutrients or resistance to proteolysis

Not relevant for this product.

B.2(b) Information on the potential allergenicity of any new proteins, including:

B.2(b)(i) Source of the new proteins

As described in A.2(a)(i)(i), The coding sequence for the Cry1A.2 and Cry1B.2 proteins are derived from the bacterium *Bacillus thuringiensis*:

Kingdom: Bacteria
Phylum: Firmicutes
Class: Bacilli
Order: Bacillales
Family: Bacillaceae
Genus: *Bacillus*

The Cry1A.2 and Cry1B.2 proteins are derived from genetic elements that code for crystalline proteins (Cry) that are expressed as parasporal inclusions (or δ-endotoxins) in the ubiquitous gram-positive bacterium *Bacillus thuriengensis* (*Bt)* (Gill *et al.*, 1992; Schnepf *et al.*, 1998; Vachon *et al.*, 2012). *Bt* isolates have a long, documented history of safe use in agriculture and safe human consumption. Since the first *Bt* isolate was registered as a pesticide in 1961, over 180 microbial *Bt* products have been registered in the United States (U.S.), with more than 120 microbial products registered in the European Union (EU) (Hammond, 2004). *Bt* microbial biopesticides have been safely and directly applied to consumed agricultural commodities including berry crops, cabbage, grapes, tomatoes, celery, lettuce, and spinach (U.S. EPA, 1998). For certain crops, a significant percentage of the total US grown crop has been treated with *Bt* crystal/spore preparations (*e.g.*, blackberries (50%), celery (46%), and cabbage (39%)) (U.S. EPA, 1998). In Europe, residual levels of *Bt* microbes of up to 100,000 CFUs (colony forming units) were observed on fresh vegetables following application of *Bt* microbial pesticides (Frederiksen *et al.*, 2006). Thus, the use of *Bt* microbials for pest control in

agriculture, including in organic farming, provides a 50-year history of safe consumption of food crops sprayed with *Bt* microbial pesticides.

B.2(b)(ii) A bioinformatics comparison of the amino acid sequence of the novel protein to known allergens

B.2(b)(ii)(i) Structural similarity of Cry1A.2 and Cry1B.2 to known allergens

Please refer to Appendix **9** for detailed methods and results from the bioinformatics comparison of the amino acid sequence of Cry1A.2 and Cry1B.2 proteins to known allergens.

The Codex guidelines for the evaluation of the allergenicity potential of introduced proteins (Codex Alimentarius, 2009) are based on the comparison of amino acid sequences between introduced proteins and allergens. Allergenic cross-reactivity may be possible if the introduced protein is found to have at least 35% amino acid identity with an allergen over any segment of at least 80 amino acids. The Codex guideline also suggests that a sliding window search with a scientifically justified peptide size be used to identify immunologically relevant peptides in otherwise unrelated proteins. Therefore, Cry1A.2 protein sequence and Cry1B.2 protein sequence were assessed for the extent of sequence similarities with known allergens, gliadins, and glutenins using the FASTA sequence alignment tool along with an eight-amino acid sliding window search (Codex Alimentarius, 2009; Thomas *et al.*, 2005). The methods used are summarized below. The data generated from these analyses confirm that the Cry1A.2 protein and Cry1B.2 protein do not share amino acid sequence similarities with known allergens, gliadins, or glutenins.

The FASTA program directly compares amino acid sequences (i.e., primary, linear protein structure). This alignment data may be used to infer shared higher order structural similarities between two sequences (i.e., secondary and tertiary protein structures). Proteins that share a high degree of similarity throughout the entire sequence are often homologous. By definition, homologous proteins have common secondary structures, and three-dimensional configuration, and, consequently, may share similar functions. The allergen, gliadin, and glutenin protein sequence database (AD_2023) was obtained as the "COMprehensive Protein Allergen REsource" (COMPARE) database from the Health and Environmental Sciences Institute (HESI) and was used for the evaluation of sequence similarities of Cry1A.2 protein and Cry1B.2 protein shared with all proteins in the database. The AD_2023 database contains 2,631 sequences. When used to align the sequence of the introduced protein to each protein in the database, the FASTA algorithm produces an *E*-score (expectation score) for each alignment. The *E*-score is a statistical measure of the likelihood that the observed similarity score could have occurred by chance in a search. A larger *E*-score indicates a low degree of similarity between the query sequence and the sequence from the database. Typically, alignments between two sequences which have an *E*-score of less than or equal to 1×10-5 are considered to have meaningful homology. Results indicate that the Cry1A.2 protein sequence and Cry1B.2 protein sequence do not share meaningful similarity with sequences in the allergen database. No alignment met or exceeded the threshold of 35% identity over 80 amino acids recommended by Codex Alimentarius (2009) or had an *E*-score of less than or equal to 1×10-5.

A second bioinformatic tool, an eight-amino acid sliding window search, was used to specifically identify short linear polypeptide matches to known allergens. It is possible that proteins structurally unrelated to allergens, gliadins, and glutenins may contain smaller immunologically meaningful epitopes. An amino acid sequence may have allergenic potential

if it has an exact sequence identity of at least eight linearly contiguous amino acids with a potential allergen epitope (Hileman *et al.*, 2002; Metcalfe *et al.*, 1996). Using a sliding window of less than eight amino acids can produce matches containing considerable uncertainty depending on the length of the query sequence (Silvanovich *et al.*, 2006), and is not useful to the allergy assessment process (Thomas *et al.*, 2005). No eight contiguous amino acid identities were detected when the Cry1A.2 protein sequence and Cry1B.2 protein sequence were compared to the proteins in the AD_2023 sequence database.

The bioinformatic results demonstrated there were no biologically relevant sequence similarities to allergens when the Cry1A.2 protein sequence and Cry1B.2 protein sequence were used as a query for a FASTA search of the AD_2023 database. Furthermore, no short (eight amino acid) polypeptide matches were shared between the Cry1A.2 and CryB.2 protein sequences and proteins in the allergen database. These data show that the Cry1A.2 protein sequence and Cry1B.2 protein sequences lack both structurally and immunologically relevant similarities to known allergens, gliadins, and glutenins.

B.2(b)(iii) The new protein's structural properties, including, but not limited to, its susceptibility to enzymatic degregation (e.g. proteolysis), heat and/or acid stability

For digestibility of Cry1A.2 and Cry1B.2 proteins, refer to Section B.2(a)(ii).

B.2(b)(iii)(i) Heat susceptibility of the MON 94637 Cry1A.2 protein

The effect of heat treatment on the activity of the *Bt*-produced Cry1A.2 protein was evaluated. The method for evaluating heat stability is described in Appendix **12**.

Temperature can have a profound effect on the structure and function of proteins. Heat treatment is widely used in the preparation of foods derived from soybean grain (Hammond and Jez, 2011). It is reasonable that such processing will have an effect on the functional activity and structure of Cry1A.2 protein when consumed in different food products derived from MON 94637, thus reducing any potential safety concerns posed by the protein. Therefore, an assessment of the effect of heating on Cry1A.2 was conducted as a surrogate for the conditions encountered during the preparation of foods from MON 94637 grain.

In the study, heat treated samples and an unheated control sample of Cry1A.2 protein were analyzed: 1) using an insect bioassay to assess the impact of temperature on the functional activity of the Cry1A.2 protein; and 2) using SDS-PAGE to assess the impact of temperature on protein integrity.

Aliquots of Cry1A.2 protein were heated to 25ºC, 37ºC, 55ºC, 75ºC and 95ºC for either 15 or 30 minutes, while a separate aliquot of Cry1A.2 protein was maintained on ice for the duration of the heat treatments to serve as a temperature control. The effect of heat treatment on the activity of Cry1A.2 was evaluated using an insect bioassay. The effect of heat treatment on the integrity of the Cry1A.2 protein was evaluated using SDS-PAGE analysis of the heated and temperature control Cry1A.2 protein samples.

Results of the functional activity assay for Cry1A.2 protein incubated at a range of temperatures for 15 or 30 minutes are listed in Table 22 and Table 23, respectively. The EC_{50} values were determined as the concentration of Cry1A.2 (µg/ml diet) that resulted in 50% growth inhibition relative to the control treatment, in a SBL insect bioassay. The control sample had an EC_{50} of 0.058 µg Cry1A.2 protein/ml diet, thus demonstrating that protein activity was maintained during incubation on ice.

Functional activity of the Cry1A.2 protein was not impacted following heat treatments at 25, 37 and 55ºC for 15 and 30 minutes with a slight reduction in activity evident at the 55°C for 30 minute heat treatment. No functional activity in an SBL bioassay was observerd after the incubation at ≥75°C for 15 or 30 minutes, As a result, an EC_{50} could not be determined.

The results of the SDS-PAGE analysis of the heat-treated samples incubated for 15 and 30 minutes are illustrated in Figure 37 and Figure 38, respectively. The control sample loaded on each gel (Figure 37 and Figure 38, lane 2) showed equivalent band intensity to the 100% reference standard (Figure 37 and Figure 38, lane 8), demonstrating that the Cry1A.2 protein was stable on ice during the incubation period. No apparent decrease in band intensity of the 124.4 kDa Cry1A.2 protein was observed in the test samples when heated at temperatures of 25 or 37°C for 15 or 30 minutes. Aggregation products were evident at 55°C for both 15 and 30 minutes. A decrease in the intensity of the main Cry1A.2 band was evident at 75°C with the most prominent loss of band intensity observed at 30 minutes. In addition, degradation and aggregation products were also evident at 75°C for both the 15 and 30 minute heat treatments. Incubation for 15 and 30 minutes at 95°C resulted in a significant loss of the Cry1A.2 band intensity with the greatest loss evident after the 30 minute heat treatment. Additionally, both the 15 and 30 minute heat treatments at 95°C exhibited increased aggregation and degradation.

These data demonstrate that the Cry1A.2 protein behaves with a predictable tendency toward protein denaturation and loss of functional activity at elevated temperatures. Heat treatment is widely used in the preparation of foods containing components derived from soybean grain. Therefore, it is reasonable to conclude that Cry1A.2 protein would not be consumed as an active protein in food products due to standard processing practices that include heat treatment.

Table 22. EC_{50} Values and 95% Confidence Limits (CI) for the Heat-treated Cry1A.2 Protein After 15 Minutes

Temperature	EC_{50} (µg Cry1A.2/ml diet)	95% CI (µg Cry1A.2/ml diet)
0 ºC (control)	0.058	0.054 – 0.064
25ºC	0.079	0.070 – 0.090
37ºC	0.071	0.063 – 0.081
55ºC	0.073	0.065 – 0.081
75ºC[1]	N/A[2]	N/A
95ºC[1]	N/A[2]	N/A

[1] No EC_{50} value and 95% CI were estimated since no dose-response relationship was observed
[2] NA: no EC50 determined due to inadequate mortality

Table 23. EC_{50} Values and 95% Confidence Limits (CI) for the Heat-treated Cry1A.2 Protein After 30 Minutes

Temperature	EC_{50} (µg Cry1A.2/ml diet)	95% CI (µg Cry1A.2/ml diet)
0 ºC (control)	0.058	0.054 – 0.064
25ºC	0.092	0.080 – 0.110
37ºC	0.064	0.045 – 0.091
55ºC	0.190	0.170 – 0.220
75ºC[1]	N/A[2]	N/A
95ºC[1]	N/A[2]	N/A

[1] No EC_{50} value and 95% CI were estimated since no dose-response relationship was observed
[2] NA: no EC50 determined due to inadequate mortality

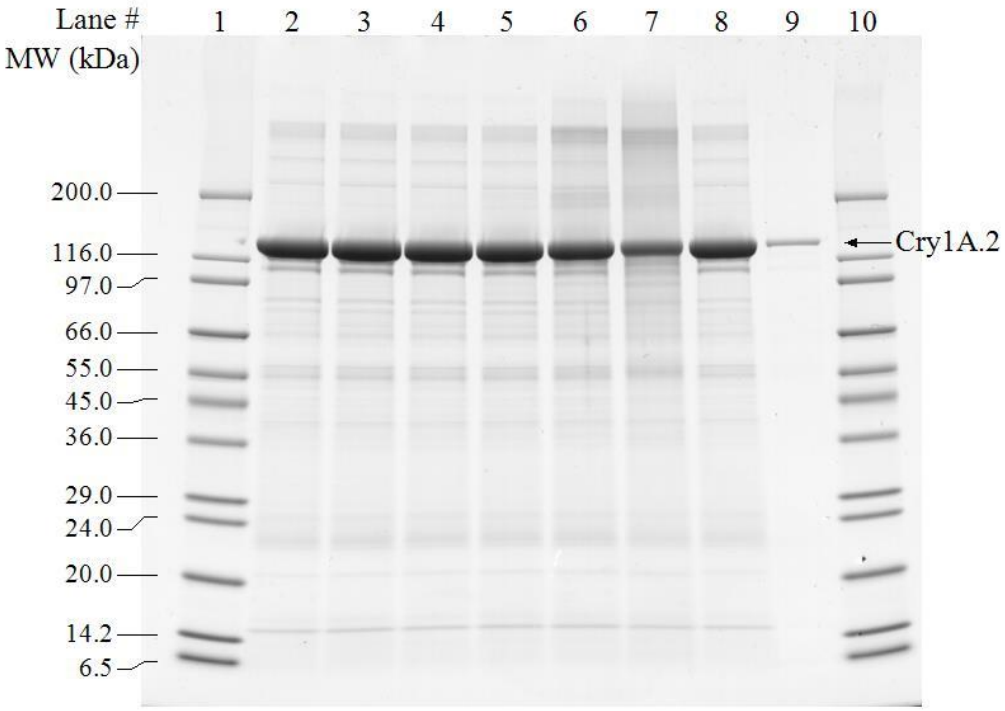

Figure 37. SDS-PAGE of Cry1A.2 Protein Demonstrating the Effect After 15 Minutes at Elevated Temperatures on Protein Structural Stability

Heat-treated samples of Cry1A.2 (3.0 µg total protein) separated on a Tris-glycine 4-20 % polyacrylamide gel under denaturing and reducing conditions. The gel was stained with Brilliant Blue G-Colloidal. Approximate molecular weights (kDa) are shown on the left and correspond to molecular weight standards in lanes 1 and 10.

Lane	Description	Total Amount
1	SigmaMarker Wide Standards	5.0 µl
2	Cry1A.2 Protein Control	3.0 µg
3	Cry1A.2 Protein 25ºC	3.0 µg
4	Cry1A.2 Protein 37ºC	3.0 µg
5	Cry1A.2 Protein 55ºC	3.0 µg
6	Cry1A.2 Protein 75ºC	3.0 µg
7	Cry1A.2 Protein 95ºC	3.0 µg
8	Cry1A.2 Protein Reference 100% Equivalence	3.0 µg
9	Cry1A.2 Protein Reference 10% Equivalence	0.3 µg
10	SigmaMarker Wide Standards	5.0 µl

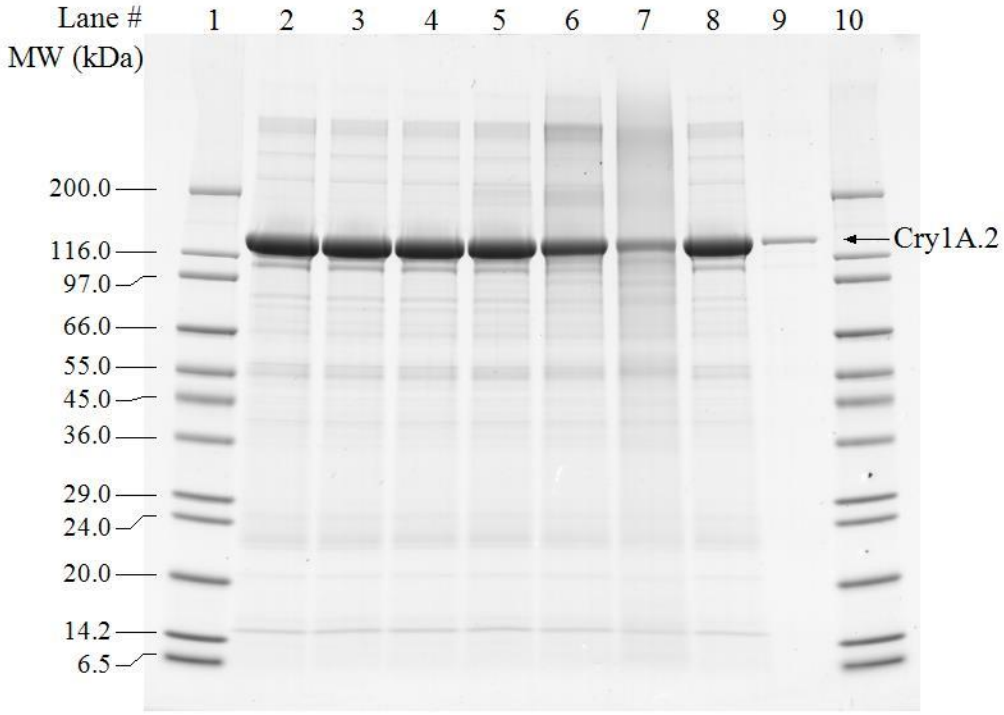

Figure 38. SDS-PAGE of Cry1A.2 Protein Demonstrating the Effect After 30 Minutes at Elevated Temperatures on Protein Structural Stability

Heat-treated samples of Cry1A.2 (3.0 µg total protein) separated on a Tris-glycine 4-20 % polyacrylamide gel under denaturing and reducing conditions. The gel was stained with Brilliant Blue G-Colloidal. Approximate molecular weights (kDa) are shown on the left and correspond to molecular weight standards in lanes 1 and 10.

Lane	Description	Total Amount
1	SigmaMarker Wide Standards	5.0 µl
2	Cry1A.2 Protein Control	3.0 µg
3	Cry1A.2 Protein 25ºC	3.0 µg
4	Cry1A.2 Protein 37ºC	3.0 µg
5	Cry1A.2 Protein 55ºC	3.0 µg
6	Cry1A.2 Protein 75ºC	3.0 µg
7	Cry1A.2 Protein 95ºC	3.0 µg
8	Cry1A.2 Protein Reference 100% Equivalence	3.0 µg
9	Cry1A.2 Protein Reference 10% Equivalence	0.3 µg
10	SigmaMarker Wide Standards	5.0 µl

B.2(b)(iii)(ii) Heat susceptibility of the MON 94637 Cry1B.2 protein

The effect of heat treatment on the activity of the *Bt*-produced Cry1B.2 protein was evaluated using purified protein. The method for evaluating heat stability is described in Appendix **13**.

As previously stated, temperature can have a profound effect on the structure and function of proteins. Heat treatment is widely used in the preparation of foods derived from soybean grain (Hammond and Jez, 2011). It is reasonable that such processing will have an effect on the functional activity and structure of Cry1B.2 protein when consumed in different food products derived from MON 94637, thus reducing any potential safety concerns posed by the protein. Therefore, an assessment of the effect of heating was conducted as a surrogate for the conditions encountered during the preparation of foods from MON 94637 grain.

In the study, heat treated samples and an unheated control sample of Cry1B.2 protein were analyzed: 1) using an insect bioassay to assess the impact of temperature on the functional activity of the Cry1B.2 protein; and 2) using SDS-PAGE to assess the impact of temperature on protein integrity.

Aliquots of Cry1B.2 protein were heated to 25ºC, 37ºC, 55ºC, 75ºC and 95ºC for either 15 or 30 minutes, while a separate aliquot of Cry1B.2 protein was maintained on ice for the duration of the heat treatments to serve as a temperature control. The effect of heat treatment on the activity of Cry1B.2 was evaluated using a insect bioassay (Appendix **13**). The effect of heat treatment on the integrity of the Cry1B.2 protein was evaluated using SDS-PAGE analysis of the heated and temperature control Cry1B.2 protein samples.

Results of the functional activity assay for Cry1B.2 protein incubated at a range of temperatures for 15 or 30 minutes are listed in Table 24 and Table 25, respectively. The EC_{50} values were determined as the concentration of Cry1B.2 (µg/ml diet) that resulted in 50% growth inhibition relative to the control treatment, in a SBL insect bioassay.The control sample had an EC_{50} of 9.3 µg Cry1B.2 protein/ml diet, thus demonstrating that protein activity was maintained during incubation on ice.

Functional activity of the Cry1B.2 protein was not impacted following heat treatments at 25°C, 37°C and 55ºC for 15 and 30 minutes. No functional activity in an SBL bioassay was observed after the incubation at ≥75°C for 15 or 30 minutes. As a result, an EC_{50} could not be determined.

The results of the SDS-PAGE analysis of the heat-treated samples incubated for 15 and 30 minutes are illustrated in Figure 39 and Figure 40 respectively. The control sample loaded on each gel (Figure 39 and Figure 40 lane 2) showed equivalent band intensity to the 100% reference standard (Figure 39 and Figure 40, lane 8), demonstrating that the Cry1B.2 protein was stable on ice during the incubation period. No apparent decrease in band intensity of the 132.6 kDa Cry1B.2 protein was observed in the test samples when heated at temperatures of 25°C, 37°C or 55°C for 15 or 30 minutes. A decrease in the intensity of the main Cry1B.2 band was evident at 75°C with the most prominent loss of band intensity observed at 30 minutes. In addition, degradation and aggregation products were also evident at 75°C for both the 15 and 30 heat treatments. Incubation for 15 and 30 minutes at 95°C resulted in a significant loss of the Cry1B.2 band intensity with the greatest loss evident after the 30 minute heat treatment. Additionally, both the 15 and 30 minute heat treatments at 95°C exhibited increased aggregation and degradation throughout.

These data demonstrate that the Cry1B.2 protein behaves with a predictable tendency toward protein denaturation and loss of functional activity at elevated temperatures. Heat treatment is widely used in the preparation of foods containing components derived from soybean grain. Therefore, it is reasonable to conclude that Cry1B.2 protein would not be consumed as an active protein in food products due to standard processing practices that include heat treatment.

Table 24. EC_{50} Values and 95% Confidence Limits (CI) for the Heat-Treated Cry1B.2 Protein After 15 Minutes

Temperature	EC_{50} (µg Cry1B.2/ml diet)	95% CI (µg Cry1B.2/ml diet)
0 ºC (control)	9.3	7.0 - 12
25ºC	8.3	6.8 – 10
37ºC	7.8	7.0 – 8.7
55ºC	8.0	6.9 – 9.3
75ºC[1]	N/A[2]	N/A
95ºC[1]	N/A[2]	N/A

[1] No EC_{50} value or 95% CI was estimated since no dose-response relationship was observed
[2] NA: no EC50 determined due to inadequate mortality

Table 25. EC_{50} Values and 95% Confidence Limits (CI) for the Heat-Treated Cry1B.2 Protein After 30 Minutes

Temperature	EC_{50} (µg Cry1B.2/ml diet)	95% CI (µg Cry1B.2/ml diet)
0 ºC (control)	9.3	7.0 – 12
25ºC	9.5	8.2 – 11
37ºC	8.1	7.5 – 8.8
55ºC	8.6	7.1 – 10
75ºC[1]	N/A[2]	N/A
95ºC[1]	N/A[2]	N/A

[1] No EC_{50} value or 95% CI was estimated since no dose-response relationship was observed
[2] NA: no EC50 determined due to inadequate mortality

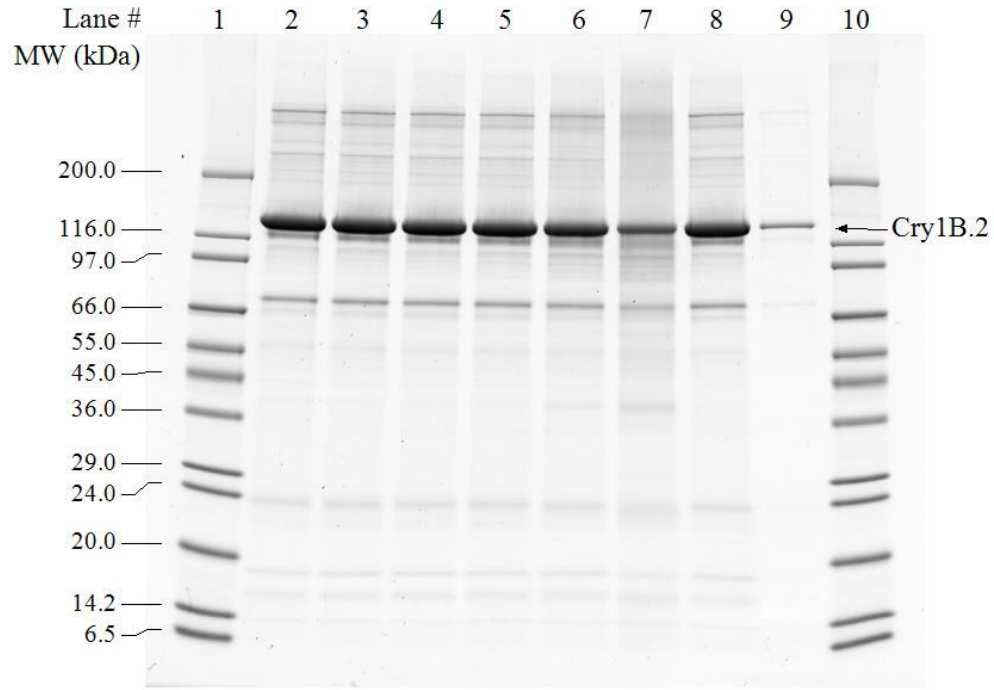

Figure 39. SDS-PAGE of Cry1B.2 Protein Demonstrating the Effect After 15 Minutes at Elevated Temperatures on Protein Structural Stability

Heat-treated samples of Cry1B.2 (3.0 µg total protein) separated on a Tris-glycine 4-20 % polyacrylamide gel under denaturing and reducing conditions. The gel was stained with Brilliant Blue G-Colloidal. Approximate molecular weights (kDa) are shown on the left and correspond to molecular weight standards in lanes 1 and 10.

Lane	Description	Total Amount
1	SigmaMarker Wide Standards	5.0 µl
2	Cry1B.2 Protein Control	3.0 µg
3	Cry1B.2 Protein 25ºC	3.0 µg
4	Cry1B.2 Protein 37ºC	3.0 µg
5	Cry1B.2 Protein 55ºC	3.0 µg
6	Cry1B.2 Protein 75ºC	3.0 µg
7	Cry1B.2 Protein 95ºC	3.0 µg
8	Cry1B.2 Protein Reference 100% Equivalence	3.0 µg
9	Cry1B.2 Protein Reference 10% Equivalence	0.3 µg
10	SigmaMarker Wide Standards	5.0 µl

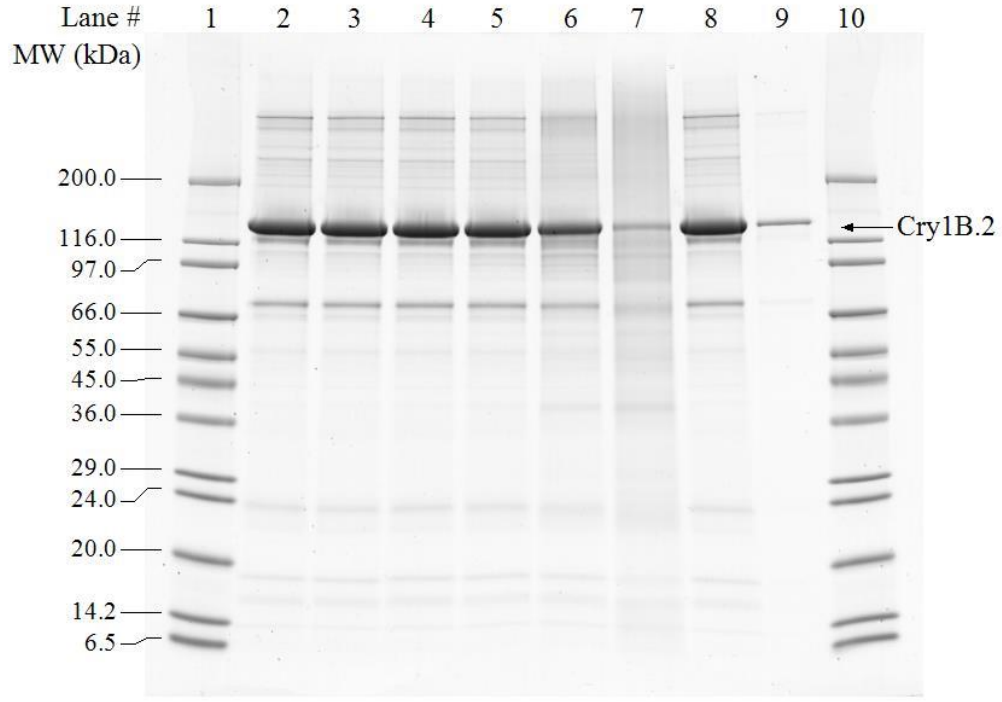

Figure 40. SDS-PAGE of Cry1B.2 Protein Demonstrating the Effect After 30 Minutes at Elevated Temperatures on Protein Structural Stability

Heat-treated samples of Cry1B.2 (3.0 µg total protein) separated on a Tris-glycine 4-20 % polyacrylamide gel under denaturing and reducing conditions. The gel was stained with Brilliant Blue G-Colloidal. Approximate molecular weights (kDa) are shown on the left and correspond to molecular weight standards in lanes 1 and 10.

Lane	Description	Total Amount
1	SigmaMarker Wide Standards	5.0 µl
2	Cry1B.2 Protein Control	3.0 µg
3	Cry1B.2 Protein 25ºC	3.0 µg
4	Cry1B.2 Protein 37ºC	3.0 µg
5	Cry1B.2 Protein 55ºC	3.0 µg
6	Cry1B.2 Protein 75ºC	3.0 µg
7	Cry1B.2 Protein 95ºC	3.0 µg
8	Cry1B.2 Protein Reference 100% Equivalence	3.0 µg
9	Cry1B.2 Protein Reference 10% Equivalence	0.3 µg
10	SigmaMarker Wide Standards	5.0 µl

B.2(b)(iv) Specific serum screening where a new protein is derived from a source known to be allergenic or has sequence homology with a known allergen

Not relevant for this product.

B.2(b)(v) Information on whether the new protein(s) have a role in the elicitation of gluten-sensitive enteropathy, in cases where the introduced genetic material is obtained from wheat, rye, barley, oats, or related cereal grains

Not relevant for this product.

B.3 Other (non-protein) New Substances

Not applicable.

B.3(a) The identity and biological function of the substance

Not applicable.

B.3(b) Whether the substance has previously been safely consumed in Food

Not applicable.

B.3(c) Potential dietary exposure to the substance

Not applicable.

B.3(d) where RNA interference has been used

B.3(d)(i) the role of any endogenous target gene and any changes to the food as a result of silencing that gene

Not applicable.

B.3(d)(ii) The expression levels of the RNA transcript

Not applicable.

B.3(d)(iii) The specificity of the RNA interference

Not applicable.

B.4 Novel Herbicide Metabolites in GM Herbicide-Tolerant Plants

Not applicable. MON 94637 produces only insecticidal proteins.

B.5 Compositional Assessment

Safety assessments of biotechnology-derived crops follow the comparative safety assessment process (Codex Alimentarius, 2009) in which the composition of grain and/or other raw agricultural commodities of the biotechnology-derived crop are compared to the appropriate conventional control that has a history of safe use. For soybean, assessments are performed based on the general principles outlined in the OECD consensus document for soybean composition (OECD, 2012).

A review of compositional assessments conducted according to OECD guidelines, that encompassed a total of seven biotechnology-derived crop varieties, nine countries, and eleven growing seasons, concluded that incorporation of biotechnology-derived agronomic traits has had little impact on crop composition compared to other sources of variation. Most compositional variation is attributable to growing region, agronomic practices, and genetic background (Harrigan *et al.*, 2010). Numerous scientific publications have further documented the extensive variability in the concentrations of crop components that reflect the influence of environmental and genetic factors as well as extensive conventional breeding efforts to improve nutrition, agronomics, and yield (Harrigan *et al.*, 2010; Harrigan *et al.*, 2009; Ridley *et al.*, 2011; Zhou *et al.*, 2011).

Compositional equivalence between biotechnology-derived and conventional crops supports an "equal or increased assurance of the safety of foods derived from genetically modified plants" (OECD, 2002). OECD consensus documents on compositional considerations for new crop varieties emphasize quantitative measurements of key nutrients and known anti-nutrients. These quantitative measurements effectively discern any compositional changes that could imply potential nutritional or safety (e.g., antinutritional) concerns. Levels of the components in grain and/or other raw agricultural commodities of the biotechnology-derived crop product are compared to: 1) corresponding levels in a conventional comparator, a genetically similar conventional line, grown concurrently under similar field conditions, and 2) natural ranges from data published in the scientific literature or in publicly-available databases (e.g. AFSI Crop Composition Database). This second comparison places any potential differences between the assessed crop and its comparator in the context of the well-documented variation in the concentrations of crop nutrients and anti-nutrients.

This section provides analyses of concentrations of key nutrients, anti-nutrients and isoflavones in grain and forage of MON 94637 compared to that of a conventional control soybean with a similar genetic background, grown and harvested under similar conditions. The production of materials for compositional analyses used a sufficient variety of field trial sites, reflecting a range of environmental conditions under which MON 94637 is expected to be grown and robust field designs (randomized complete block design with four replicates). Samples were subjected to sensitive analytical methods that allow quantitative and accurate measurements of key components. The information provided in this section addresses relevant factors in Codex Plant Guidelines, Section 4, paragraphs 44 and 45 for compositional analyses (Codex Alimentarius, 2009).

B.5(a) The levels of relevant key nutrients, toxicants and anti-nutrients in the food produced using gene technology compared with the levels in an appropriate comparator (usually non-GM counterpart). A statistical analysis of the data must be provided

B.5(a)(i) Compositional equivalence of MON 94637 grain and forage to conventional soybean

For detailed methods and results of composition analysis of MON 94637 compared to conventional soybean control, please refer to Appendix **14**.

Grain and forage samples were collected from MON 94637 and a conventional control at five sites grown in the United States during 2021. The field sites were planted in a randomized complete block design with four blocks per site. MON 94637 and the conventional control were grown under agronomic field conditions typical for the different growing regions.

The compositional analysis provided a comprehensive comparative assessment of the levels of key nutrients, anti-nutrients and isoflavones in grain and forage of MON 94637 and the conventional control.

The evaluation of MON 94637 followed considerations relevant to the compositional quality of soybean as defined by the OECD consensus document (OECD, 2012). Harvested grain samples were assessed for moisture and levels of nutrients including proximates (protein, total fat and ash), amino acids (18 components), fatty acids (22 components), carbohydrates by calculation, fiber (acid detergent fiber (ADF) and neutral detergent fiber (NDF)), minerals (calcium and phosphorus) and vitamins (vitamin E and vitamin K_1). Grain samples were also assessed for levels of other components including anti-nutrients (phytic acid, raffinose, soybean lectin, stachyose and trypsin inhibitor) and isoflavones (daidzein, genistein and glycitein). Harvested forage samples were assessed for moisture and levels of nutrients including proximates (protein, total fat and ash), carbohydrates by calculation, and fiber (ADF and NDF). In all, 66 different components were analyzed.

Of the 66 measured components, 11 components (caprylic acid, capric acid, lauric acid, myristoleic acid, pentadecanoic acid, pentadecenoic acid, heptadecenoic acid, gamma linolenic acid, eicosadienoic acid, eicosatrienoic acid and arachidonic acid in grain) had more than 50% of the observations below the assay limit of quantitation (LOQ) and were excluded from statistical analysis. Moisture values for grain and forage were measured for conversion of components from fresh to dry weight but were not statistically analyzed. Therefore, 53 components were statistically analyzed (Table 26 through Table 32).

The statistical comparisons of MON 94637 and the conventional control were based on compositional data combined across all field sites. Statistically significant differences were identified at the 5% level ($\alpha = 0.05$). A statistically significant difference between MON 94637 and the conventional control does not necessarily imply biological relevance from a food safety perspective. Therefore, any statistically significant differences observed between MON 94637 and the conventional control were evaluated further to determine whether the detected difference indicated a biologically relevant compositional change or supported a conclusion of compositional equivalence, as follows:

Step 1 – Determination of the Magnitude of Difference between Test (MON 94637) and Conventional Control Means

The difference in mean values between MON 94637 and the conventional control was determined for use in subsequent steps. For protein and amino acids only, the relative magnitude of the difference (percent change relative to the control) between MON 94637 and the conventional control was determined to allow an assessment of any observed difference in amino acids in relation to the difference in protein.

Step 2 – Assessment of the Difference in the Context of Natural Variation within the Conventional Control across Multiple Sites

The relative impact of MON 94637 was evaluated in the context of variation within the conventional control germplasm grown across multiple sites (i.e., variation due to environmental influence). This step assessed the mean difference between MON 94637 and the conventional control in the context of the individual replicate values for the conventional control range value (maximum value minus the minimum value). When a mean difference is less than the variability seen due to natural environmental variation within the single, closely related germplasm, the difference is typically not a food safety concern (Venkatesh *et al.*, 2014).

Step 3 – Assessment of the Difference in the Context of Natural Variation Due to Multiple Sources

The relative impact of MON 94637 on composition was also evaluated in the context of sources of natural variation such as environmental and germplasm influences. This assessment determined whether the component mean value of MON 94637 was within the natural variability defined by the literature values and/or the AFSI Crop Composition Database (AFSI CCDB)[8] values (Table 33). This natural variability is important in assessing the biological relevance to food and feed safety of statistically significant differences in composition between MON 94637 and the conventional control.

These evaluations of natural variation are important as crop composition is known to be greatly influenced by environment and variety (Harrigan *et al.*, 2010). Although used in the comparative assessment process, detection of statistically significant differences between MON 94637 and the conventional control mean values does not imply a meaningful contribution by MON 94637 to compositional variability. Only if the impact of MON 94637 on levels of components is large relative to natural variation inherent to conventional soybean would the difference in composition be potentially meaningful from a food safety and nutritional perspective. Differences between MON 94637 the conventional control that are within the observed natural variation for soybean are not meaningful, therefore the results support a conclusion of compositional equivalence.

There were no statistically significant differences ($p<0.05$) for 48 of the 53 components analyzed. There were three components (palmitoleic acid, heptadecanoic acid and behenic acid) in grain and two components (protein and carbohydrates by calculation) in forage that

[8] Effective May 1, 2020, the ILSI RF publishing the CCDB became an unaffiliated non-profit scientific organization, no longer part of the ILSI federation, and changed its name to Agriculture and Food Systems Institute (AFSI). There is no change to the current structure or function of the CCDB, only name change: AFSI CCDB. The CCDB working group and their website still the same https://www.cropcomposition.org/

showed a statistically significant difference ($p<0.05$) between MON 94637 and the conventional control.

For palmitoleic acid, heptadecanoic acid and behenic acid in grain, the magnitudes of differences ranged from 0.0041% Total FA (heptadecanoic acid) to 0.0094% Total FA (behenic acid) (Table 27). As shown in Table 27, the magnitude of differences for the three fatty acids between MON 94637 and the conventional control were less than the corresponding conventional control range values. This indicates that MON 94637 does not impact levels of these components more than the natural variation within the conventional control grown at multiple locations. The mean levels of the three fatty acids were within the natural variability of these components as published in the scientific literature on soybean composition and/or the AFSI CCDB (Table 33). The data demonstrated that MON 94637 was not a major contributor to variation in fatty acid levels in soybean and confirmed the compositional equivalence of MON 94637 to the conventional control in levels of these components.

For protein in forage, the difference was -1.17% dw (Table 32). As shown in Table 32, the magnitude of difference for protein between MON 94637 and the conventional control was less than the corresponding conventional control range values. This indicates that MON 94637 does not impact levels of this component more than the natural variation within the conventional control grown at multiple locations. The mean level of protein was within the natural variability of this component as published in the scientific literature on soybean composition and/or the AFSI CCDB (Table 33). The data demonstrated that MON 94637 was not a major contributor to variation in protein levels in soybean forage and confirmed the compositional equivalence of MON 94637 to the conventional control in levels of this component.

For carbohydrates by calculation in forage, the difference was 1.82% dw (Table 32). As shown in Table 32, the magnitude of difference for carbohydrates by calculation between MON 94637 and the conventional control was less than the corresponding conventional control range values. This indicates that MON 94637 does not impact levels of this component more than the natural variation within the conventional control grown at multiple locations. The mean level of carbohydrates by calculation was within the natural variability of this component as published in the scientific literature on soybean composition and/or the AFSI CCDB (Table 33). The data demonstrated that MON 94637 was not a major contributor to variation in carbohydrates by calculation or fiber levels in soybean forage and confirmed the compositional equivalence of MON 94637 to the conventional control in levels of this component.

Conclusions

Compositional analysis was conducted on grain and forage of MON 94637 and the conventional control grown at five sites in the United States during the 2021 field season. Of the 53 components statistically assessed, 48 showed no statistically significant differences ($p<0.05$) between MON 94637 and the conventional control. A total of three components (palmitoleic acid, heptadecanoic acid and behenic acid) in grain and two components (protein and carbohydrates by calculation) in forage showed a statistically significant difference ($p<0.05$) between MON 94637 and the conventional control. For these components, the mean difference in component values between MON 94637 and the conventional control was less than the range of the conventional control values. The MON 94637 mean component values were within the range of values observed in the literature and/or the AFSI CCDB.

These results support the overall conclusion that MON 94637 soybean was not a major contributor to variation in component in grain or forage and confirmed the compositional equivalence of MON 94637 to the conventional control in levels of these components. The statistically significant differences observed were not compositionally meaningful from a food safety perspective.

Table 26. Summary of Soybean Grain Protein and Amino Acids for MON 94637 and the Conventional Control

Component (% dw)[1]	MON 94637 Mean (S.E.)[2] Range	Control Mean (S.E.) Range	Control Range Value[3]	Difference (Test minus Control) Mean (S.E.)	p-Value	% Relative[4]
Protein	39.25 (0.51) 36.57 - 40.97	39.17 (0.51) 37.46 - 41.25	3.80	0.081 (0.33)	0.810	0.21
Alanine	1.57 (0.017) 1.46 - 1.71	1.58 (0.017) 1.49 - 1.65	0.15	-0.014 (0.012)	0.249	-0.88
Arginine	2.68 (0.058) 2.26 - 2.92	2.65 (0.058) 2.28 - 2.87	0.59	0.024 (0.040)	0.549	0.90
Aspartic Acid	4.38 (0.057) 4.12 - 4.96	4.41 (0.057) 4.19 - 4.77	0.58	-0.034 (0.064)	0.595	-0.77
Cystine	0.58 (0.028) 0.40 - 0.71	0.56 (0.028) 0.41 - 0.74	0.33	0.022 (0.021)	0.295	4.02
Glutamic Acid	7.01 (0.098) 6.52 - 7.76	7.05 (0.098) 6.59 - 7.57	0.98	-0.049 (0.078)	0.531	-0.70
Glycine	1.61 (0.024) 1.42 - 1.80	1.60 (0.024) 1.47 - 1.73	0.26	0.0095 (0.022)	0.663	0.59

Table 26. Summary of Soybean Grain Protein and Amino Acids for MON 94637 and the Conventional Control (Continued)

Component (% dw)[1]	MON 94637 Mean (S.E.)[2] Range	Control Mean (S.E.) Range	Control Range Value[3]	Difference (Test minus Control) Mean (S.E.)	p-Value	% Relative[4]
Histidine	1.00 (0.015) 0.84 - 1.12	1.00 (0.015) 0.89 - 1.08	0.19	0.0032 (0.018)	0.863	0.32
Isoleucine	1.73 (0.023) 1.57 - 1.89	1.73 (0.023) 1.62 - 1.80	0.18	0.0028 (0.018)	0.880	0.16
Leucine	2.86 (0.037) 2.61 - 3.05	2.88 (0.037) 2.64 - 3.00	0.35	-0.019 (0.023)	0.410	-0.67
Lysine	2.39 (0.032) 2.16 - 2.70	2.42 (0.032) 2.31 - 2.62	0.32	-0.034 (0.032)	0.282	-1.42
Methionine	0.59 (0.018) 0.43 - 0.74	0.59 (0.018) 0.51 - 0.68	0.18	0.0039 (0.021)	0.853	0.66
Phenylalanine	1.87 (0.035) 1.54 - 2.13	1.87 (0.035) 1.63 - 2.05	0.42	0.0069 (0.036)	0.847	0.37
Serine	1.95 (0.028) 1.76 - 2.11	1.96 (0.028) 1.77 - 2.10	0.33	-0.0027 (0.022)	0.905	-0.14

Table 26. Summary of Soybean Grain Protein and Amino Acids for MON 94637 and the Conventional Control (Continued)

Component (% dw)[1]	MON 94637 Mean (S.E.)[2] Range	Control Mean (S.E.) Range	Control Range Value[3]	Difference (Test minus Control) Mean (S.E.)	p-Value	% Relative[4]
Proline	1.90 (0.026) 1.70 - 2.06	1.91 (0.026) 1.76 - 1.99	0.24	-0.0076 (0.020)	0.706	-0.40
Threonine	1.48 (0.018) 1.33 - 1.57	1.48 (0.018) 1.38 - 1.56	0.18	-0.0048 (0.014)	0.737	-0.32
Tryptophan	0.46 (0.0055) 0.43 - 0.49	0.46 (0.0055) 0.43 - 0.48	0.055	0.0028 (0.0049)	0.566	0.61
Tyrosine	1.10 (0.022) 0.93 - 1.26	1.10 (0.022) 0.90 - 1.27	0.37	0.0027 (0.027)	0.919	0.25
Valine	1.75 (0.022) 1.60 - 1.87	1.75 (0.022) 1.64 - 1.85	0.21	0.0030 (0.018)	0.873	0.17

[1]dw=dry weight
[2] Mean (S.E.) = least-square mean (standard error)
[3]Maximum value minus minimum value for the control soybean variety
[4]The relative magnitude of the difference in mean values between MON 94637 and the control, expressed as a percent of the control.

Table 27. Summary of Soybean Grain Total Fat and Fatty Acids for MON 94637 and the Conventional Control

				Difference (Test minus Control)	
Component	MON 94637 Mean (S.E.)[1] Range	Control Mean (S.E.) Range	Control Range Value[2]	Mean (S.E.)	p-Value
Total Fat (% dw)[3]	18.59 (0.28) 17.34 - 20.10	18.77 (0.28) 17.63 - 19.88	2.25	-0.18 (0.12)	0.121
14:0 Myristic (% Total FA)[4]	0.057 (0.0041) 0.025 - 0.074	0.059 (0.0041) 0.049 - 0.071	0.022	-0.0018 (0.0018)	0.342
16:0 Palmitic (% Total FA)	12.19 (0.14) 11.37 - 12.57	12.22 (0.14) 11.55 - 12.54	0.99	-0.036 (0.052)	0.503
16:1 Palmitoleic (% Total FA)	0.065 (0.0038) 0.030 - 0.077	0.072 (0.0038) 0.058 - 0.086	0.028	-0.0062 (0.0017)	<0.001
17:0 Heptadecanoic (% Total FA)	0.061 (0.0015) 0.030 - 0.073	0.065 (0.0015) 0.058 - 0.075	0.017	-0.0041 (0.0018)	0.021
18:0 Stearic (% Total FA)	3.96 (0.051) 3.74 - 4.37	3.93 (0.051) 3.70 - 4.20	0.50	0.039 (0.043)	0.387
18:1 Oleic (% Total FA)	19.57 (0.26) 18.30 - 23.50	19.25 (0.26) 18.03 - 20.60	2.57	0.32 (0.35)	0.374
18:2 Linoleic (% Total FA)	55.12 (0.20) 52.03 - 56.22	55.46 (0.20) 54.40 - 56.79	2.39	-0.33 (0.26)	0.221

Table 27. Summary of Soybean Grain Total Fat and Fatty Acids for MON 94637 and the Conventional Control (Continued)

Component	MON 94637 Mean (S.E.)[1] Range	Control Mean (S.E.) Range	Control Range Value[2]	Difference (Test minus Control) Mean (S.E.)	p-Value
18:3 Linolenic (% Total FA)	8.31 (0.19) 7.33 - 8.88	8.28 (0.19) 7.49 - 9.01	1.53	0.030 (0.10)	0.779
20:0 Arachidic (% Total FA)	0.28 (0.0045) 0.26 - 0.31	0.28 (0.0045) 0.25 - 0.30	0.042	0.0021 (0.0039)	0.596
20:1 Eicosenoic (% Total FA)	0.13 (0.0067) 0.10 - 0.15	0.13 (0.0067) 0.11 - 0.15	0.046	-0.0017 (0.0020)	0.398
22:0 Behenic (% Total FA)	0.26 (0.0058) 0.22 - 0.29	0.27 (0.0058) 0.25 - 0.29	0.042	-0.0094 (0.0030)	0.007

[1] Mean (S.E.) = least-square mean (standard error)
[2]Maximum value minus minimum value for the control soybean variety
[3]dw=dry weight
[4]FA=Fatty Acid
The following components with more than 50% of observations below the assay LOQ were excluded from statistical analysis: caprylic acid, capric acid, lauric acid, myristoleic acid, pentadecanoic acid, pentadecenoic acid, heptadecenoic acid, gamma linolenic acid, eicosadienoic acid, eicosatrienoic acid and arachidonic acid.

Table 28. Summary of Soybean Grain Carbohydrates by Calculation and Fiber for MON 94637 and the Conventional Control

Component (% dw)[1]	MON 94637 Mean (S.E.)[2] Range	Control Mean (S.E.) Range	Control Range Value[3]	Difference (Test minus Control) Mean (S.E.)	Difference (Test minus Control) p-Value
Carbohydrates by Calculation	37.40 (0.41) 35.14 - 39.16	37.33 (0.41) 35.67 - 38.31	2.64	0.069 (0.29)	0.817
ADF	13.60 (0.25) 12.12 - 16.30	13.65 (0.25) 12.59 - 14.76	2.17	-0.05 (0.34)	0.886
NDF	15.82 (0.23) 14.18 - 17.41	15.62 (0.23) 14.60 - 16.58	1.98	0.20 (0.22)	0.366

[1]dw=dry weight
[2]Mean (S.E.) = least-square mean (standard error)
[3]Maximum value minus minimum value for the control soybean variety

Table 29. Summary of Soybean Grain Ash and Minerals for MON 94637 and the Conventional Control

Component (% dw)[1]	MON 94637 Mean (S.E.)[2] Range	Control Mean (S.E.) Range	Control Range Value[3]	Difference (Test minus Control) Mean (S.E.)	Difference (Test minus Control) p-Value
Ash	4.76 (0.081) 4.46 - 5.09	4.72 (0.081) 4.41 - 5.03	0.62	0.034 (0.020)	0.090
Calcium	0.27 (0.011) 0.18 - 0.31	0.26 (0.011) 0.18 - 0.31	0.13	0.012 (0.0080)	0.145
Phosphorus	0.66 (0.0093) 0.61 - 0.74	0.65 (0.0093) 0.60 - 0.70	0.11	0.014 (0.0083)	0.114

[1]dw = dry weight

[2]Mean (S.E.) = least-square mean (standard error)
[3]Maximum value minus minimum value for the control soybean variety

Table 30. Summary of Soybean Grain Vitamins for MON 94637 and the Conventional Control

Component[1]	MON 94637 Mean (S.E.)[2] Range	Control Mean (S.E.) Range	Control Range Value[3]	Difference (Test minus Control) Mean (S.E.)	Difference (Test minus Control) p-Value
Vitamin E (mg/100g dw)	2.59 (0.24) 1.71 - 3.68	2.43 (0.24) 1.67 - 3.49	1.83	0.16 (0.082)	0.077
Vitamin K_1 (µg/g dw)	0.74 (0.055) 0.46 - 0.94	0.73 (0.055) 0.56 - 0.89	0.33	0.013 (0.029)	0.646

[1]dw=dry weight; Common names of vitamins: E=α-Tocopherol; K_1=phylloquinone
[2]Mean (S.E.) = least-square mean (standard error)
[3]Maximum value minus minimum value for the control soybean variety

Table 31. Summary of Soybean Grain Anti-Nutrients and Isoflavones for MON 94637 and the Conventional Control

				Difference (Test minus Control)	
Component	MON 94637 Mean (S.E.)[1] Range	Control Mean (S.E.) Range	Control Range Value[2]	Mean (S.E.)	p-Value
Phytic Acid (% dw)[3]	1.50 (0.034) 1.31 - 1.78	1.47 (0.034) 1.34 - 1.67	0.33	0.029 (0.026)	0.274
Raffinose (% dw)	0.98 (0.066) 0.76 - 1.29	0.94 (0.066) 0.69 - 1.29	0.60	0.037 (0.037)	0.334
Soybean Lectin (mg/g dw)	1.90 (0.047) 1.61 - 2.53	1.99 (0.047) 1.73 - 2.28	0.55	-0.085 (0.053)	0.112
Stachyose (% dw)	4.51 (0.14) 3.56 - 4.91	4.71 (0.14) 3.90 - 5.87	1.97	-0.21 (0.13)	0.136
Trypsin Inhibitor (TIU/mg dw)	28.36 (2.09) 11.70 - 41.87	26.14 (2.09) 14.42 - 38.27	23.85	2.22 (2.28)	0.332
Daidzein (µg/g dw)	1067.68 (100.66) 638.06 - 1320.11	1077.73 (100.66) 672.90 - 1327.15	654.26	-10.06 (39.92)	0.805
Genistein (µg/g dw)	768.94 (69.57) 454.84 - 953.08	809.17 (69.57) 511.81 - 1016.04	504.22	-40.23 (30.21)	0.207
Glycitein (µg/g dw)	143.44 (6.04) 115.57 - 161.18	143.38 (6.04) 123.12 - 182.44	59.32	0.053 (6.72)	0.993

[1]Mean (S.E.) = least-square mean (standard error)
[2]Maximum value minus minimum value for the control soybean variety

Table 32. Summary of Soybean Forage Proximates, Carbohydrates by Calculation, Fiber and Minerals for MON 94637 and the Conventional Control

				Difference (Test minus Control)	
Component[1]	MON 94637 Mean (S.E.)[2] Range	Control Mean (S.E.) Range	Control Range Value[3]	Mean (S.E.)	p-Value
Protein (% dw)	20.62 (0.64) 17.62 - 23.75	21.80 (0.64) 17.70 - 24.03	6.33	-1.17 (0.37)	0.002
Total Fat (% dw)	8.63 (0.49) 6.86 - 11.05	9.25 (0.49) 6.28 - 12.38	6.11	-0.62 (0.45)	0.199
Carbohydrates by Calculation (% dw)	64.68 (0.89) 61.50 - 69.98	62.86 (0.89) 58.09 - 68.17	10.08	1.82 (0.50)	0.003
ADF (% dw)	31.22 (1.03) 25.27 - 41.54	33.39 (1.03) 26.91 - 47.60	20.69	-2.17 (1.41)	0.150
NDF (% dw)	35.74 (1.37) 28.21 - 50.40	37.20 (1.37) 29.00 - 48.83	19.83	-1.45 (1.67)	0.400
Ash (% dw)	6.06 (0.30) 4.52 - 7.32	6.09 (0.30) 4.82 - 6.87	2.05	-0.029 (0.17)	0.865

[1]dw=dry weight

[2]Mean (S.E.) = least-square mean (standard error)

B.5(b) Information on the range of natural variation for each constituent measured to allow for assessment of biological significance should any statistically significant difference be identified

Table 33. Literature and AFSI Database Ranges for Components in Soybean Grain and Forage

Tissue Components[1]	Literature Range[2]	AFSI Range[3]
Grain Nutrients		
Proximates		
protein (% dw)	34.78-43.35[a]; 32.29-42.66[b]	29.51-46.80
total fat (% dw)	14.40-20.91[a]; 15.10-23.56[b]	6.97-25.00
ash (% dw)	4.61-6.32[a]; 4.32-5.88[b]	3.73-10.90
Amino Acids		
alanine (% dw)	1.62-1.89[a]; 1.43-1.93[b]	1.15-2.35
arginine (% dw)	2.57-3.34[a]; 2.15-3.05[b]	1.73-3.93
aspartic acid (% dw)	4.16-5.02[a]; 4.01-5.72[b]	3.13-6.83
cystine (% dw)	0.52-0.69[a]; 0.41-0.71[b]	0.31-0.93
glutamic acid (% dw)	6.52-8.19[a]; 5.49-8.72[b]	4.35-10.90
glycine (% dw)	1.59-1.90[a]; 1.41-1.99[b]	1.16-2.55
histidine (% dw)	0.96-1.13[a]; 0.86-1.24[b]	0.20-1.59
isoleucine (% dw)	1.59-2.00[a]; 1.41-2.02[b]	1.20-2.48
leucine (% dw)	2.79-3.42[a]; 2.39-3.32[b]	2.04-4.13
lysine (% dw)	2.36-2.77[a]; 2.19-3.15[b]	1.79-3.94
methionine (% dw)	0.45-0.63[a]; 0.39-0.65[b]	0.29-1.15
phenylalanine (% dw)	1.82-2.29[a]; 1.62-2.44[b]	1.40-2.73
proline (% dw)	1.83-2.23[a]; 1.63-2.25[b]	1.32-2.95
serine (% dw)	1.95-2.42[a]; 1.51-2.30[b]	0.86-2.80
threonine (% dw)	1.44-1.71[a]; 1.23-1.74[b]	1.07-2.18
tryptophan (% dw)	0.30-0.48[a]; 0.41-0.56[b]	0.254-0.746
tyrosine (% dw)	1.27-1.53[a]; 0.74-1.31[b]	0.74-2.32
valine (% dw)	1.68-2.11[a]; 1.50-2.13[b]	1.24-2.66
Fatty Acids		
myristic acid (% Total FA)	0.063-0.11[b]; ND-0.2[f]	0.056-0.243
palmitic acid (% Total FA)	9.80-12.63[b]; 8.0-13.5 [f]	8.03-15.99
palmitoleic acid (% Total FA)	0.055-0.14[b]; ND-0.2[f]	0.055-0.247
heptadecanoic acid (% Total FA)	0.076-0.13[b]; ND-0.1[f]	0.071-0.166
stearic acid (% Total FA)	3.21-5.63[b]; 2.0-5.4[f]	2.68-6.74
oleic acid (% Total FA)	16.69-35.16[b]; 17-30[f]	14.5-46.3
linoleic acid (% Total FA)	44.17-57.72[b]; 48.0-59.0[f]	34.8-72.5
linolenic acid (% Total FA)	4.27-9.90[b]; 4.5-11.0[f]	3.00-12.84
arachidic acid (% Total FA)	0.35-0.57[b]; 0.1-0.6[f]	0.167-0.611
eicosenoic acid (% Total FA)	0.13-0.30[b]; ND-0.5[f]	0.110-0.387
behenic acid (% Total FA)	0.35-0.65[b]; ND-0.7[f]	0.181-0.723
Carbohydrates By Calculation		
carbohydrates by calculation (% dw)	32.75-40.98[a]; 29.88-43.48[b]	25.2-55.8

Table 33. Literature and AFSI Database Ranges for Components in Soybean Grain and Forage (Continued)

Tissue Components[1]	Literature Range[2]	AFSI Range[3]
Fiber		
ADF (% dw)	9.22-26.26[a]; 11.81-19.45[b]	4.60-35.30
NDF (% dw)	10.79-23.90[a]; 13.32-23.57[b]	7.38-31.90
Minerals		
calcium (% dw)	0.24-0.41[c]	0.09-0.49
phosphorus (% dw)	0.40-0.61[c]	0.21-0.94
Vitamins		
vitamin E (mg/100g dw)	1.29-4.80[a]; 1.12-8.08[b]	0.193-12.738
vitamin K_1 (µg/g dw)	0.49-0.909[d]	0.07-2.07
Grain Other		
Anti-Nutrients		
phytic acid (% dw)	0.41-1.92[a]; 0.81-2.66[b]	0.2855-2.8600
raffinose (% dw)	0.26-0.84[a]; 0.43-1.85[b]	0.1778-1.8542
soybean lectin (mg/g dw)	1.82-2.92[e]	0.7764-9.3500
stachyose (% dw)	1.53-3.04[a]; 1.97-6.65[b]	0.6183-6.8900
trypsin inhibitor (TIU/mg dw)	20.79-59.03[a]; 18.14-42.51[b]	3.23-118.68
Isoflavones		
daidzein (µg/g dw)	224.03-1571.91[a]; 198.95-1458.24[b]	60.04-3,061.20
genistein (µg/g dw)	338.24-1488.89[a]; 148.06-1095.57[b]	35.71-2,837.20
glycitein (µg/g dw)	52.72-298.57[a]; 32.42-255.94[b]	14.10-1,630.00
Forage Nutrients		
Proximates		
protein (% dw)	16.48-24.29[a]; 12.68-23.76[b]	9.51-46.25
total fat (% dw)	2.65-9.87[a]; 2.96-7.88[b]	0.3-20.0
ash (% dw)	5.28-9.24[a]; 4.77-8.54[b]	2.866-36.600
Carbohydrates By Calculation		
carbohydrates by calculation (% dw)	62.25-72.30[a]; 60.61-77.26[b]	27.8-80.6
Fiber		
acid detergent fiber (% dw)	23.86-50.89[a]; 25.49-47.33[b]	12.845-64.100
neutral detergent fiber (% dw)	19.61-43.70[a]; 30.96-64.19[b]	19.26-82.00

[1]dw = dry weight; FA = Fatty Acid.

[2]Literature range references: [a](Lundry *et al.*, 2008); [b](Berman *et al.*, 2009); [c](Bellaloui *et al.*, 2011); [d](Thompson *et al.*, 2016); [e](Breeze *et al.*, 2015); [f](Codex Alimentarius, 2021) ND = non-detectable <0.05% Total FA.

[3]AFSI range is from AFSI CCDB, 2022 (Accessed February 22, 2022).

B.5(c) The levels of any other constituents that may potentially be influenced by the genetic modification, as a result, for example, of downstream metabolic effects, compared with the levels in an appropriate comparator as well as the range of natural variation.

Considering mode of action of proteins expressed in MON 94637 in B.1(a), and composition analysis in B.5(a), it is not anticipated that any other constituents would be influenced by the genetic modification.

C. INFORMATION RELATED TO THE NUTRITIONAL IMPACT OF THE FOOD PRODUCED USING GENE TECHNOLOGY

There are no nutritional impacts on the food derived from MON 94637. This product is developed to confer insect protection. It is not a nutritionally altered product.

D. OTHER INFORMATION

The data and information presented in this submission demonstrate that the food derived from MON 94637 are as safe and nutritious as those derived from commercially-available, conventional soybean for which there is an established history of safe consumption. No additional studies are considered necessary to demonstrate the safety of MON 94367.

STATUTORY DECLARATION pursuant to Statutory Declarations Act 1959

I [redacted], Regulatory Affairs Lead at Bayer CropScience Pty Ltd, Level 4, 109 Burwood Road, Hawthorn, Vic. 3122, make the following declaration under the Statutory Declarations Act 1959:

1. the information provided in this application fully sets out the matters required,

2. the information provided in this application is true to the best of my knowledge and belief,

3. no information has been withheld that might prejudice this application, to the best of my knowledge and belief.

I understand that a person who intentionally makes a false statement in a statutory declaration is guilty of an offence under section 11 of the Statutory Declarations Act 1959, and I believe that the statements in this declaration are true in every particular.

[redacted]

[redacted]

Signature of person making the declaration

Declared at Hawthorn on 4th June 2024

Before me

[redacted]

Level 4, 109 Burwood Road, Hawthorn, Vic. 3122, an Australian Legal Practitioner within the meaning of the Legal Profession Uniform Law (Victoria)

////////////////

04 June 2024

Bayer CropScience Pty Ltd
ABN 87 000 226 022

Level 4, 109 Burwood Road
Hawthorn VIC 3122
Australia

Tel. +61 3 9248 6888

crop.bayer.com.au

PART 4 REFERENCES

UNPUBLISHED REPORTS BEING SUBMITTED

Appendix 1. M-815737-01-1. Molecular Characterization of Insect-Protected Soybean MON 94637.

Appendix 2. M-835402-01-1. Updated Bioinformatics Evaluation of the T-DNA in MON 94637 Utilizing the AD_2023, TOX_2023, and PRT_2023 Databases

Appendix 3. M-835404-01-1. Updated Bioinformatics Evaluation of Putative Flank-Junction Peptides in MON 94637 Utilizing the AD_2023, TOX_2023, and PRT_2023 Databases

Appendix 4. M-829572-01-1. Segregation Analysis of the T-DNA Insert in Insect Protected MON 94637 Soybean Across Three Generations

Appendix 5. M-822244-01-1. Demonstration of the Presence of Cry1A.2 and Cry1B.2 Proteins in Soybean Seed Samples Across Multiple Generations of MON 94637

Appendix 6. M-830877-01-1. Characterization of the Cry1A.2 Protein Purified from the Seed of MON 94637 Soybean and Comparison of the Physicochemical and Functional Properties of the Plant-Produced and *Bacillus thuringiensis* (*Bt*)-Produced Cry1A.2 Proteins

Appendix 7. M-830878-01-1. Characterization of the Cry1B.2 Protein Purified from the Seed of MON 94637 Soybean and Comparison of the Physicochemical and Functional Properties of the Plant-Produced and *Bacillus thuringiensis* (*Bt*)-Produced Cry1B.2 Proteins.

Appendix 8. M-824045-02-1. Amended Report for SCR-2022-0316: Assessment of Cry1A.2 and Cry1B.2 Protein Levels in Soybean Flower, Forage, Grain, Over Season Leaf 1 (OSL1), and Root Tissues Collected from MON 94637 Produced in United States Field Trials in 2021

Appendix 9. M-835406-01-1. Updated Bioinformatics Evaluation of Cry1A.2 and Cry1B.2 in MON 94637 Utilizing the AD_2023, TOX_2023, and PRT_2023 Databases

Appendix 10. M-827971-06-1. Assessment of the *In Vitro* Digestibility of *Bacillus Thuringiensis*-produced Cry1A.2 by Pepsin and Pancreatin

Appendix 11. M-827969-02-1 Assessment of the *in vitro* Digestibility of *Bacillus thuringiensis*-produced Cry1B.2 by Pepsin and Pancreatin

Appendix 12. M-827773-01-1 The Effect of Heat Treatment on the Functional Activity of *Bacillus thuringiensis*-produced Cry1A.2 Protein

Appendix 13. M-827770-01-1 The Effect of Heat Treatment on the Functional Activity of *Bacillus thuringiensis*-produced Cry1B.2 Protein

Appendix 14. M-822352-02-1 Compositional Analyses of Soybean Grain and Forage Harvested from MON 94637 Grown in the United States During the 2021 Season

PUBLISHED REFERENCES

Anderson, J.E., J.-M. Michno, T.J.Y. Kono, A.O. Stec, B.W. Campbell, S.J. Curtin and R.M. Stupar. 2016. Genomic variation and DNA repair associated with soybean transgenesis: A comparison to cultivars and mutagenized plants. BMC Biotechnology 16:41.

ASA. 2022. SoyStats 2022: A reference guide to soybean facts and figures. American Soybean Association, St. Louis, Missouri. https://soygrowers.com/wp-content/uploads/2022/06/22ASA-002-Soy-Stats-Final-WEB.pdf [Accessed April 14, 2024].

Axelos, M., C. Bardet, T. Liboz, A. Le Van Thai, C. Curie and B. Lescure. 1989. The gene family encoding the *Arabidopsis thaliana* translation elongation factor EF-1α: Molecular cloning, characterization and expression. Molecular and General Genetics 219:106-112.

Barker, R.F., K.B. Idler, D.V. Thompson and J.D. Kemp. 1983. Nucleotide sequence of the T-DNA region from the *Agrobacterium tumefaciens* octopine Ti plasmid pTi15955. Plant Molecular Biology 2:335-350.

Baum, J.A. 1998. Transgenic *Bacillus thuringiensis*. Phytoprotection 79:127-130.

Baum, J.A., T.B. Johnson and B.C. Carlton. 1999. *Bacillus thuringiensis*: Natural and recombinant bioinsecticide products. Pages 189-209 in Methods in Biotechnology: Biopesticides: Use and Delivery. Volume 5. F.R. Hall and J.J. Menn (eds.). Humana Press Inc., Totowa, New Jersey.

Bäumlein, H., W. Boerjan, I. Nagy, R. Bassüner, M. Van Montagu, D. Inzé and U. Wobus. 1991. A novel seed protein gene from *Vicia faba* is developmentally regulated in transgenic tobacco and *Arabidopsis* plants. Molecular and General Genetics 225:459-467.

Bautista-Zapanta, J.-n., K. Suzuki and K. Yoshida. 2002. Characterization of four ribosomal RNA operons in the genome of *Agrobacterium tumefaciens* MAFF301001. Nucleic Acids Research S2:91-92.

Beck, E., G. Ludwig, E.A. Auerswald, B. Reiss and H. Schaller. 1982. Nucleotide sequence and exact localization of the neomycin phosphotransferase gene from transposon Tn*5*. Gene 19:327-336.

Bellaloui, N., J.R. Smith, A.M. Gillen and J.D. Ray. 2011. Effects of maturity, genotypic background, and temperature on seed mineral composition in near-isogenic soybean lines in the early soybean production system. Crop Science 51:1161-1171.

Berman, K.H., G.G. Harrigan, S.G. Riordan, M.A. Nemeth, C. Hanson, M. Smith, R. Sorbet, E. Zhu and W.P. Ridley. 2009. Compositions of seed, forage, and processed fractions from insect-protected soybean MON 87701 are equivalent to those of conventional soybean. Journal of Agricultural and Food Chemistry 57:11360-11369.

Betz, F.S., B.G. Hammond and R.L. Fuchs. 2000. Safety and advantages of *Bacillus thuringiensis*-protected plants to control insect pests. Regulatory Toxicology and Pharmacology 32:156-173.

Bevan, M., W.M. Barnes and M.-D. Chilton. 1983. Structure and transcription of the nopaline synthase gene region of T-DNA. Nucleic Acids Research 11:369-385.

Biron, D.G., C. Brun, T. Lefevre, C. Lebarbenchon, H.D. Loxdale, F. Chevenet, J.-P. Brizard and F. Thomas. 2006. The pitfalls of proteomics experiments without the correct use of bioinformatics tools. Proteomics 6:5577-5596.

Bradshaw, R.A., W.W. Brickley and K.W. Walker. 1998. N-terminal processing: The methionine aminopeptidase and N^{α}-acetyl transferase families. Trends in Biochemical Sciences 23:263-267.

Bravo, A., S.S. Gill and M. Soberón. 2007. Mode of action of *Bacillus thuringiensis* Cry and Cyt toxins and their potential for insect control. Toxicon 49:423-435.

Bravo, A., S. Likitvivatanavong, S.S. Gill and M. Soberón. 2011. *Bacillus thuringiensis*: A story of a successful bioinsecticide. Insect Biochemistry and Molecular Biology 41:423-431.

Breeze, M.L., E. Leyva-Guerrero, G.R. Yeaman, Y. Dudin, R. Akel, P. Brune, F. Claussen, C. Dharmasri, J. Golbach, R. Guo, C. Maxwell, L. Privalle, H. Rogers, K. Liu, G. Shan, M. Yarnall, D. Thiede and N. Gillikin. 2015. Validation of a method for quantitation of soybean lectin in commercial varieties. Journal of the American Oil Chemists' Society 92:1085-1092.

Bueno, A.F., S.V. Paula-Moraes, D.L. Gazzoni and A.F. Pomari. 2013. Economic thresholds in soybean-integrated pest management: Old concepts, current adoption, and adequacy. Neotropical Entomology 42:439-447.

Cade, R., K. Burgin, K. Schilling, T.-J. Lee, P. Ngam, N. Devitt and D. Fajardo. 2018. Evaluation of whole genome sequencing and an insertion site characterization method for molecular characterization of GM maize. Journal of Regulatory Science 6:1-14.

Caetano-Anollés, G., M. Wang, D. Caetano-Anollés and J.E. Mittenthal. 2009. The origin, evolution and structure of the protein world. Biochemical Journal 417:621-637.

Chen, D., W.J. Moar, A. Jerga, A. Gowda, J.S. Milligan, E.C. Bretsynder, T.J. Rydel, J.A. Baum, A. Semeao, X. Fu, V. Guzov, K. Gabbert, G.P. Head and J.A. Haas. 2021. *Bacillus thuringiensis* chimeric proteins Cry1A.2 and Cry1B.2 to control soybean lepidopteran pests: New domain combinations enhance insecticidal spectrum of activity and novel receptor contributions. PLoS ONE 16:e0249150.

Codex Alimentarius. 2009. Foods derived from modern biotechnology. Second Edition. Codex Alimentarius Commission, Joint FAO/WHO Food Standards Programme, Food and Agriculture Organization of the United Nations, Rome, Italy.

Codex Alimentarius. 2021. Codex standard for named vegetable oils. Codex-Stan 210-1999. Codex Alimentarius Commission, Joint FAO/WHO Food Standards Programme, Food and Agriculture Organization of the United Nations, Rome, Italy.

Coruzzi, G., R. Broglie, C. Edwards and N.-H. Chua. 1984. Tissue-specific and light-regulated expression of a pea nuclear gene encoding the small subunit of ribulose-1,5-bisphosphate carboxylase. The EMBO Journal 3:1671-1679.

Crickmore, N., D.R. Zeigler, J. Feitelson, E. Schnepf, J. Van Rie, D. Lereclus, J. Baum and D.H. Dean. 1998. Revision of the nomenclature for the *Bacillus thuringiensis* pesticidal crystal proteins. Microbiology and Molecular Biology Reviews 62:807-813.

de Maagd, R.A., A. Bravo, C. Berry, N. Crickmore and H.E. Schnepf. 2003. Structure, diversity, and evolution of protein toxins from spore-forming entomopathogenic bacteria. Annual Review of Genetics 37:409-433.

de Maagd, R.A., A. Bravo and N. Crickmore. 2001. How *Bacillus thuringiensis* has evolved specific toxins to colonize the insect world. Trends in Genetics 17:193-199.

Deist, B.R., M.A. Rausch, M.T. Fernandez-Luna, M.J. Adang and B.C. Bonning. 2014. Bt toxin modification for enhanced efficacy. Toxins 6:3005-3027.

Depicker, A., S. Stachel, P. Dhaese, P. Zambryski and H.M. Goodman. 1982. Nopaline synthase: Transcript mapping and DNA sequence. Journal of Molecular and Applied Genetics 1:561-573.

EFSA. 2012. Conclusion on the peer review of the pesticide risk assessment of the active substance *Bacillus thuringiensis* subsp. *kurstaki* (strains ABTS 351, PB 54, SA 11, SA 12, EG 2348). EFSA Journal 10:2540.

Federici, B.A. and J.P. Siegel. 2008. Safety assessment of *Bacillus thuringiensis* and Bt crops used in insect control. Pages 45-102 in Food Safety of Proteins in Agricultural Biotechnology. B.G. Hammond (ed.). CRC Press, Boca Raton, Florida.

Fisher, R. and L. Rosner. 1959. Toxicology of the microbial insecticide, Thuricide. Journal of Agricultural and Food Chemistry 7:686-688.

Fling, M.E., J. Kopf and C. Richards. 1985. Nucleotide sequence of the transposon Tn*7* gene encoding an aminoglycoside-modifying enzyme, 3"(9)-*O*-nucleotidyltransferase. Nucleic Acids Research 13:7095-7106.

Fraley, R.T., S.G. Rogers, R.B. Horsch, P.R. Sanders, J.S. Flick, S.P. Adams, M.L. Bittner, L.A. Brand, C.L. Fink, J.S. Fry, G.R. Galluppi, S.B. Goldberg, N.L. Hoffmann and S.C. Woo. 1983. Expression of bacterial genes in plant cells. Proceedings of the National Academy of Sciences of the United States of America 80:4803-4807.

Frederiksen, K., H. Rosenquist, K. Jørgensen and A. Wilcks. 2006. Occurrence of natural *Bacillus thuringiensis* contaminants and residues of *Bacillus thuringiensis*-based insecticides on fresh fruits and vegetables. Applied and Environmental Microbiology 72:3435-3440.

Gao, Y., K.J. Fencil, X. Xu, D.A. Schwedler, J.R. Gilbert and R.A. Herman. 2006. Purification and characterization of a chimeric Cry1F δ-endotoxin expressed in transgenic cotton plants. Journal of Agricultural and Food Chemistry 54:829-835.

Giglione, C., A. Boularot and T. Meinnel. 2004. Protein N-terminal methionine excision. Cellular and Molecular Life Sciences 61:1455-1474.

Gill, S.S., E.A. Cowles and P.V. Pietrantonio. 1992. The mode of action of *Bacillus thuringiensis* endotoxins. Annual Review of Entomology 37:615-636.

Giza, P.E. and R.C.C. Huang. 1989. A self-inducing runaway-replication plasmid expression system utilizing the Rop protein. Gene 78:73-84.

Hadley, W.M., S.W. Burchiel, T.D. McDowell, J.P. Thilsted, C.M. Hibbs, J.A. Whorton, P.W. Day, M.B. Friedman and R.E. Stoll. 1987. Five-month oral (diet) toxicity/infectivity study of *Bacillus thuringiensis* insecticides in sheep. Fundamental and Applied Toxicology 8:236-242.

Hammond, B. 2004. A review of the food/feed safety and benefits of *Bacillus thuringiensis* protein containing insect-protected crops. Pages 103-123 in Agricultural Biotechnology: Challenges and Prospects. M.K. Bhalgat, W.P. Ridley, A.S. Felsot, and J.N. Seiber (eds.). American Chemical Society, Washington, D.C.

Hammond, B.G. and J.M. Jez. 2011. Impact of food processing on the safety assessment for proteins introduced into biotechnology-derived soybean and corn crops. Food and Chemical Toxicology 49:711-721.

Harrigan, G.G., D. Lundry, S. Drury, K. Berman, S.G. Riordan, M.A. Nemeth, W.P. Ridley and K.C. Glenn. 2010. Natural variation in crop composition and the impact of transgenesis. Nature Biotechnology 28:402-404.

Harrigan, G.G., W.P. Ridley, K.D. Miller, R. Sorbet, S.G. Riordan, M.A. Nemeth, W. Reeves and T.A. Pester. 2009. The forage and grain of MON 87460, a drought-tolerant corn hybrid, are compositionally equivalent to that of conventional corn. Journal of Agricultural and Food Chemistry 57:9754-9763.

Heinrichs, E.A. and R. Muniappan. 2018. Integrated pest management for tropical crops: Soyabeans. CAB Reviews 13:1-44.

Hensley, K., E.J. Benaksas, R. Bolli, P. Comp, P. Grammas, L. Hamdheydari, S. Mou, Q.N. Pye, M.F. Stoddard, G. Wallis, K.S. Williamson, M. West, W.J. Wechter and R.A. Floyd. 2004. New perspectives on Vitamin E: γ–tocopherol and carboxyethylhydroxy chroman metabolites in biology and medicine. Free Radical Biology & Medicine 36:1-15.

Hernandez-Garcia, C.M. and J.J. Finer. 2014. Identification and validation of promoters and *cis*-acting regulatory elements. Plant Science 217-218:109-119.

Herrmann, K.M. 1995. The shikimate pathway: Early steps in the biosynthesis of aromatic compounds. The Plant Cell 7:907-919.

Hileman, R.E., A. Silvanovich, R.E. Goodman, E.A. Rice, G. Holleschak, J.D. Astwood and S.L. Hefle. 2002. Bioinformatic methods for allergenicity assessment using a comprehensive allergen database. International Archives of Allergy and Immunology 128:280-291.

Horikoshi, R.J., P.M. Dourado, G.U. Berger, D.d.S. Fernandes, C. Omoto, A. Willse, S. Martinelli, G.P. Head and A.S. Corrêa. 2021. Large-scale assessment of lepidopteran soybean pests and efficacy of Cry1Ac soybean in Brazil. Scientific Reports 11:15956.

Hunt, A.G. 1994. Messenger RNA 3’ end formation in plants. Annual Review of Plant Physiology and Plant Molecular Biology 45:47-60.

Illergård, K., D.H. Ardell and A. Elofsson. 2009. Structure is three to ten times more conserved than sequence - A study of structural response in protein cores. Proteins 77:499-508.

Klee, H.J., Y.M. Muskopf and C.S. Gasser. 1987. Cloning of an *Arabidopsis thaliana* gene encoding 5-enolpyruvylshikimate-3-phosphate synthase: Sequence analysis and manipulation to obtain glyphosate-tolerant plants. Molecular and General Genetics 210:437-442.

Kovalic, D., C. Garnaat, L. Guo, Y. Yan, J. Groat, A. Silvanovich, L. Ralston, M. Huang, Q. Tian, A. Christian, N. Cheikh, J. Hjelle, S. Padgette and G. Bannon. 2012. The use of next generation sequencing and junction sequence analysis bioinformatics to achieve molecular characterization of crops improved through modern biotechnology. The Plant Genome 5:149-163.

Krause, E., H. Wenschuh and P.R. Jungblut. 1999. The dominance of arginine-containing peptides in MALDI-derived tryptic mass fingerprints of proteins. Analytical Chemistry 71:4160-4165.

Liu, K.S. 2004. Soybeans as a powerhouse of nutrients and phyhtochemicals. Pages 1-22 in Soybeans as Functional Foods and Ingredients. AOCS Press, Champaign, Illinois.

Lundry, D.R., W.P. Ridley, J.J. Meyer, S.G. Riordan, M.A. Nemeth, W.A. Trujillo, M.L. Breeze and R. Sorbet. 2008. Composition of grain, forage, and processed fractions from second-generation glyphosate-tolerant soybean, MON 89788, is equivalent to that of conventional soybean (*Glycine max* L.). Journal of Agricultural and Food Chemistry 56:4611-4622.

Mazodier, P., P. Cossart, E. Giraud and F. Gasser. 1985. Completion of the nucleotide sequence of the central region of Tn*5* confirms the presence of three resistance genes. Nucleic Acids Research 13:195-205.

McClintock, J.T., C.R. Schaffer and R.D. Sjoblad. 1995. A comparative review of the mammalian toxicity of *Bacillus thuringiensis*-based pesticides. Pesticide Science 45:95-105.

Mendelsohn, M., J. Kough, Z. Vaituzis and K. Matthews. 2003. Are *Bt* crops safe? Nature Biotechnology 21:1003-1009.

Messina, M.J. 1999. Legumes and soybeans: Overview of their nutritional profiles and health effects. American Journal of Clinical Nutrition 70:439S-450S.

Metcalfe, D.D., J.D. Astwood, R. Townsend, H.A. Sampson, S.L. Taylor and R.L. Fuchs. 1996. Assessment of the allergenic potential of foods derived from genetically engineered crop plants. Critical Reviews in Food Science and Nutrition 36:S165-S186.

Norris, S.R., S.E. Meyer and J. Callis. 1993. The intron of *Arabidopsis thaliana* polyubiquitin genes is conserved in location and is a quantitative determinant of chimeric gene expression. Plant Molecular Biology 21:895-906.

OECD. 2002. Report of the OECD workshop on the toxicological and nutritional testing of novel foods. SG/ICGB(1998)1/FINAL. Organisation for Economic Co-operation and Development, Paris, France.

OECD. 2007. Consensus document on safety information on transgenic plants expressing *Bacillus thuringiensis*-derived insect control proteins. ENV/JM/MONO(2007)14. Organisation for Economic Co-operation and Development, Paris, France.

OECD. 2012. Revised consensus document on compositional considerations for new varieties of soybean [*Glycine max* (L.) Merr.]: Key food and feed nutrients, anti-nutrients, toxicants and allergens. ENV/JM/MONO(2012)24. Series on the Safety of Novel Foods and Feeds No. 25. Organisation for Economic Co-operation and Development, Paris, France.

Oerke, E.-C. 2006. Centenary review: Crop losses to pests. Journal of Agricultural Science 144:31-43.

Piper, K.R., S.B. von Bodman, I. Hwang and S.K. Farrand. 1999. Hierarchical gene regulatory systems arising from fortuitous gene associations: Controlling quorum sensing by the opine regulon in *Agrobacterium*. Molecular Microbiology 32:1077-1089.

Rademacher, T.W., R.B. Parekh and R.A. Dwek. 1988. Glycobiology. Annual Review of Biochemistry 57:785-838.

Richins, R.D., H.B. Scholthof and R.J. Shepherd. 1987. Sequence of figwort mosaic virus DNA (caulimovirus group). Nucleic Acids Research 15:8451-8466.

Ridley, W.P., G.G. Harrigan, M.L. Breeze, M.A. Nemeth, R.S. Sidhu and K.C. Glenn. 2011. Evaluation of compositional equivalence for multitrait biotechnology crops. Journal of Agricultural and Food Chemistry 59:5865-5876.

Rogers, S.G. 2000. Promoter for transgenic plants. Patent 6,018,100, U.S. Patent Office, Washington, D.C.

Salomon, S. and H. Puchta. 1998. Capture of genomic and T-DNA sequences during double-strand break repair in somatic plant cells. The EMBO Journal 17:6086-6095.

Schafer, F.Q., E.E. Kelley and G.R. Buettner. 2003. Oxidative stress and antioxidant intervention. Pages 849-869 in Critical Reviews of Oxidative Stress and Aging: Advances in Basic Science, Diagnostics and Intervention. R.G. Cutler and H. Rodriguez (eds.). World Scientific, New Jersey.

Schnepf, E., N. Crickmore, J. van Rie, D. Lereclus, J. Baum, J. Feitelson, D.R. Zeigler and D.H. Dean. 1998. *Bacillus thuringiensis* and its pesticidal crystal proteins. Microbiology and Molecular Biology Reviews 62:775-806.

Siegel, J.P. 2001. The mammalian safety of *Bacillus thuringiensis*-based insecticides. Journal of Invertebrate Pathology 77:13-21.

Silvanovich, A., M.A. Nemeth, P. Song, R. Herman, L. Tagliani and G.A. Bannon. 2006. The value of short amino acid sequence matches for prediction of protein allergenicity. Toxicological Sciences 90:252-258.

Sutcliffe, J.G. 1979. Complete nucleotide sequence of the *Escherichia coli* plasmid pBR322. Cold Spring Harbor Symposia on Quantitative Biology 43:77-90.

Thomas, K., M. Aalbers, G.A. Bannon, M. Bartels, R.J. Dearman, D.J. Esdaile, T.J. Fu, C.M. Glatt, N. Hadfield, C. Hatzos, S.L. Hefle, J.R. Heylings, R.E. Goodman, B. Henry, C. Herouet, M. Holsapple, G.S. Ladics, T.D. Landry, S.C. MacIntosh, E.A. Rice, L.S. Privalle, H.Y. Steiner, R. Teshima, R. van Ree, M. Woolhiser and J. Zawodny. 2004. A multi-laboratory evaluation of a common in vitro pepsin digestion assay protocol used in assessing the safety of novel proteins. Regulatory Toxicology and Pharmacology 39:87-98.

Thomas, K., G. Bannon, S. Hefle, C. Herouet, M. Holsapple, G. Ladics, S. MacIntosh and L. Privalle. 2005. In silico methods for evaluating human allergenicity to novel proteins: International Bioinformatics Workshop Meeting Report, 23-24 February 2005. Toxicological Sciences 88:307-310.

Thompson, M.M., A. Niemuth, J. Sabbatini, D. Levin, M.L. Breeze, X. Li, T. Perez, M. Taylor and G.G. Harrigan. 2016. Analysis of vitamin K_1 in soybean seed: Assessing levels in a lineage representing over 35 years of breeding. Journal of the American Oil Chemists' Society 93:587-594.

U.S. EPA. 1986. Pesticide fact sheet number 93: *Bacillus thuringiensis.* EPA/540/FS-87/025. U.S. Environmental Protection Agency, Washington, D.C.

U.S. EPA. 1996. *Bacillus thuringiensis* Cry1A(b) delta-endotoxin and the genetic material necessary for its production in all plants; Exemption from requirement of a tolerance. Federal Register 61:40340-40343.

U.S. EPA. 1998. Reregistration eligibility decision (RED): *Bacillus thuringiensis*. EPA738-R-98-004. U.S. Environmental Protection Agency, Washington, D.C.

U.S. EPA. 2001. Biopesticides registration action document: *Bacillus thuringiensis* plant-incorporated protectants (October 15, 2001). U.S. Environmental Protection Agency, Washington, D.C. http://www.epa.gov/pesticides/biopesticides/pips/bt_brad.htm [Accessed July 24, 2013].

Vachon, V., R. Laprade and J.-L. Schwartz. 2012. Current models of the mode of action of *Bacillus thuringiensis* insecticidal crystal proteins: A critical review. Journal of Invertebrate Pathology 111:1-12.

Venkatesh, T.V., M.L. Breeze, K. Liu, G.G. Harrigan and A.H. Culler. 2014. Compositional analysis of grain and forage from MON 87427, an inducible male sterile and tissue selective glyphosate-tolerant maize product for hybrid seed production. Journal of Agricultural and Food Chemistry 62:1964-1973.

VKM. 2016. Risk assessment of the biological plant protection product Turex 50 WG, with the organism *Bacillus thuringiensis* ssp. *aizawai* CG-91. Opinion of the Panel on Plant Protection Product of the Norwegian Scientific Committee for Food Safety. VKM Report 2016:20.

Wingfield, P.T. 2017. N-terminal methionine processing. Current Protocols in Protein Science 88:6.14.11-16.14.13.

Ye, X., E.J. Williams, J. Shen, J.A. Esser, A.M. Nichols, M.W. Petersen and L.A. Gilbertson. 2008. Plant development inhibitory genes in binary vector backbone improve quality event efficiency in soybean transformation. Transgenic Research 17:827-838.

Ye, X., E.J. Williams, J. Shen, S. Johnson, B. Lowe, S. Radke, S. Strickland, J.A. Esser, M.W. Petersen and L.A. Gilbertson. 2011. Enhanced production of single copy backbone-free transgenic plants in multiple crop species using binary vectors with a pRi replication origin in *Agrobacterium tumefaciens*. Transgenic Research 20:773-786.

Zambryski, P., A. Depicker, K. Kruger and H.M. Goodman. 1982. Tumor induction by *Agrobacterium tumefaciens*: Analysis of the boundaries of T-DNA. Journal of Molecular and Applied Genetics 1:361-370.

Zastrow-Hayes, G.M., H. Lin, A.L. Sigmund, J.L. Hoffman, C.M. Alarcon, K.R. Hayes, T.A. Richmond, J.A. Jeddeloh, G.D. May and M.K. Beatty. 2015. Southern-by-sequencing: A robust screening approach for molecular characterization of genetically modified crops. The Plant Genome 8:1-15.

Zhou, J., G.G. Harrigan, K.H. Berman, E.G. Webb, T.H. Klusmeyer and M.A. Nemeth. 2011. Stability in the composition equivalence of grain from insect-protected maize and seed from glyphosate-tolerant soybean to conventional counterparts over multiple seasons, locations, and breeding germplasms. Journal of Agricultural and Food Chemistry 59:8822-8828.